Russian Original Vol. 40, No. 3, March, 1976

September, 1976

SATEAZ 40(3) 243-348 (1976)

SOVIET ATOMIC ENERGY

АТОМНАЯ ЭНЕРГИЯ
(ATOMNAYA ÉNERGIYA)

TRANSLATED FROM RUSSIAN

CONSULTANTS BUREAU, NEW YORK

SOVIET ATOMIC ENERGY

Soviet Atomic Energy is a cover-to-cover translation of *Atomnaya Énergiya*, a publication of the Academy of Sciences of the USSR.

An agreement with the Copyright Agency of the USSR (VAAP) makes available both advance copies of the Russian journal and original glossy photographs and artwork. This serves to decrease the necessary time lag between publication of the original and publication of the translation and helps to improve the quality of the latter. The translation began with the first issue of the Russian journal.

Consultants Bureau journals appear about six months after the publication of the original Russian issue. For bibliographic accuracy, the English issue published by Consultants Bureau carries the same number and date as the original Russian from which it was translated. For example, a Russian issue published in December will appear in a Consultants Bureau English translation about the following June, but the translation issue will carry the December date. When ordering any volume or particular issue of a Consultants Bureau journal, please specify the date and, where applicable, the volume and issue numbers of the original Russian. The material you will receive will be a translation of that Russian volume or issue.

Subscription
$107.50 per volume (6 Issues)
2 volumes per year
Prices somewhat higher outside the United States.

Single Issue: $50
Single Article: $15

CONSULTANTS BUREAU, NEW YORK AND LONDON

c/b
227 West 17th Street
New York, New York 10011

Published monthly. Second-class postage paid at Jamaica, New York 11431.

Soviet Atomic Energy is abstracted or indexed in *Applied Mechanics Reviews, Chemical Abstracts, Engineering Index, INSPEC—Physics Abstracts and Electrical and Electronics Abstracts, Current Contents,* and *Nuclear Science Abstracts.*

SOVIET ATOMIC ENERGY

A translation of *Atomnaya Énergiya*

September, 1976

Volume 40, Number 3 March, 1976

CONTENTS

	Engl.	Russ.
ARTICLES		
Gas-Phase Composition in the Fuel Rods at Novyi Voronezh Nuclear Power Station — A. T. Ageenkov, A. A. Buravtsov, E. M. Valuev, L. I. Golubev, Z. V. Ershova, V. V. Kravtsev, and A. F. Skvoev	243	203
Spatial Nonuniformity of Fuel Burnup in VVÉR Reactors — L. I. Golubev, L. I. Gorobtsov, G. A. Kulakov, V. D. Simonov, and M. A. Sunchagashev	247	207
Observation of Vacant Porosity in Metals upon Their Irradiation by Accelerated Iron Ions — G. N. Flerov, V. S. Barashenkov, S. Ya. Lebedev, G. N. Akap'ev, V. E. Dubinskii, V. G. Rodionova, S. I. Rudnev, and S. Ya. Surkov	251	211
ÉLV-1 Electron Accelerator for Industrial Use — G. I. Budker, V. A. Gaponov, B. M. Korabel'nikov, G. S. Krainov, S. A. Kuznetsov, N. K. Kuksanov, V. I. Kondrat'ev, and R. A. Salimov	256	216
Grazing Scattering of Fast Electrons by the Surface of a Solid — V. I. Boiko, V. V. Evstigneev, B. A. Kononov, A. L. Plotnikov, and E. A. Gorbachev	261	221
Microdosimetric Determination of Radiation Quality Factors — I. V. Filyushkin	267	227
The Development of Gamma-Resonance (Mössbauer) Spectroscopy in the Soviet Union — I. P. Suzdalev	274	234
New Books from Atomizdat	280	239
DEPOSITED ARTICLES		
Dynamics of Transmission of High-Frequency Power during Magnetosonic Heating of a Plasma in a Tokamak	281	240
Applicability of the Method of Magnetosonic Heating for Thermonuclear Parameters of a Plasma in a Tokamak	282	241
Method of Correction of Macroscopic Constants of Fast Systems Based on Results of Individual Experiments — Yu. Yu. Vasil'ev, V. N. Gurin, and B. G. Dubovskii	283	242
Optimal Electron-Positron Conversion at High Energies — V. A. Tayurskii	284	242
Calculation of Released Energy and Total Track Lengths of Charged Particles in Showers in Xenon — M. Ya. Borkovskii and S. P. Kruglov	284	243
LETTERS		
Moments of Neutron Density Distribution Functions — A. A. Kostritsa and E. I. Neimotin	286	244
Efficiency of a Scintillation Gamma Detector in an Isotropic Radiating Medium — Yu. A. Sapozhnikov, V. A. Lopatin, and V. P. Ovcharenko	289	246
Single-Channel Alpha Spectrometer for Measurement of Radon Daughter Product Concentrations — N. I. Antipin, Yu. V. Kuznetsov, and L. S. Ruzer	291	247
Algorithm for Monte Carlo Simulation of Compton Scattering Including Gamma-Ray Polarization — N. L. Kuchin, K. K. Popkov, and I. N. Trofimov	293	249
Semiconductor Radiometer-Spectrometer for Measurement of Surface Contamination by Alpha-Radioactive Materials — V. A. Manchuk and A. A. Petushkov	295	250
An Apparatus for Assaying Helium in Constructional Materials — A. I. Dashkovskii, A. G. Zaluzhnyi, D. M. Skorov, O. M. Sorozhuk, and M. V. Cherednichenko-Alchevskii	297	251

CONTENTS

(continued)

	Engl.	Russ.
Surface Blister Bursting – B. A. Kalin, N. M. Kirilin, A. A. Pisarev, D. M. Skorov, V. G. Tel'kovskii, S. K. Fedyaev, and G. N. Shishkin	299	252
Temperature Dependence of Erosion of Stainless Steels under Ionic Bombardment – A. D. Gurov, B. A. Kalin, N. M. Kirilin, A. A. Pisarev, D. M. Skorov, V. G. Tel'kovskii, S. K. Fedyaev, and G. N. Shishkin	301	254
Diffusion Coefficients and Solubility of Vanadium, Niobium, and Cerium in Beryllium – V. M. Anan'in, V. P. Gladkov, A. V. Svetlov, D. M. Skorov, and V. I. Tenishev	304	256
Diffusion and Solubility of Aluminum in Beryllium – V. P. Gladkov, A. V. Svetlov, D. M. Skorov, V. I. Tenishev, and A. N. Shabalin	306	257
Relative Measurements of the Spectral Characteristics of Neutron Distributions by the Activation Ratios Method – R. D. Vasil'ev, E. I. Grigor'ev, and V. P. Yarnya	308	259
Monte Carlo Solution of Gamma–Gamma Logging Problems for Large Distances from the Source – R. T. Khamatdinov	311	260
COMECON CHRONICLES		
Symposium on "The Drawing-Up of Apparatus Systems of Nuclear Instrument Making for Laboratory and Industrial Applications – A. S. Tuchina	314	263
Comecon Collaboration Notes	316	264
INFORMATION		
50 Years of Corresponding Member of the Academy of Sciences of the SSSR, A. M. Baldin – N. N. Bogolyubov, A. A. Kuznetsov, and I. N. Semenyushkin	318	265
CONFERENCES AND MEETINGS		
Seminar on the Operating Cycles of Nuclear Power Stations – B. B. Baturov, O. M. Glazkov, and R. R. Ionaitis	320	266
International Symposium on Gas-Cooled Reactors – I. Kh. Ganev	323	267
The Soviet–French Seminar on Water-Cooled/Water-Moderated Power Reactors – V. P. Denisov	326	269
Symposium on the Transplutonium Elements – K. Shvetsovii	328	270
IAEA Symposium on the Natural Nuclear Reactor at Oklo – V. A. Pchelkin	330	271
Conference of the International Committee on Nuclear Data – G. B. Yan'kov	332	272
All-Union Conference on the Application of Charged-Particle Accelerators in the National Economy – O. A. Gusev	334	273
2nd International Symposium on Plasma Chemistry – Yu. N. Tumanov	336	274
3rd International Conference on the Measurement of Low Levels of Radioactivity and Their Application – A. K. Lavrukhina	339	275
All-Union Seminar on the Radiation Stability of Organic Materials – Yu. Ya. Shavarin	341	277
NEW FACILITIES		
A Facility for Producing a Beam of Electrons with Energies of up to 250 KeV and with a Power of Up to 1000 kW – M. M. Brovin, A. A. Bushuev, V. A. Gapanov, A. I. Grishehenko, S. S. Zhukovskii, V. E. Nekhaev, V. S. Nikolaev, V. V. Ryazanov, R. A. Salimov, E. P. Semenov, and A. F. Serov	342	277
BIBLIOGRAPHY		
A. I. Moskvin. Coordination Chemistry of the Actinides – Reviewed by A. M. Rozen	343	278
V. M. Gorbachev, Yu. S. Zamyatnin, and A. A. Lbov. The Principal Characteristics of Isotopes of the Heavy Elements – Reviewed by N. A. Vlasov	345	278
A. P. Zimon. Decontamination – Reviewed by O. M. Zaraev	346	279

The Russian press date (podpisano k pechati) of this issue was 2/25/1976. Publication therefore did not occur prior to this date, but must be assumed to have taken place reasonably soon thereafter.

ARTICLES

GAS-PHASE COMPOSITION IN THE FUEL RODS AT NOVYI VORONEZH NUCLEAR POWER STATION

A. T. Ageenkov, A. A. Buravtsov,
E. M. Valuev, L. I. Golubev,
Z. V. Ershova, V. V. Kravtsev,
and A. F. Skvoev

UDC 621.039

Gaseous and volatile fission products (krypton, xenon, tritium, and iodine) may be released from a nuclear fuel and penetrate into the volume of the fuel-free rod. The amount and composition of the gas are of interest from the viewpoint of fuel rod operation and subsequent fuel processing. Particular attention here is needed to the radioisotopes tritium, ^{85}Kr, ^{129}I, and ^{131}I.

We examined pins from two cassettes in the second section of this power station, which had worked, respectively, for 190 and 500 effective days at specific powers of 155 and 142 W/cm and which had been allowed to cool for two years and one year, respectively. We took pins from rows III and IV in the sets.

The mean burnup factors were 7500 and 19,100 MW-days/ton U, respectively. The calculated amounts of tritium and ^{85}Kr, corrected for decay, were respectively 0.1 ± 0.01 and 2.1 ± 0.2 Ci/pin for the first set and 0.24 ± 0.02 and 5.3 ± 0.4 Ci/pin for the second set.

The method consisted of piercing the sheath and determining the gas composition. First of all, the sets of pins were mechanically dismantled, the sheaths were checked for sealing, and the burnup factors were determined for the individual pins, for which purpose γ scanning was used to measure the ^{137}Cs content. The measured burnup differed from the calculated value by not more than 20%. The sheath was pierced at a distance of 80 mm from the lower end of the pin in a hot cell using a sealed piercer (Fig. 1),

TABLE 1. Trapped Gas Sampling

Collection conditions		Number of pins in (1st and 2nd cassettes)									
		48*	61	72	73	85	48*	61	72	73	85
After piercing sheath	Zeolite trap	+	–	–	+	+	+	–	–	+	+
	Manganese reactor	+	+	+	+	–	–	+	+	–	–
Flushing at: 40—50° C	No. of flushing cycles	2	2	1	2	1	1	2	1	2	2
	Flushing time, h	0,5 0,5	0,3 0,3	0,8	0,7 12	0,3	0,5	0,5 60	0,3	0,5 1,0	0,5 1,0
Flushing with heat treatment (200°C)	Zeolite trap	–	+	+	–	–	–	+	+	–	–
	Manganese reactor	–	–	–	+	+	–	–	–	+	+
	Flushing time, h	–	10	10	16	16	–	10	10	16	16

*No heat treatment; + and – denote trap and reactor present or absent.

Translated from Atomnaya Énergiya, Vol. 40, No. 3, pp. 203-206, March, 1976. Original article submitted August 28, 1975.

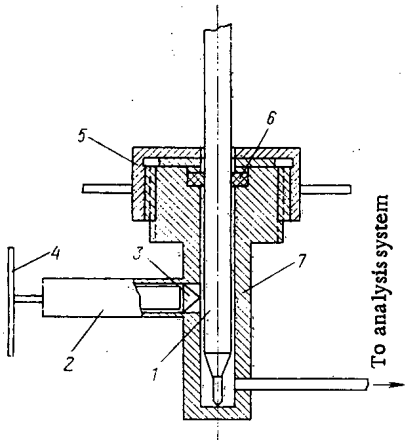

Fig. 1

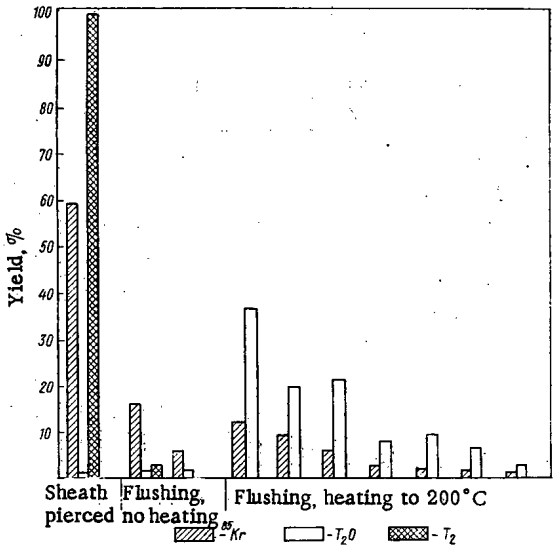

Fig. 2

Fig. 1. The sealed pin opener: 1) fuel pin; 2) shaft with bellows seal; 3) puncture needle; 4) handle; 5) pressure nut; 6) vacuum insert; 7) body.

Fig. 2. Distribution of ^{85}Kr, tritium, and tritiated water by operations.

which was heated to 100-120°C. The cavity in the pin opener was connected by a metal pipe to the gas effluent system in the working space. The gas from the opener was passed either through a zeolite absorber for water or else bypassed the absorber and went to a manganese reducer; the connecting pipe between the opener and the hydrogen generator was heated. The gas effluent system was fitted with a mercury pump, a rotary vacuum pump, gauges, and standard tubes. The pipework and working sections were evacuated to less than 0.1 mm Hg before piercing the pin. Gas was pumped into an ampoule by a mercury pump down to a pressure of 1 mm Hg, which corresponded to collecting over 95% of the gas. More complete gas recovery was provided by flushing the spaces with ordinary hydrogen at room temperature and at elevated temperatures. Hydrogen flushing without heating (pin temperatures of 40-50°C) was performed directly in the opener. The gas release at elevated temperatures was examined in an oven having 12 sealed 3-m channels (Table 1).

The gas was analyzed with an apparatus consisting of a KhL-3 gas chromatograph, a 5-cm^3 volume proportional counter containing a tungsten wire of diameter 50 μ, and appropriate electronic equipment.

A 1-ml volume gas sample was introduced into the chromatograph; the 3-m-length column contained CaA zeolite at 50°C, and the carrier-gas flow rate of 30 cm^3/min provided for separation of helium, hydrogen, krypton, and xenon, which were then passed sequentially through the proportional counter, which recorded the radioactivity due to the tritium and ^{85}Kr. Propane was supplied at a flow rate of 8 cm^3/min to the counter to provide for stable operation. The limits of detection for tritium and ^{85}Kr at the ±15% level were 10^{-9} Ci, while the corresponding limits for helium and hydrogen were 0.002 ml, and for the stable isotopes of krypton and xenon 0.03 ml/sample. The system was calibrated periodically on a standard gas mixture: H_e, H_2, tritium, and ^{85}Kr.

Checks were done immediately before the apparatus was set up in the hot cell; the equivalent was fitted with tubes containing gaseous tritium, tritiated water, and ^{85}Kr. The method collected 100% of the gaseous tritium and krypton and over 95% of the tritiated water. Tables 2 and 3 and Fig. 2 show the results with the irradiated pins. The total amount of gas was 14.5-21.1 cm^3. The chromatograph revealed helium and hydrogen in the gas. The helium constituted 65-95% by volume, and the hydrogen less than 32%. The contents of other stable isotopes were less than the limit of detection. Quantitative determinations were made for tritium and ^{85}Kr amongst the radioisotopes. Also, the counter detected a low activity ($1 \cdot 10^{-7}$-$1.2 \cdot 10^{-6}$ Ci/pin) of a gaseous compound, whose time of emergence lay between those for nitrogen and krypton. It was assumed that this compound was tritiated methane, but a check failed to confirm this.

TABLE 2. Amounts and Compositions of Gases in Pins

Content per pin	Number of pins in 1st and 2nd cassettes									
	48	61	72	73	85	48	61	72	73	85
Total gas cm^3	19,5	16,3	14,8	24,8	14,5	16,6	16,9	18,1	25,2	17,3
Helium, vol.%	82	89	85	65	95	95	90	91	84	83
H_2, vol.%	15	11	15	32	Not obs.	Not obs.	10	9	15	Not abs.
Gaseous tritium, $Ci \cdot 10^{-7}$	1,2	2,8	4,1	3,9	0,7	4,1	2,8	3,1	5,6	2,0
Tritiated water, $Ci \cdot 10^{-7}$	1,2	540	540	2000	2000	16	660	680	2400	2400
^{85}Kr, $Ci \cdot 10^{-3}$	2,7	1,8	3,0	3,5	3,4	1,9	2,3	3,4	5,4	11,0

The amounts of tritium and ^{85}Kr are of the most interest, along with the form of the tritium. The form taken by tritium in oxide fuel rods has not been discussed in the literature. The radiochromatograms indicated that the tritium is present in the gaseous state and as water. The gaseous tritium was identified from a comparison of the standard and sample gases. Water is a simple compound of hydrogen capable of being sorbed on solids at ordinary temperatures and being desorbed on heating. Figure 2 and Table 2 show that the gas collected on piercing the pins without heating contained mainly gaseous tritium ($7.0 \cdot 10^{-8}$-$4.1 \cdot 10^{-7}$ Ci), no matter whether the zeolite absorber was used or the manganese device. The first batch of gas at 40-50°C contains almost all the gaseous tritium, 58% of the krypton, and only 0.3% of the tritiated water. Flushing with hydrogen without heating yielded 4-13% of the krypton and about 1% T_2O. Heating a pin to 200°C produced a considerable release of T_2O (76% in the first three cycles) and also of krypton (23%). Subsequently (cycles 4-7), the release of ^{85}Kr remained at the background level (0.4-0.7%), while the T_2O continued to be released (5-7% per cycle). As there was a decreasing yield of tritiated water, one can assume that at this stage we had collected not less than 70% of the tritium sorbed as water in the fuel. A higher temperature is required to release the tritiated water completely.

The amounts of tritium and ^{85}Kr go with the calculated values to indicate that the gas from these pins contains only small proportions of these isotopes (0.12-0.27 and 0.06-0.28%, respectively). The fuel releases only a low proportion of the volatile fission products because of the comparatively low temperature during irradiation. It has been reported [1, 2] that the release becomes appreciable at the growth temperature for columnar UO_2 crystals (above 1600°C). The temperatures of the fuel pins at this power station were much lower (less than 1400-1500°C) because it has been found [3] that there were no columnar grains on examining the fuel rods.

The composition of the gas phase has thus been examined for these fuel pins for burnup factors of 7500 and 19,000 MW-day/ton U. The amount of gas in a pin is 14.5-21.1 cm^3 NTP (95% confidence range). The main components by volume are helium (65-95%) and ordinary hydrogen (less than 32%). The radioisotopes were ^{85}Kr and tritium in gaseous form and as water, the latter being the main form of tritium in these pins (99%). Unheated pins (40-50°C) released $2\text{-}8 \cdot 10^{-4}$% of the tritium and 0.04-0.13% of the ^{85}Kr;

TABLE 3. Yields of Gaseous Fission Products in Gas from VVÉR Pins at 200°C

Fission products	Mean ($\bar{X}$)	$S = \sqrt{\frac{\Sigma (X_i - \bar{X})^2}{n-1}}$ SD	95% confidence range
Gas volume:			
cm^3 per 1 pin	18,4	3,8	$14,5 \leqslant \bar{X} \leqslant 21,1$
cm^3 per 1 g U	$1,7 \cdot 10^{-2}$	$3,6 \cdot 10^{-3}$	$1,4 \cdot 10^{-2} \leqslant \bar{X} \leqslant 2,0 \cdot 10^{-2}$
^{85}Kr, Ci	$3,5 \cdot 10^{-3}$	$1,2 \cdot 10^{-3}$	$2 \cdot 10^{-3} \leqslant \bar{X} \leqslant 4 \cdot 10^{-3}$
Water (tritium), Ci	$2,2 \cdot 10^{-4}$	$4,0 \cdot 10^{-5}$	$2 \cdot 10^{-4} \leqslant \bar{X} \leqslant 2,3 \cdot 10^{-4}$
Hydrogen (tritium), Ci	$3,5 \cdot 10^{-7}$	$3,6 \cdot 10^{-7}$	$1,0 \cdot 10^{-7} \leqslant \bar{X} \leqslant 6,2 \cdot 10^{-7}$

the corresponding figures for heating to 200°C are 0.05-0.1% and 0.1-0.2% of the total amounts. No effect from the extent of burnup on the yield of gaseous fission products was found in the presence of the fluctuations in these values.

LITERATURE CITED

1. B. Lastman, Radiation Effects in Uranium Dioxide [Russian translation], Atomizdat, Moscow (1964), p. 145.
2. R. Carroll, Nucl. Safety, 10, No. 3, 210 (1969).
3. V. Ya. Gabeskiriya et al., At. Énerg., 30, No. 3, 247 (1971).

SPATIAL NONUNIFORMITY OF FUEL BURNUP IN VVÉR REACTORS

L. I. Golubev, L. I. Gorobtsov,
G. A. Kulakov, V. D. Simonov,
and M. A. Sunchugashev

UDC 621.039.516.22

The fuel component in the cost of the electrical power from a nuclear station is reduced as the mean burnup increases; an effective way of increasing the mean burnup is to reduce the spatial nonuniformity in the burnup. This has required a detailed study of the burnup in the VVÉR reactors at Novyi Voronezh nuclear power station in order to establish the effects of various factors on the nonuniformity in height and section of cassettes. The data substantially supplement and refine calculated characteristics and provide a basis for improved structure in reactor cores.

Research Methods and Choice of Isotopes. The burnup nonuniformity was examined via the spatial distribution of the fission-product concentration, as measured by γ spectrometry with a Ge(Li) detector and a multichannel pulse-height analyzer.

We used ^{137}Cs, ^{134}Cs, and ^{106}Ru – the basis for choosing these isotopes [1, 2] being briefly as follows:

1. The amount of ^{137}Cs produced is directly proportional to the burnup, so the distribution of ^{137}Cs characterizes the nonuniformity in burnup.
2. The yield of ^{106}Ru from ^{239}Pu is almost 12 times that of ^{235}U, so the distribution of ^{106}Ru can characterize the burnup of ^{239}Pu.
3. ^{134}Cs is formed mainly by activation of ^{133}Cs (the direct yield of ^{134}Cs in fission is negligible). Therefore, the amount of ^{134}Cs formed is proportional to the square of the integral neutron flux [2].

The areas of the photoelectric peaks for these isotopes were measured by channel summation, with subtraction of a linear approximation for the γ background. We processed the peaks for ^{137}Cs, ^{106}Ru, and

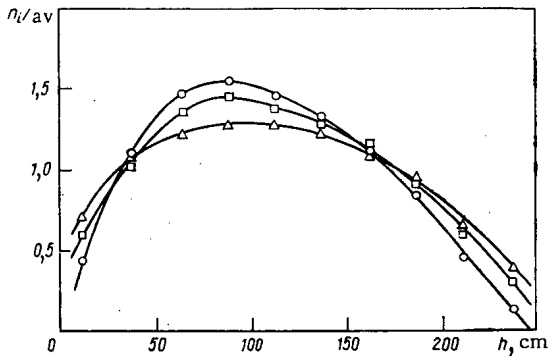

Fig. 1

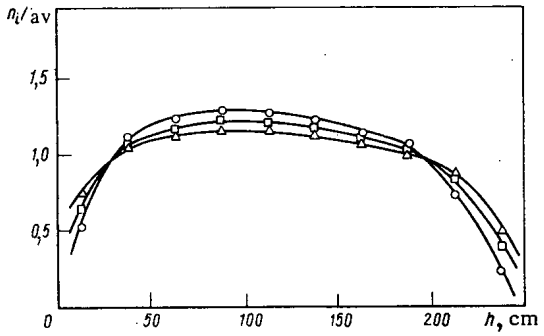

Fig. 2

Fig. 1. Relative distributions of ^{137}Cs (Δ), ^{106}Ru (□), and ^{134}Cs (○) over the height of a cassette in the first section of the Novyi Voronezh nuclear power station.

Fig. 2. Relative distributions of fission products over the height h of a cassette in the second section (symbols as Fig. 1).

Translated from Atomnaya Énergiya, Vol. 40, No. 3, pp. 207-210, March, 1976. Original article submitted January 3, 1975; revision submitted October 1, 1975.

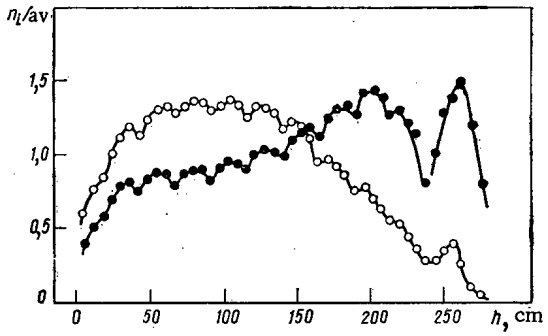

Fig. 3. Relative distribution of the thermal-neutron flux over the height h of the reactor core in the second section: ○) at start of cycle; ●) at end.

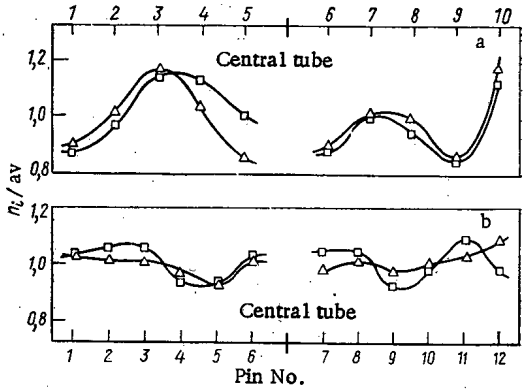

Fig. 4. Relative distributions of: Δ) ^{137}Cs; □) ^{106}Ru over a cassette in: a) first section; b) second section.

^{134}Cs at energies of 661.6, 622.1, 604.7, and 796 + 801 keV, respectively. The errors of measurement for these did not exceed 3% for ^{137}Cs and ^{134}Cs, or 5% for ^{106}Ru. The data were processed with a Nairi computer.

Spatial Distribution of the Burnup in a Cassette. This was determined from the γ spectra for the individual pins; the measuring equipment has previously been described [1].

Each pin was measured at 10 equally separated points along the length (at 25-cm intervals). This gave the fission-product distribution. We made measurements on 20 pins from the cassettes. The fission-product distribution in the cross section of a cassette was constructed from the mean contents for each pin; similarly, the distribution over the height of a cassette was obtained by averaging the height distributions for all the rods.

We characterize the distributions via the nonuniformity factors k_z (height) and k_d (diameter), which were determined as the ratios of the maximum areas for the photoelectric peaks to the mean values:

$$k_z = \frac{S_{z\,\max}}{S_{z\,\mathrm{av}}};\quad k_d = \frac{S_{d\,\max}}{S_{d\,\mathrm{av}}}.$$

Height Distribution of Burnup. Figure 1 shows the distributions of ^{137}Cs, ^{106}Ru, and ^{134}Cs for the first block at this power station as obtained by averaging for 20 pins. The calculated mean burnup [3] for this cassette was 17.5 kg/ton U, which agrees satisfactorily with the observed 18.9 ± 2.6 in the same units [1]. These distributions gave the following results: k_z = 1.30 ± 0.02; 1.46 ± 0.05; 1.56 ± 0.05, respectively. The nonuniformity for ^{137}Cs agreed well with the calculated value k_z = 1.29.

The maximum burnup occurred at 80-110 cm from the bottom (Fig. 1), i.e., below the middle of the core; this shift was due to the effects of the control cassettes.

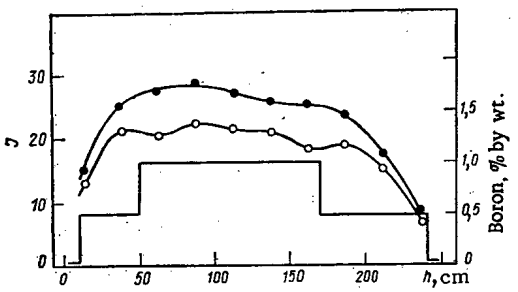

Fig. 5. Relative distribution of ^{137}Cs over the height h of pins: ●) No. 1; ○) No. 4; and –) boron content in rod.

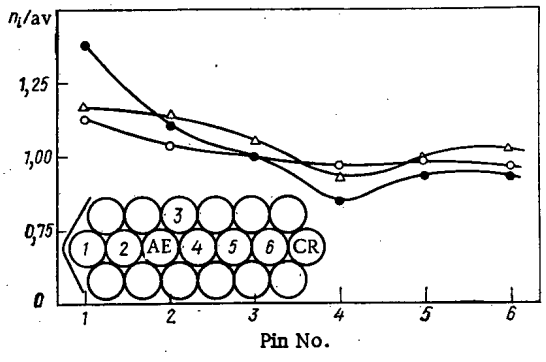

Fig. 6. Radial distribution of heat output in cassette containing boron rod for degrees of burnup (kg/ton U): ●) 0.0; Δ) 9.6; ○) 22.

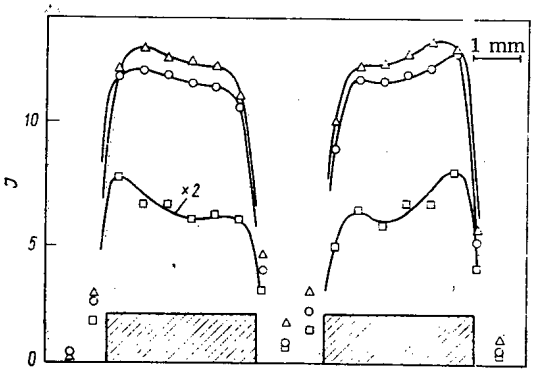

Fig. 7. Relative fission-product activities I over the diameter of specimen No. 1 for a burnup of 19.3 kg/ton U: Δ) ^{137}Cs; □) ^{106}Ru; ○) ^{134}Cs.

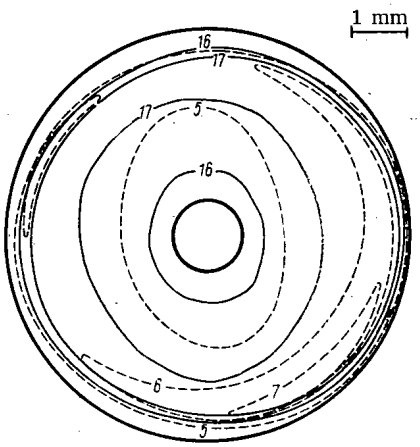

Fig. 8. Relative distributions of ^{137}Cs (——) and ^{106}Ru (– – –) over the cross section of specimen No. 2 at a burnup of 32.2 kg/ton U (the numbers denote the lines of equal activity).

Figure 2 shows the similar distributions for the second set (calculated burnup 19.1 kg/ton U, observed 22.6 ± 2.4). The nonuniformity was appreciably less in this case: k_z = 1.17 ± 0.01, 1.23 ± 0.02, 1.30 ± 0.02 for ^{137}Cs, ^{106}Ru, and ^{134}Cs, respectively, because this section had much of the excess reactivity balanced by boric acid dissolved in the coolant, so almost all the solid absorbers were completely removed from the core during operation at full power. The maximum burnup here was also somewhat shifted towards the bottom, but less so; however, during the running time the maximum power release shifted to the upper part of the cassettes, as is clear from Fig. 3, which shows the height distributions of the thermal-neutron fluxes at the start and end of a run, which were determined from the activation of copper wires in the measurement channel (second section). Local minima seen in Fig. 3 reflect the effects of the stainless-steel spaces on the neutron flux.

Burnup Distribution over the Cassette Cross Section. The cores of the VVÉR had various features responsible for nonuniform burnup distribution over the cross section. These include water gaps at the outside and center of the cassette, adjacent cassettes differing in enrichment and burnup, and the control units.

Figure 4 shows the distributions of ^{137}Cs and ^{106}Ru for both units at this power station; the distribution over the diameter for the first unit shows increased burnup in pins Nos. 3, 7, and 8, which are furthest from the water gaps, and also in pin No. 10, which is closer than the others to the emergency-shutdown rod. This nonuniformity is due to variation in the neutron spectrum hardness over the cross section.

In the second unit, where the water contained boron, the burnup was more uniformly distributed over the cassette.

Effects of Absorbing Elements on the Burnup Distribution. The absorbing elements in this reactor are used to compensate the excess reactivity and consist of zirconium rods containing boron; they are placed amongst the fuel pins in the cassettes. The boron is unevenly distributed along the length of the rod.

Figure 5 shows the ^{137}Cs distribution for pin No. 4, which is next to an absorbing rod, and also for pin No. 1, which is far from that rod (see Fig. 6). Although the burnup distribution in No. 4 is more uniform than that in No. 1, the extent of burnup in No. 4 is less by 20%.

The absorbing rod produces considerable nonuniformity in the distribution over the cross section (Fig. 6). This is one reason for abandoning the use of such rods.

Fission-Product Distribution in a Pin Cross Section. We examined this aspect of the fuel burnup within a pin also, for which purpose we made up a special system consisting of a lead castle in which there

was a collimator, a fitting column for the container holding the specimen, and a displacement mechanism, which moved the specimen relative to the collimator slit in diameter and azimuth. The measurements were made with a tungsten slot collimator of length 70 mm and a slot size 0.3 × 0.6 mm.

We examined the fission-product distribution over the cross section for two specimens from one of the cassettes in the second unit. The specimens were epoxide-resin impregnated pieces of pin of height 5 mm, which were cut from parts with different degrees of burnup (calculated value 19.3 kg/ton U for No. 1 and 32.2 kg/ton U for No. 2).

Figure 7 shows the fission-product distribution over one of the diameters for No. 1; there is a fall from the edge to the center, which indicates self-screening. The nonuniformity factor averaged over six diameters was 1.08 for ^{137}Cs, as against 1.25 for ^{106}Ru. The ^{106}Ru distribution monitors the burnup of ^{239}Pu, and it indicates the self-screening for the resonant-neutron flux, since ^{239}Pu is formed mainly by capture of resonant neutrons by ^{238}U. The nonuniformity for No. 2, which had the higher burnup, was of the same type as for No. 1, but less pronounced: k_d for ^{137}Cs and ^{106}Ru were 1.05 and 1.21, respectively, which is clearly due to the reduced self-screening for the thermal neutrons as the extent of burnup increases.

Figure 8 shows the fission-product distribution in the cross section for No. 2 (these curves were constructed in the same way as those of [5]). There is an azimuthal nonuniformity in the distributions of ^{137}Cs and ^{106}Ru, being more pronounced for the latter.

CONCLUSIONS

1. The cassettes of the VVÉR show considerable nonuniformity in burnup over the height and cross section; this tends to decrease as the general burnup increases.

2. Absorbing elements reduce the nonuniformity in the height distribution somewhat, but increase the nonuniformity over the cross section of the cassette and substantially reduce the extent of burnup in adjacent fuel pins.

3. Boron control produces substantially less nonuniformity in burnup both in height and cross section.

4. There is considerable nonuniformity in burnup across the cross section of a fuel pin on account of self-screening; there is also appreciable azimuthal asymmetry in burnup in a pin, which is particularly prominent for ^{239}Pu, as is clear from the distribution of ^{106}Ru.

LITERATURE CITED

1. O. A. Miller et al., At. Énerg., 27, No. 4, 281 (1969).
2. O. Eder and M. Lammer, in: Proc. IAEA Symp; "Nuclear Data in Science and Technology," Vienna, 1, 233 (1973).
3. V. D. Sidorenko and E. V. Belyaeva, Institute of Atomic Energy (IAE) Preprint 29/895 (1966).
4. A. V. Sukhikh et al., At. Énerg., 32, No. 4, 318 (1972).
5. A. N. Kamyshan et al., Institute of Atomic Energy (IAE) Preprint 9/774 (1968).

OBSERVATION OF VACANT POROSITY IN METALS UPON THEIR IRRADIATION BY ACCELERATED IRON IONS

G. N. Flerov, V. S. Barashenkov,
S. Ya. Lebedev, G. N. Akap'ev,
V. E. Dubinskii, V. G. Rodionova,
S. I. Rudnev, and S. Ya. Surkov

UDC 621.039.53

Investigations of construction materials subjected to irradiation in reactors with large total fluxes of rapid neutrons at high temperatures have shown the formation of vacant porosity, which is accompanied by an increase in the dimensions (swelling) of these materials [1, 2, 3]. Such swelling (it amounts to 7% for 304 stainless steel at a total rapid neutron flux of $7.8 \cdot 10^{22}$ neutrons per square centimeter and an irradiation temperature of 500°C) causes very serious problems for the designers of power reactors using rapid neutrons.

Since the fluxes of rapid neutrons in operating reactors do not exceed 10^{15} neutrons/(cm^2 · sec), it is necessary, in order to obtain a noticeable effect, to irradiate the sample being investigated for a year and more, which significantly complicates the study of the swelling phenomenon. One can also observe the process of the formation of vacant porosity during the bombardment of a material by accelerated ions. There is no fundamental difference in the action of neutron irradiation and ion beams on construction materials, since in both cases there occurs, as a result of the primary act of radiation damage, a displacement of an atom in the crystalline lattice of the irradiated material, which produces a cascade of successive displacements of other atoms. This process continues as long as the atoms expelled in preceding collisions can transmit in succeeding collisions with atoms at rest an energy exceeding the displacement energy.

Neutrons of a reactor's active zone directly cause displacement, on the average, in less than 10% of the total number of atoms participating in a collisional cascade. The remaining 90% of the atoms undergo displacements in the succeeding stages of the cascade [4].

Due to the large cross sections of the elastic interaction of an ion with the target atoms, the rate of creation of defects in a material irradiated by heavy ions is higher by several orders of magnitude than in a material irradiated by an equivalent neutron dose [10^{-6} displacements/(atom · sec) in a reactor, 10^{-3} displacements/(atom · sec) in an accelerator]. Therefore, an observable porosity can be achieved in the case of ion irradiation in only a few hours.

However, one should note that the rate of creation of radiation defects should not be too great: those diffusion processes that take place during extended irradiation in a reactor should have time to occur in the target during its irradiation in the accelerator. This requirement is evidently fulfilled only at rather high temperatures of the irradiated target, since the diffusion coefficients of point defects grow rapidly with a temperature increase.

The main difference in irradiation by neutrons and ions consists of the fact that because of the small collisional cross section of a neutron with the atom of a lattice, $\sim 10^{-24}$ cm^2, and the large mean free path, neutrons create displacements distributed practically uniformly throughout the entire volume of the irradiated material, whereas in the case of irradiation by heavy ions displacements of atoms occur only in a thin surface layer of the target, whereby the degree of destruction of the crystalline lattice varies with depth even in this thin layer.

Translated from Atomnaya Énergiya, Vol. 40, No. 3, pp. 211-215, March, 1976. Original article submitted May 21, 1975.

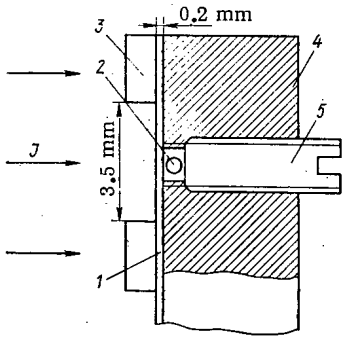

Fig. 1

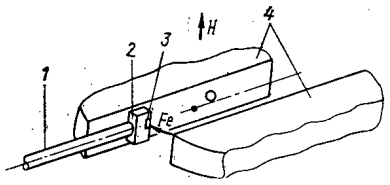

Fig. 2

Fig. 1. Target element: 1) target; 2) thermocouples; 3) cover plate; 4) target holder; 5) screw.

Fig. 2. Layout of the target arrangement inside the chamber of the U-300 cyclotron: 1) probe; 2) copper shield; 3) input window; 4) the cyclotron dees; H is the magnetic field.

In the case of ion irradiation the possibility arises of studying separately the dependence of pore formation on the content of gaseous atom impurities and on the degree of destruction of the crystalline lattice, which it is impossible to accomplish in the case of irradiation in a reactor.

It is easy to provide in the case of ion irradiation accurate control and constancy of the samples' temperature, which is especially important, since the investigations of construction materials irradiated in rapid reactors have shown that the range of irradiation temperature at which radiation porosity arises is comparatively small: 0.25-0.6 T_{melt}°K [3].

An important advantage of irradiation by heavy ions consists also of the fact that the samples are not activated: this significantly simplifies the work with such samples and also speeds up the acquisition of the necessary information.

An inadequacy of the method of simulating radiation defects with the help of beams of heavy ions is the extremely limited number of techniques with whose help one can study the structure and properties of a material, which is explained by the small thickness of the layer in which the defects created by the ion beam are concentrated. In practice, electron microscopy has proven to be the only suitable technique.

The goal of this paper is the investigation of the possibility of using accelerators of multiply charged ions to simulate the radiation defects of reactor construction materials produced by rapid neutrons.

The experiments were conducted with the U-300 accelerator of the Nuclear Research Laboratory of the Joint Institute for Nuclear Research, which permits obtaining intense beams of heavy ions of all the elements right up to xenon.

The sources developed in the Nuclear Research Laboratory of the Joint Institute for Nuclear Research make it possible to create intense beams of multiply charged ions not only in the case of elements which form gaseous compounds but also in the case of solid materials [5, 6]. Just this kind of source with a solid material was used in the present work to obtain iron ions.

Requirements on the Ion Beam. The ion beam should alter the chemical composition of the irradiated material as little as possible in the simulation of the radiation defects of reactor materials. In particular, one should avoid irradiation by the ions of those elements which, entering into the sample, form insoluble precipitates or compounds in it. The formation of insoluble phases can significantly alter the damaged state of the metal or alloy being investigated. Compounds formed by the light elements B, C, N, and O are the most critical in this respect in the case of the irradiation of metals. It is undesirable to use ions of the inert gases, since they have exceedingly low solubility in metals, and the formation of bubbles occurs in the case of supersaturation, especially at high temperatures, when the mobility of interstitial gas atoms is high.

And so it is desirable in the simulation of radiation swelling to carry out the irradiation of pure metals with ions of the same kind as the irradiated target and of alloys with ions of the element making

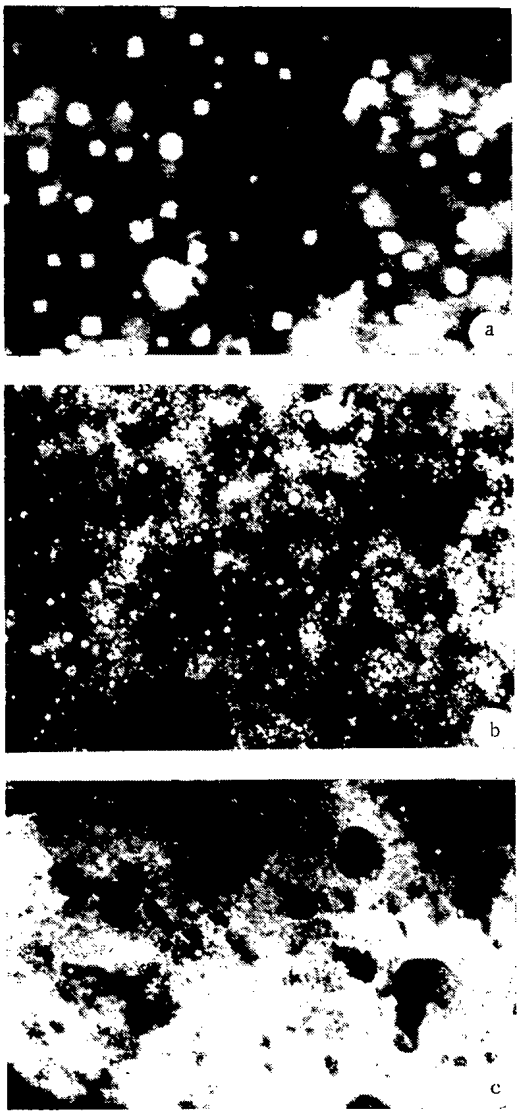

Fig. 3. Electron microscope micrographs of irradiated samples of a) nickel, b) 1Kh18N9T steel, and c) 0Kh16N15M3B steel. (×135,000).

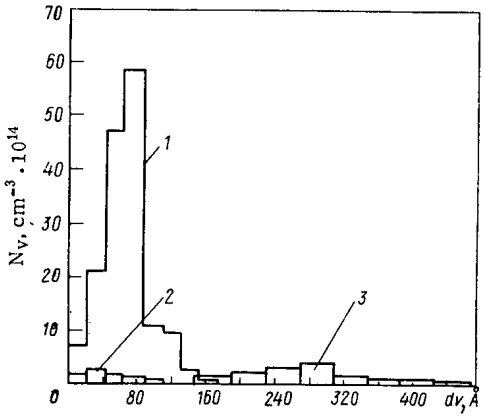

Fig. 4. Distribution of the number of pores per unit volume as a function of diameter: 1) 1Kh18N3T steel; 2) 0Kh16N15M3B steel; 3) nickel.

up most of the given alloy in order to provide for the best correspondence to the samples irradiated in a reactor.

The investigation of pore formation in metals [7] irradiated in reactors and by an accelerator has shown that in some cases the regions adjacent to the surfaces of samples do not contain pores. Such regions are spread over a depth of the order of 1000 Å. One should take account of this fact in the simulation; therefore, it is necessary to use ions having an energy sufficient for the predominant creation of radiation defects at a depth exceeding several thousands of angstroms.

The application of ions of low energies ~100 keV is of definite interest [8, 9, 10]; however, it is possible to derive only a qualitative trend, and quantitative relations are sought due to the damaged layer's nearness to the sample's surface and the nonuniformity in the depth distribution of displacements.

In the experiments which were conducted an internal (not separated out from the accelerator) beam of triply charged iron atoms $_{56}Fe^{+3}$ was used at a radius of R = 57.* The energy of the ions at this radius is E(R) = 2.08·10^{-3}, and R^2 = 6.8 MeV, which corresponds to an average mean free path in nickel of 1.5 microns.

Experimental Procedure. The target design should provide for obtaining the maximum number of displacements per atom in the region of the displacement peak, measurement of the irradiation dose, and control and maintenance throughout the entire experiment of a specified temperature of the sample being irradiated. Since the heat liberated by the ion beam at the target is completely sufficient to heat it up to the necessary temperature, additional heating is not required. The amount of heat transfer was varied in accordance with the size of the radiating surface of the target holder. In order to increase the density of the ion flux at a specified temperature, it is advisable to use not the limiting energy of ions in the cyclotron but a lower energy of several MeV, for which one should locate the target inside the cyclotron at a small radius. A decrease in the ion energy results in an increase in the number of displacements per atom also at the peak due to a smaller scatter in the mean free path.

One of the four target elements used is shown in Fig. 1. The sample 1 in the form of foil with a thickness of 200 microns was held between the holder 4 and the cover plate 3. The temperature was

* This amounts to ~1/3 of the maximum orbital radius of ions in the U-300 accelerator.

TABLE 1. Chemical Composition of the Nickel Foil

Element	Content, mass %	Element	Content, mass %
Ni	99,9	Co	$3 \cdot 10^{-3}$
Mg	$2 \cdot 10^{-2}$	Mo	10^{-3}
Si	$2 \cdot 10^{-2}$	Cr	$6 \cdot 10^{-3}$
Cu	$1,7 \cdot 10^{-2}$	Sb	$3 \cdot 10^{-3}$
Fe	$2 \cdot 10^{-3}$	Mn	$1,7 \cdot 10^{-4}$

TABLE 2. Results of the Calculation of Pore Characteristics Based on the Histograms Obtained

Material	$\frac{\Delta V}{V}$, %*	N_v, cm^{-3}	$\langle V \rangle$, cm^3†	$\langle d_v \rangle$, Å‡	$\langle \tilde{d}_v \rangle$, Å**
1Kh18N9T steel	1,01	$1,6 \cdot 10^{16}$	$6,25 \cdot 10^{-19}$	74	106
0Kh16N15M3B steel	0,015	$4,8 \cdot 10^{14}$	$3,1 \cdot 10^{-19}$	50	84
Nickel	2,5	10^{15}	$2,5 \cdot 10^{-17}$	290	310

*Amount of swelling.
†Average pore volume.
‡Average pore diameter for spheres or the average value of the interplanar spacing for square grains of cubo-octahedrons of the type (100).
**Corresponding size of a pore of average volume.

measured with the aid of a Chromel–Alumel thermocouple 2 in a case 0.5 mm in diameter attached to the foil by a screw 5.

The current in the ion beam was measured by an integrator. The target itself, reliably isolated from ground, was used as the collector. The resistance of the target's isolation significantly exceeded the integrator's input resistance at all working temperatures.

The use of the target as the collector became possible due to the presence of the cyclotron's strong magnetic field, which prevents the emergence of secondary electrons from the target.

Since the accelerating high-frequency voltage creates strong electromagnetic inductions, the target was covered on all sides by a water-cooled copper shield. The beam was incident on the target through an aperture (input window) in a tantalum diaphragm attached to the copper shield.

The design of the collector permitted constant control of the absolute value of the beam's current.

The sample prepared for irradiation was placed into the holder (see Fig. 1) and attached at the end of a special device — a probe, which was introduced through a vacuum lock to within the cyclotron into a space between the dees (Fig. 2). Shifting the probe with respect to radius and also the smooth regulation of the ion beam's intensity from the cyclotron's control panel permitted the exact establishment of the irradiated sample's temperature and maintaining it within specified limits. The temperature was measured by four Chromel–Alumel thermocouples and controlled from the cyclotron panel.

The solid source of iron ions operated stably for many hours, providing a total ion flux no less than $3 \cdot 10^{16}$ ions/($cm^2 \cdot h$).

At a current density of 3-4 $\mu A/cm^2$ the target's temperature was 500°C. The irradiation was carried out for 2-4 h, during which 20 displacements/atom arose in nickel and 40 displacements/atom in the steels.

For investigation by an electron microscope the irradiated samples must be prepared in the form of thin foils (thickness of 0.05-0.1 μ), have almost parallel sides, and have a clean surface [11]. The latter requirement is especially important, since a thin layer of amorphous material not producing contrast can, upon scanning, sharply reduce the sample's transparency because of a strong diffusive scattering of the electrons.

Rolled foils 200 μ thick of nickel and of 1Kh18N9T and 0Kh16N15M3B steels were selected as the initial materials (Table 1).

Strips 10 × 25 mm in size were cut out of the foils, which were subjected to electrical polishing in an electrolyte composed of a mixture of orthophosphoric acid (88%) and chrome anhydride (12%) in order to impart the necessary degree of smoothness to the surface. The chemical composition of the electrolyte, the electrical conditions, and the polishing time were established by experimental means. The quality of the surface was checked with an MIM-7 optical microscope.

In order to remove the internal stresses and regulate the material's structure, the strips were subjected to recrystallization annealing in a vacuum (10^{-5} torr) for 1 h at a temperature of 800°C for nickel and 1100°C for the steels. The average size of the grains after annealing was 15-20 μ in the steels and in the nickel.

As is well known, the development of vacant porosity occurs in a narrow layer ~500 Å thick. It is necessary to remove a layer 1.5 microns thick by electrical polishing in order to attain regions having the maximum displacement density.

The amount of etched material was determined by the gravimetric method, after which samples 3 mm in diameter, which were thinned down to a thickness of 1000-1500 Å, were cut out of the irradiated foil. This thinning down was conducted in two stages: First, the samples were subjected to polishing in a silver–phosphoric electrolyte, and then they were finally brought to the necessary thickness in a phosphorochrome electrolyte. After thinning, the samples were scanned with the electron microscope.

Results of the Measurements and Discussion of Them. Typical microphotographs of the samples of nickel and 1Kh18N9T and 0Kh16N15M3B steels are shown in Fig. 3. The pores in the nickel are far larger and have faceting. Their shape is close to a cubo-octahedron. The shape of the pores in the steels is spherical within the limits of the microscope's resolution. Depleted zones 900 Å in width are observed near the boundaries of the grains [7]. In addition, segregations are observed which appear in the dark field and give reflections upon electron diffraction.

Histograms of the distribution of the number of pores per unit volume N_V as a function of their diameter are given in Fig. 4. The results of calculations based on these histograms are presented in Table 2.

It is obvious from Table 2 that the swelling of 0Kh16N15M3B steel is less at an irradiation temperature of 500°C by two orders of magnitude than for the other materials investigated. The temperature of the samples is close to the lower swelling boundary [3].

Following the papers [12, 13], one can find that the swelling of materials in a power reactor at a temperature of ~400°C corresponds to the experimental conditions described above.

If the relatively small swelling of 0Kh16N15M3B steel is observed at other temperatures and total fluxes $\sim 10^{23}$ neutrons/cm^2, then one could regard the indicated steel as a very promising construction material for reactors using rapid neutrons.

The authors are grateful to Yu. P. Tret'yakov for providing for the reliable operation of the ion source during irradiation of the metals.

LITERATURE CITED

1. S. Pugh, M. Loretto, and D. Morris, in: Proc. BNES Reading Europ. Conf. on Voids Formed by Irradiation of Reactor Materials, Harwell, March 24-25 (1971).
2. J. Corbett and L. Janiello, in: Proc. AEC Symp. "Radiation-induced voids in metals," New York, June 9-11, Conf.-710601.
3. D. Norris, Radiation Effects, 14, 15 (1972).
4. G. Kulcinski et al., Nucl. Instrum. and Methods, 94, 365 (1971).
5. Yu. P. Tret'yakov et al., Preprint P7-4477 of the Joint Institute for Nuclear Research, Dubna (1969).
6. A. S. Pasyuk and Yu. P. Tret'yakov, Preprint P7-6668 of the Joint Institute for Nuclear Research, Dubna (1972).
7. J. Brimhall and B. Mastel, J. Nucl. Mater., 33, 186 (1969).
8. S. Ya. Lebedev and S. D. Panin, Pribory i Tekh. Éksperim., No. 3, 179 (1973).
9. S. Ya. Lebedev, S. D. Panin, and S. I. Rudnev, At. Énerg., 39, No. 5, 362 (1975).
10. V. I. Krotov, S. Ya. Lebedev, and V. N. Bykov, At. Énerg., 37, No. 4, 343 (1974).
11. P. Khirsh and A. Khovi, Electron Microscopy of Thin Crystals [in Russian], Mir, Moscow (1968).
12. S. Golubov, Yu. Konobeev, and A. Subbotin, Phys. Solid State, 18, No. 2, 81 (1973).
13. S. Ya. Lebedev, S. D. Panin, and S. I. Rudnev, At. Énerg., 38, No. 6, 426 (1975).

ÉLV-1 ELECTRON ACCELERATOR FOR INDUSTRIAL USE

G. I. Budker, V. A. Gaponov,
B. M. Korabel'nikov, G. S. Krainov,
S. A. Kuznetsov, N. K. Kuksanov,
V. I. Kondrat'ev, and R. A. Salimov

UDC 621.384.654

Type ÉLV accelerators have been designed at the Institute of Nuclear Physics of the Siberian Branch of the Academy of Sciences of the USSR in 1971-1973 for general use as high-power radiation sources. The pilot model of an ÉLV-1 accelerator satisfactorily passed long-term tests (several thousands of operating hours), has been recommended for industrial applications by an Interdepartmental Commission, and accepted for mass production.

Operating Principles and Circuit of Accelerator. The accelerator (Fig. 1) consists of an accelerating voltage generator, an accelerator tube mounted inside the generator, a system for extracting the accelerated electron beam into the atmosphere, and electrical supply, measuring, and control circuits. The generator with the accelerator tube is located in a boiler filled with gas at a pressure of 4-6 kgf/cm^2. The beam accelerated in the tube is swept by the deflection system in two mutually perpendicular directions and is extracted into the atmosphere through a rectangular titanium window. The accelerating voltage generator is a step-up transformer with a sectional secondary winding. The alternating voltage induced in secondary sections is converted into dc voltage by a full-wave, voltage-doubler rectifying circuit. The secondary sections are connected in series with respect to dc and are isolated from each other with respect to ac. A chain of 24 rectifying sections is loaded onto the accelerator tube with a voltage divider. The transformer primary is fed from a VPL-50 inverter whose output voltage does not exceed 208 V at 388 Hz.

Capacitors C_2 and C_3 are used to match the VPL-50 inverter to the accelerating voltage generator. The top coil supplies the heater and anode circuits of the injector, and the voltage divider is used for measuring the accelerating voltage.

The specifications of the ÉLV-1 accelerator are listed below.

Energy range of accelerated electrons, keV	400-1000
Electron beam power over the entire energy range, kW	20
Accelerating voltage ripple over load, %	2.5
Total loss in accelerator, kW	3.5
Dimensions of exit window, mm:	
length	980
width	75
Dimensions of accelerator including the vacuum and deflection systems, mm:	
height	3.8
width	1.6
Mass, tons	8

Accelerating Voltage Generator. The primary winding and rectifying sections, whose coils are parts of the secondary winding of the step-up transformer, are mounted inside the boiler (Fig. 2) on a disk-shaped magnetic circuit. The primary winding is a Textolite form wound on the inside with a twin, 12-mm copper tube which carries cooling water. To improve coupling with rectifier coils, the primary winding (W = 30) has a conical form. On the high-voltage side, the primary winding turns are covered with a split,

Translated from Atomnaya Énergiya, Vol. 40, No. 3, pp. 216-220, March, 1976. Original article submitted May 26, 1975.

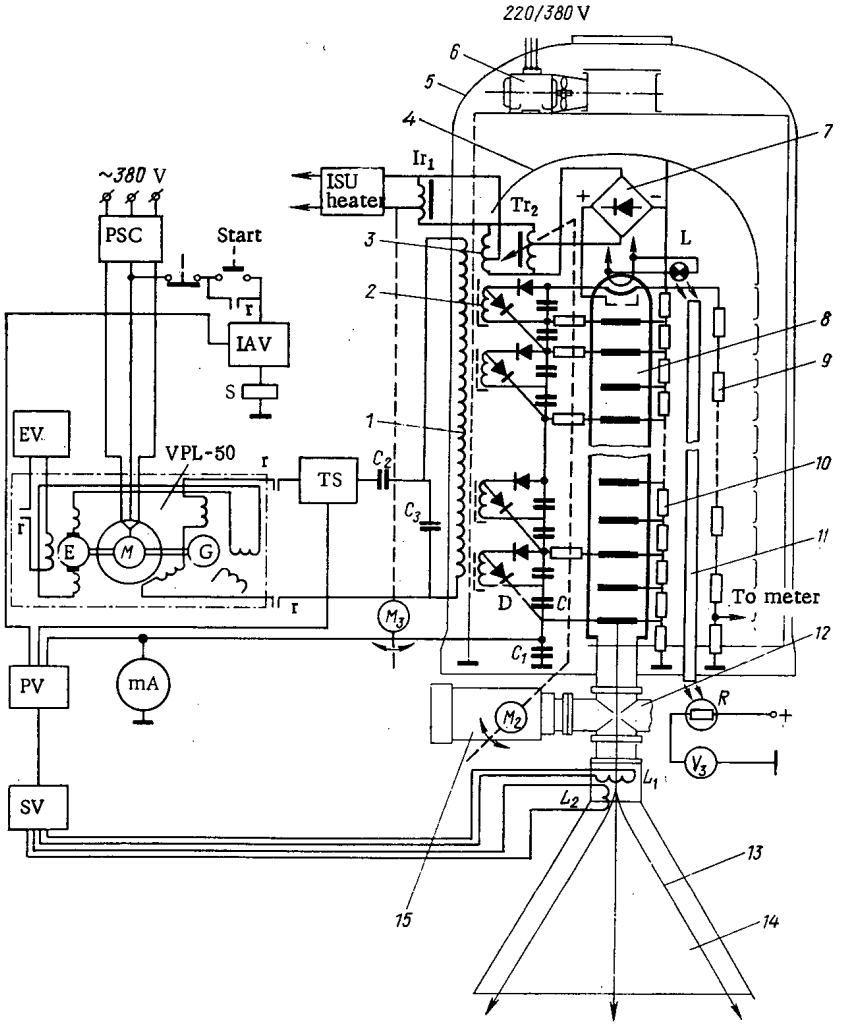

Fig. 1. Electrical circuit of accelerator: 1) primary winding; 2) rectifying section; 3) top coil; 4) high-voltage electrode; 5) boiler; 6) fan; 7) anode voltage supply; 8) accelerator tube; 9, 10) generator and tube voltage dividers; 11) light guide; 12) adapter; 13) beam; 14) funnel; 15) vacuum pump; SU) sweep unit; IAU) interlock and alarm unit; R) photoresistor; L_1 and L_2) sweep coils.

stainless-steel shield. The rectifying sections, stacked one above the other into one pile, are covered by the bottom end of the high-voltage electrode which carries the top coil, two variable transformers of the beam current control circuit, and the injector power supply. The output voltage of the variable transformers is controlled by means of two control shafts. Electrostatic shielding of the high-voltage end of the rectifier column is provided by a hemispherical high-voltage electrode with radial grooves on its outside casing. To reduce the diameter of the installation and the eddy current loss in the boiler walls, the generator has two ring- and disc-shaped magnetic circuits made of É-43 transformer steel and radially stacked. The ring-shaped magnetic circuit is covered with a metal shield on which the fan is mounted.

In addition, the generator is fitted with resistive divider for measuring the total accelerating voltage, mounted beside the accelerating tube, and with a device for controlling the injector heater current (see Fig. 1, items 9 and 11).

Rectifier Section (Figs. 3 and 4). All rectifier section components are mounted on a split metal rim with three Textolite segments fastened to it. Supporting inserts used for joining and centering the sections are cemented to the segments. The coil is mounted on a sliding strip and is covered with a split external shield. The coil consists of 3130 turns of 0.35-mm PÉV-2 wire. Interlayer insulation is provided by cable paper. The coil is wound on a separable frame and is impregnated with an epoxy compound. One

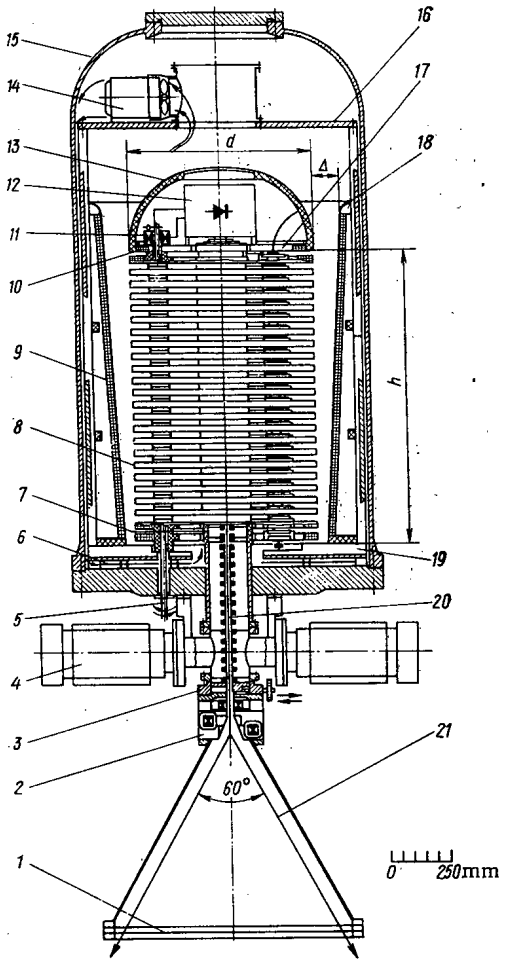

Fig. 2. Accelerator construction: 1) exit window foil; 2) deflection system; 3) slide valve; 4) vacuum pumps; 5) control shaft; 6) cooler; 7) accelerating tube; 8) rectifier section; 9) primary winding; 10) top coil; 11) variable transformer; 12) injector control unit; 13) high-voltage electrode; 14) fan; 15) boiler; 16) shield; 17) high-voltage electrode base; 18) magnetic circuit; 19) disk-shaped magnetic circuit; 20) electric conductor; 21) electron beam boundary.

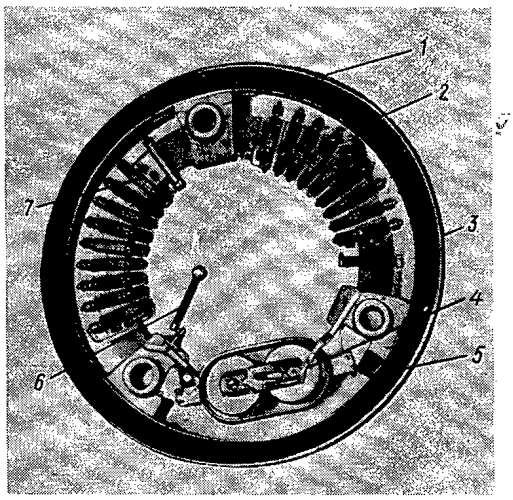

Fig. 3. Rectifier section: 1) section base; 2) coil; 3) outside shield; 4) capacitor block; 5) conductor; 6) limiter resistor; 7) diode arm.

end of the coil is connected to the outside shield which, in turn, is connected by means of a polyethylene conductor to the center point of the capacitor block. The capacitor block consists of four K15-10 ceramic capacitors ($C = 10^4$ pF, $U = 40$ kV) in a series–parallel connection. The diode arms connect the input and output of the section with inside shield of the coil – the section base rim. A limiting resistor, one end of which is connected to the appropriate accelerator tube electrode, is fastened through a leaf spring to one of the segments of the section base.

A diode arm consists of nine D1008 stud rectifiers cemented to the base. The diode chain is preceded by a choke that limits the dc current through the diodes in case of breakdown (resistance Z in Fig. 4).

Shunt capacitors, fastened to rectifier columns, ensure uniform distribution of reverse voltage over the rectifier columns. All electrical connections in the diode arm are made with 1.5-mm bare copper wire.

Accelerator Tube. The accelerator tube (Fig. 2) is built into the rectifier section column; at the bottom the tube ends in a neck which passes through the boiler bottom connected to the vacuum system. The vacuum system (two NMDO-025-1 magnetic pumps) is fastened to the boiler bottom and carries a slide valve and the deflecting system with a titanium foil exit window.

The length of the accelerator tube insulator is the same as the rectifier column height (h = 1200 mm). The insulator (Fig. 5) consists of two parts hermetically joined together by screws. A Pierce gun with a perveance of $\sim 0.4 \cdot 10^6$ A/V$^{3/2}$ is mounted on the top flange.

The electron beam current is controlled by varying the first-anode voltage supplied by the injector power supply unit. All tube electrodes are connected through a resistive divider with a total resistance of $8 \cdot 10^3$ MΩ and consisting of type KÉV-1 resistors. In addition, the second anode and some of the intermediate tube electrodes are connected to the rectifier column through 6-Ω limiting resistors. After passing the second anode the beam enters a magnetic periodical focusing system (MPFS) formed by permanent

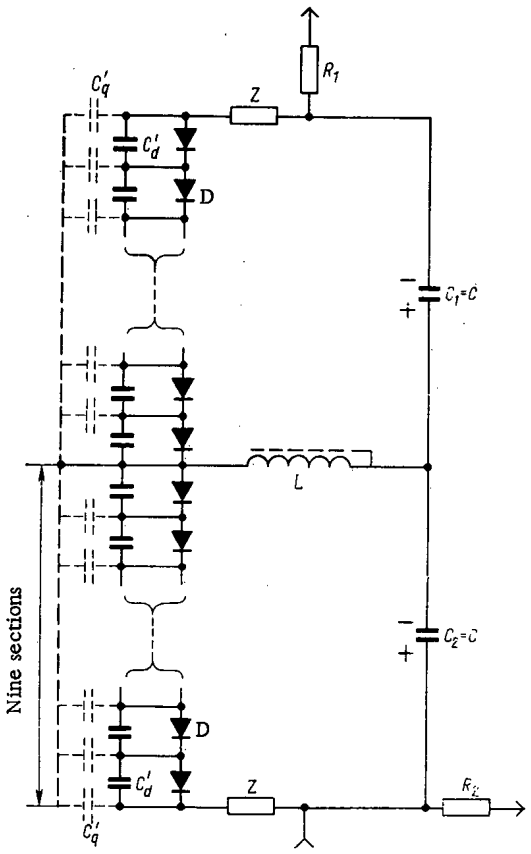

Fig. 4. Rectifier section circuit: $C_1 = C_2 = C$) filter capacitors; Z) choke resistance; D) rectifier column; R_1, R_2) limiter resistors; C'_d) shunt capacitor; C'_q) parasitic capacitance between diode arm and coil shield; L) section coil.

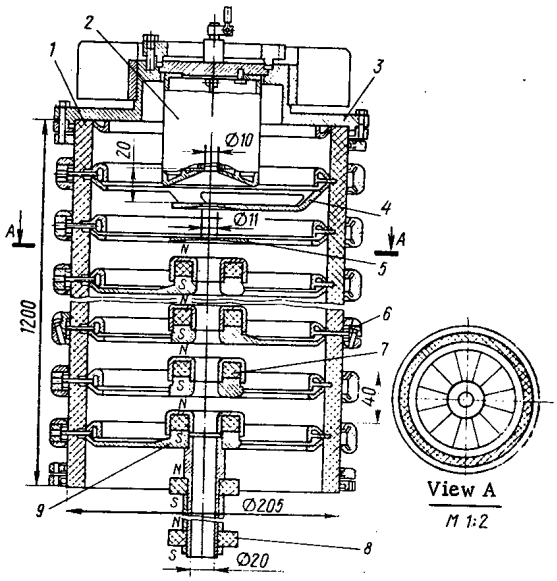

Fig. 5. Accelerator tube: 1) insulator; 2) Pierce gun; 3) top flange; 4, 5) first and second anodes; 6) screw; 7) permanent magnet; 8) MPFS channel; 9) electrode.

magnets with dimensions D × d × h = 52 × 23 × 12 and made of mark 2BA barium ferrite. The magnetic field amplitude along the axis of each magnet is ~600 G. Moving along the magnetic channel, the accelerated electron beam enters the deflecting system.

Deflecting System and Exit Window. This system consists of a funnel with exit window, line and frame scan coils, and the scan power supply. The electron beam is deflected by the magnetic field provided by scanning coils fed from a sawtooth current generator. The basic technical specifications of the system are listed below.

Deflection angle of line scan, deg	±30
Scan frequency, Hz:	
line	50
frame	1075
Dimensions of exit window, mm^2	75 × 980
Thickness of titanium foil, μ	50
Electron energy loss in foil, keV	50
Nonuniformity of beam current density along the exit window length, %	±12
Minimum air pressure at cooler inlet, kgf/cm^2	0.5

The deflection system funnel is made of stainless steel (Fig. 2) and at the point of location of the deflecting coils has thin walls through which the alternating magnetic field penetrates. The funnel ends in a rectangular flange which holds the exit window (Fig. 6).

Electrical Circuits. The asynchronous motor M_1 of a VPL-50 inverter is connected to the line through the power supply cabinet PSC (see Fig. 1). The motor rotates the generator G and exciter E of the VPL-50 inverter. The generator output voltage, and thus also the accelerating voltage, is controlled by the exciter unit EU mounted in the control desk. The generator G is connected to the primary winding through a magnetic starter S and thyristor switch TS. The latter ensures fast switching off of the accelerator

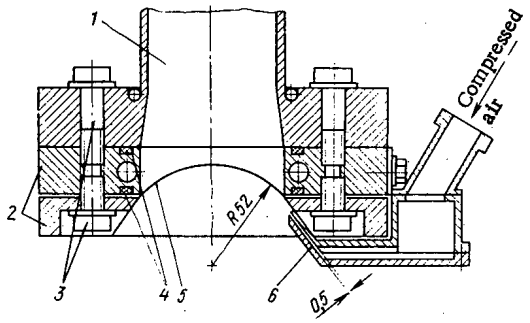

Fig. 6. Exit window: 1) funnel; 2) frames; 3) bolts; 4) seals; 5) foil; 6) cooler.

supply in case of emergencies, and consists of two TL-200 thyristors in a series–parallel connection.

The chain of rectifier sections is connected to the accelerator tube electrodes. Through variable transformers Tr_1 and Tr_2 the top coil feeds the heater circuit of the injector supply unit (ISU) and the ISU source whose output voltage is applied to the injector electrode. (The ISU and source are mounted on the high-voltage electrode.) The beam current is controlled by varying the anode voltage. The heater voltage and beam current voltage are controlled from the desk by means of electrical motors M_3 and M_2 mounted on the boiler bottom. The cathode heater is also monitored at the desk. For this, the injector heater circuit includes a lamp L whose brightness depends on the heater voltage. The light of this lamp is guided along a light pipe and falls on a photoresistor R connected in the measuring circuit.

The measuring and protection circuits are also worth mentioning. The end of the bottom rectifier section is brought out from the boiler and connected to ground through a meter. The dc component flowing through milliammeter mA corresponds to the beam current. The alternating component passing through capacitor C_2 indicates changes in the accelerating voltage in case of breakdowns in the accelerator. The voltage across C_1 is thus applied to the protection unit PU which shuts off the accelerator in case of breakdown, reduced vacuum in the tube, too high accelerating and injector heater voltages, and loss of line and frame coil currents, i.e., in all emergency situations.

In conclusion, the authors express gratitude to A. N. Skrinskii for his constant interest and help in the accelerator design.

GRAZING SCATTERING OF FAST ELECTRONS BY THE SURFACE OF A SOLID

V. I. Boiko, V. V. Evstigneev, B. A. Kononov, A. L. Plotnikov, and E. A. Gorbachev

UDC 539.124:539.171

Investigation of electron scattering by a solid-body surface as a special case of their interaction with matter is of scientific and practical interest. The flux characteristics of reflected particles carry information concerning the processes involved in their interaction with the surface layer, the structure of the surface, etc. The differential characteristics of the scattered electron fluxes are essential for solving practical problems of dosimetry, shielding [1], and radiography [2]. In particular, knowledge of the differential characteristics is required for calculating the penetration of electrons through extended inhomogeneities in matter (e.g., in a shield consisting of blocks) when the particles being trapped in holes move effectively in them due to grazing scatterings [3].

The processes involved in electron backscattering by solid bodies are being intensively investigated. The integral characteristics of low-energy (1-10 keV) electrons have been well investigated up to now [4] and the differential characteristics in this region are under investigation. Results of the investigation of the total reflection coefficient for normal [5] and oblique [6] incidence at energies up to 25 MeV have been published. The differential albedo for the megaelectron volt region (up to 1.75 MeV) is investigated in [7, 8] and there are reports [9, 10] for the high-energy region. However, these experiments are performed at grazing angles greater than 20°.

The process of backscattering is simulated by the Monte Carlo method [11, 12]; a quantum-mechanical approach [13] and a diffusion approximation for grazing angles of incidence [14] are developed.

The differential characteristics of fast electrons, scattered from the solid-body surface, for grazing angles less than 20° have not been investigated up to now due primarily to difficulties of an experimental nature, connected with the measurement of the effective signal against the background noise of the attendant radiation.

This paper is devoted to the investigation of the differential albedo of electrons with an initial energy E_0 = 3.8-8.2 MeV, undergoing grazing scattering from the surface of polycrystalline solids.

Experimental Apparatus and Procedure. The electron beam from a betatron having a high (~2%) energy homogeneity was utilized in the experiment. The beam, focused by magnetic quadrupole lenses, was monitored by a duct ionization chamber and entered the scattering chamber through an aluminum collimator, where the pressure was maintained at $\sim 10^{-2}$ mm Hg. A beam 2 mm in diameter with an angular dispersion of ±0.25° was intercepted by an additional collimator. Investigation of grazing scattering was conducted on graphite, aluminum, copper, and lead targets, whose surfaces were machined to the 5th class of precision (GOST 2.789-59). The target was deflected by an angle α = 3-30° relative to the original beam. The electrons scattered by the deflector were recorded by a FÉU-31 scintillation detector. The detector, located in a protective casing, was moved by remote control in the axial and azimuthal planes (Fig. 1). Standard amplification, discrimination, and recording units were utilized with the detector for analyzing the signal. A number of measures were taken to reduce the noise produced by the accompanying bremsstrahlung as well as by the electron radiation scattered by the structural components and the pickups from the accelerator's high-current circuits. In the first place, in order to reduce the bremsstrahlung

Translated from Atomnaya Énergiya, Vol. 40, No. 3, pp. 221-226, March, 1976. Original article submitted April 29, 1975; revision submitted September 8, 1975.

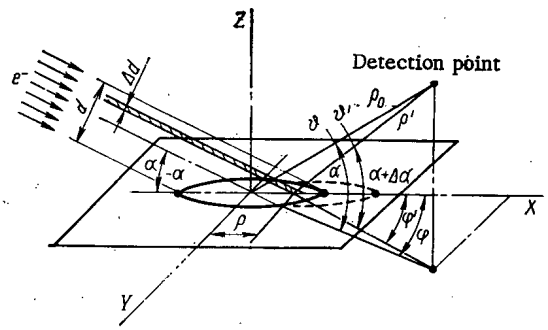

Fig. 1. Experimental geometry: ϑ and φ are angles in the axial and azimuthal planes.

background, the scattering chamber was placed behind a 10-cm lead shield and the sensitive element of the detector consisted of an organic scintillator (n-terphenyl in polystyrene with additions of RORORO) 0.5 mm thick and 1 mm in diameter. In the second place, in order to reduce the background pickups from the betatron, a proportional pulse gate [15], which opens the connecting duct only at prescribed time intervals upon discharge of the electrons at the target, was incorporated into the signal investigation duct. This time (up to 10 μsec) was set by the pulse generator, whose operation was synchronized with the operation of betatron's control circuit. The duct was unblocked during the remaining time before the next pulse, the frequency of which equaled 50 Hz.

In order to amplify the signal of the electrons scattered by the surface, the detector was placed at a distance from the deflector not great in comparison with the size of the image of the beam. The detector was collimated in such a manner that its sensitive element "scanned" the entire region of the beam's image, produced by the incident electrons and the ones scattered in the absorber. Because of the increase in the detection solid angle for small sizes of the sensitive element, one succeeded in reducing the effective signal to the background signal and even exceeding it for detection angles greater than 10°.

The total level of the γ-background was measured for each detection point and was subtracted from the total signal. The background of the electrons scattered by the walls of the chamber and the structural elements was reduced up to 1% by a special arrangement of polyethylene blocks inside of the scattering chamber. The maximum mean-square error in the measurements, including energy instability (±0.1%), intensity (±1%) of the betatron's radiation, and the statistical error in the calculation (±5%) did not exceed 8%.

The specific properties of the investigation of the characteristics of the electrons deflected during grazing scattering necessitated the use of a special method of processing the results of the experiment.

Procedure for Processing the Results of the Investigation. For the transition to a point source, the original electron beam with diameter d (see Fig. 1) and grazing angle α was split into elementary unidirectional beams Δd. In addition, the image of an elementary beam in the deflector plane $\Delta d/\sin\alpha$ was assumed to be much smaller than the distance from its center to the detection point ρ', while the angular distribution of the elementary beam was described by the function $\Phi(\vartheta', \varphi')$. The quantity measured was the function $F(\vartheta, \varphi)$, which describes a beam of particles with a total area of the image of the incident beam, as well as the one scattered in the absorber.

One should mention that for oblique incidence of the beam, the size of the image X is the sum of the sizes of the incident beam $2a = d/\sin\alpha$ and the one scattered in the deflector $\Delta a = KR_e \cos\alpha$ (here R_e is the extrapolated mean-free path of the deflector electrons). For grazing angles $\alpha = 3\text{-}30°$, we shall neglect the size of the image along Y (2 mm) as compared with X and $\rho_0 = 100$ mm and shall assume that the particles are scattered from the surface out of a narrow region of length X. Let us also neglect the angular dispersion of the incident beam (0.5°) and the angular size of the sensitive element of the detector (0.5°), taking it to be a point.

Then integration over the individual fluxes gives

$$F(\vartheta, \varphi) = \frac{1}{X} \int_{-a}^{a+\Delta a} \Phi(\vartheta', \varphi')\, d\rho, \tag{1}$$

where 1/X is the normalization coefficient, while ϑ' and φ' are connected with ρ by the relation (see Fig. 1)

$$\rho = \rho_0(\cos\vartheta \cos\varphi - \sin\vartheta \operatorname{ctg}\vartheta' \cos\varphi). \tag{2}$$

In the experiment, the function $F(\vartheta, \varphi)$ was measured for specified values of the angles ϑ and φ, i.e., for $\varphi = 0$ one plotted the distribution in the axial plane, and then for $\vartheta = \vartheta_{max}$ the distribution along the azimuth is plotted [by ϑ_{max} is understood the angle corresponding to the maximum value of $F(\vartheta, \varphi)$ at $\varphi = 0$].

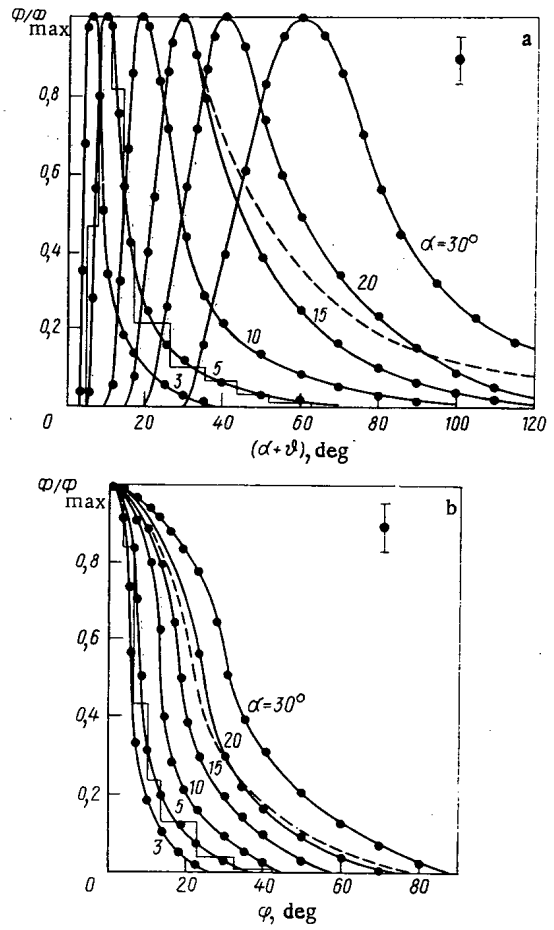

Fig. 2. Angular distribution of electrons with E_0 = 3.3 MeV, scattered from an aluminum deflector in the axial plane at $\varphi = 30°$ (a) and the azimuthal plane at $\vartheta = \vartheta_{max}$ (b): ———) function $\Phi(\vartheta, \varphi)/\Phi_0$; - - - -) function $F(\vartheta, \varphi)/\Phi_0$; the histogram was calculated by the Monte Carlo method.

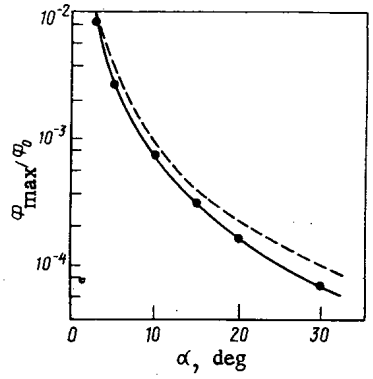

Fig. 3. Dependence of the electron flux at the maximum of the angular distributions at $\vartheta = \vartheta_{max}$; $\varphi = 0$, normalized to the initial flux, on the grazing angle of the electrons with E_0 = 3.3 MeV by an aluminum deflector: ———) experiment; - - - -) theory of O. B. Firsov [14].

Therefore, in order to simplify the calculations in Eq. (1), we take $\varphi = 0$ and find $\Phi(\vartheta)$. Then

$$\rho = \rho_0 (\cos\vartheta - \sin\vartheta \operatorname{ctg}\vartheta'). \tag{3}$$

Transforming to integration over ϑ' in Eq. (1), we obtain

$$F(\vartheta) = \frac{\rho_0}{X} \sin\vartheta \int_{\vartheta_{-a}}^{\vartheta_{a+\Delta a}} \Phi(\vartheta') \frac{d\vartheta'}{\sin^2\vartheta'}, \tag{4}$$

where it is easy to obtain the limits of integration from the relationship

$$\vartheta' = \operatorname{arc\,tg} \frac{\rho_0 \sin\vartheta}{\rho_0 \cos\vartheta - \rho}, \tag{5}$$

assuming ρ to be equal to $-a$ and $a + \Delta a$, respectively.

From Eq. (4), it is not difficult to convince oneself that for $\rho \gg X$, $F(\vartheta) \equiv \Phi(\vartheta)$.

In view of the fact that the integral in Eq. (4) is not taken in manifest form, we expand the integrand in a Fourier series, assuming the a_0 and b_n coefficients of the series to be zero:

$$\frac{\Phi(\vartheta')}{\sin^2\vartheta'} = \sum_{n=1}^{\infty} a_n \sin n\vartheta'. \tag{6}$$

Substituting Eq. (6) into Eq. (4) and integrating, we obtain a system of n equations for the a_n coefficients of the series:

$$\frac{F(\vartheta)}{\sin\vartheta} = \frac{\rho_0}{X} \sum_{n=1}^{\infty} \frac{a_n}{n} (\cos n\vartheta_{-a} - \cos n\vartheta_{a+\Delta a}), \tag{7}$$

where ϑ_{-a} and $\vartheta_{a+\Delta a}$ are functions of ϑ [see Eq. (5)].

Solving the system obtained for the coefficients a_n and substituting them into Eq. (6), we obtain the function $\Phi(\vartheta)$ for $\varphi = 0$ in the form

$$\Phi(\vartheta) = \sin^2\vartheta \sum_{n=1}^{\infty} a_n \sin n\vartheta. \tag{8}$$

We then find the flux distribution in the azimuthal plane $\Phi(\varphi)$ for $\vartheta = \vartheta_{max}$. Since $\vartheta_{max} \approx \alpha$ one can set $\vartheta' = \vartheta$ in Eq. (2) and taking into account that $\Phi(\varphi = 0) = \Phi(\vartheta_{max}) = \Phi_{max}$, we find $\Phi(\varphi)$ for $\vartheta = \vartheta_{max}$ in the form

$$\Phi(\varphi) = \sin^2\vartheta_{max} \sum_{n=1}^{\infty} a_n \sin n\vartheta_{max} \cos n\varphi. \tag{9}$$

The flux distribution functions for electrons scattered from the solid-body surface in the axial (8) and azimuthal (9) planes were calculated on an electronic computer.

The greatest difference in the functions F and Φ is observed for large ϑ and φ, i.e., when the size of the image, visible from the detection point, is comparable to the distance ρ_0 [the broken line for $F(\vartheta, \varphi)$ in Fig. 2].

Discussion of Experimental Results. In order to describe the angular distribution of the electrons scattered by the solid-body surface, we utilize the following parameters: $\Delta\vartheta$ and $\Delta\varphi$ are the halfwidths of the angular distribution in the axial and azimuthal planes; Φ_{max} is the amplitude of the angular distribution (the number of electrons at the curve's maximum); ϑ_{max} is the most probable scattering angle at the surface.

The parameters of the angular distribution for the scattered flux are determined by the contribution of the single and multiple scattering at the surface, multiple scattering in the surface layer, and diffusion of the electrons in the body of the deflector.

Let us pursue the nature of the variation of these quantities as a function of the grazing angle α of the electrons, their energy E_0, the atomic number Z, and the deflector's thickness R.

The typical dependences of the angular distributions with $\Phi_{max} = 1$ on the grazing angle are given in Fig. 2a, b. It is seen that a reduction in the grazing angle of the electrons results in a decrease in the halfwidth of the angular distributions. This is explained by the dependence of the depth of penetration of the electrons on the grazing angle, which decreases with a decrease in the angle. As a result, the number of electrons undergoing multiple and single scattering at the maximum of the distribution increases (Fig. 3).

The halfwidth of the angular distributions in the azimuthal plane is greater than in the axial plane. This is evidently connected with the great contribution of the multiple and diffusion scattering to the azimuthal distribution of the electron flux. With an increase in the atomic number of the target, the probability for the scattering of electrons at a large angle is increased and, in spite of the fact that the depth of penetration is reduced, the contribution of the diffusion component is increased and dominates for substances with large Z. As a result, the halfwidth of the angular distribution increases sharply (Fig. 4) and the halfwidths in the axial and azimuthal planes become comparable. The halfwidth of the angular distributions decreases with an increase in the energy (see Fig. 4). Analysis of the dependences of $\Delta\vartheta$ and $\Delta\varphi$ on α, Z, and E_0 indicates that, with an accuracy up to the error in the measurements, for a semiinfinite deflector they can be expressed by relations of the form

$$\begin{aligned} \Delta\vartheta &= 8 + (1.3 + 0.06Z/E_0)(\alpha - 5); \\ \Delta\varphi &= 13 + (1.8 + 0.09Z/E_0)(\alpha - 5), \end{aligned} \tag{10}$$

where $\Delta\vartheta$, $\Delta\varphi$, and α are measured in degrees; E_0 is in MeV, and the parameters vary within the limits: Z = 6-82, E_0 = 3.3-8.2 MeV, and α = 5-20°.

Thus, for a specified grazing angle α, the angular distributions are described by the ratio Z/E_0, which is found to be in agreement with the conclusion made previously for the total scattering coefficient [7]. Investigation of the grazing scattering of electrons by the solid-body surface allowed one to exhibit its characteristic peculiarities. It is found that for grazing angles $\leq 5°$ the dependence of the distribution's parameters on Z and E_0 vanishes (see Fig. 4), while the reflection angle ϑ_{max} becomes less than the grazing angle α (for $\alpha = 5°$, $\vartheta_{max} = 4°$).

The processes of single and multiple elastic scattering of electrons by the surface have the greatest effect on the characteristics of the angular distribution for grazing scattering, while multiple and diffusion scattering, which results in a broadening of the angular distribution, is expressed weakly. One can observe

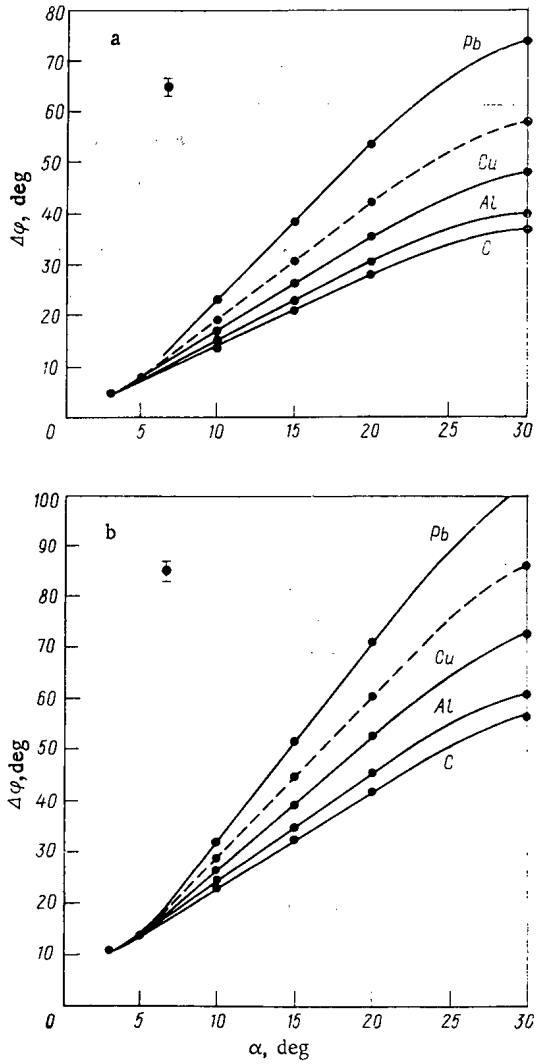

Fig. 4. Dependence of the halfwidths of angular distributions in the axial (a) and azimuthal (b) planes on α, Z, and E_0 when E_0 = 3.3 (——) and 8.2 (– – –) MeV.

the effect of multiple scattering and diffusion by reducing the thickness of the deflector.

This was done for aluminum targets by varying their thicknesses from $2R_e$ (i.e., from semiinfinite) down to $0.002R_e$ for E_0 = 5 MeV. For such a variation in the thickness of the scatterer, the halfwidth of the angular distribution of $\Delta\vartheta$ decreases from 8 to 6.5° and the maximum of the curves is reduced by a factor of 1.7, i.e., the multiple scattering and diffusion contribution vanishes. In the case of oblique incidence, one can in general express the thickness of the saturation layer R_s by the relationship

$$R_s = kR_e \sin\alpha, \tag{11}$$

where the coefficient of proportionality k depends on the energy E_0 and the atomic number Z of the scatterer. For example, when Z = 13, E_0 = 5 MeV, and α = 3; 5; and 10° k = 0.26. With an increase in Z and E_0, k increases insignificantly.

In this case, one can express the increase in the size of the image of the electron beam in the plane of the reflector due to scattering in the substance along the x axis (see Fig. 1) in this way:

$$\Delta a = kR_e \cos\alpha. \tag{12}$$

Besides the thickness, the atomic number, and the energy, the purity of the preparation of the surface of the solid affects the scattering of the electrons.

If the dependence of the electron reflection coefficient on the quality of the surface is not very important in the case of normal incidence (e.g., a surface machined to the 14th precision class reflects 5% more electrons than one machined to the 2nd class [16]), then at small grazing angles it is manifested to a greater degree. In this case, the thickness of the saturation layer becomes comparable in roughness and the increase in the relative contribution of electrons undergoing nonspecular reflection results in an increase in the halfwidth of the angular distribution. The number at the maximum of the curve is reduced by 30%, while the halfwidth of the distribution is increased by a factor of 1.2 with the substitution of a scattering surface machined to the 10th precision class by one machined to the 3rd class.

A comparison of the results of the investigation of the grazing scattering of electrons by a solid with the theory of Firsov [14] was made (the broken line in Fig. 3). Analysis indicates that the diffusion approach developed for the scattering problem satisfactorily explains the scattering of relativistic electrons. The thesis concerning the independence of the characteristics of the scattering from the reflector substance and the energy of the electrons at grazing incidence is verified experimentally. However, according to theory the halfwidths of the angular distributions are narrower than the experimental ones; this is obviously connected with the fact that the quality of the surface was not considered in the calculations, the total reflection coefficient was taken to be unity, therefore the theoretical values of the maximum flux proved to be higher than the experimental ones, especially at large angles of incidence (~30°). The results of a numerical calculation by the Monte Carlo method, conducted according to a program similar to the one in [1], neglecting the formation of secondary electrons, are in satisfactory agreement with the experimental data (the histograms in Fig. 2).

The investigations regarding the grazing scattering of fast electrons from the surface of solids allow one to conclude the following.

1. The dependence of the parameters of the angular distribution of scattered electrons ($\Delta\vartheta$, $\Delta\varphi$, ϑ_{max}, and Φ_{max}) on the atomic number Z and the energy of the electrons E_0, vividly expressed at large angles of incidence, vanishes for grazing scattering and the integral reflection coefficient converges to one.

2. The angle of reflection ϑ_{max} becomes smaller than the grazing angle α, while the ϑ_{max}/α ratio converges to one with an increase in the grazing scattering angle.

3. The angular distribution depends on the thickness of the scatterer. The quantities $\Delta\vartheta$, $\Delta\varphi$, and Φ_{max} decrease with a decrease in the thickness.

4. The quality of the reflector's surface has the greatest effect on the characteristics of the scattered electrons at grazing incidence.

5. Satisfactory agreement of the experimental curves with the calculations of Firsov [14] and by the Monte Carlo method is obtained.

LITERATURE CITED

1. V. F. Baranov, Electron Radiation Dosimetry [in Russian], Atomizdat, Moscow (1974).
2. V. D. Karataev, Author's Abstract of Candidate's Dissertation, Tomsk (1974).
3. V. I. Boiko, V. V. Evstigneev, and A. L. Plotnikov, At. Énerg., 36, No. 6, 515 (1974).
4. I. I. Davletchin, V. A. Mashinin, and A. A. Pravikov, in: Radiation Technology [in Russian], Vol. 1, Atomizdat, Moscow (1967), p. 114.
5. I. Tabata, R. Ito, and S. Okabe, Nucl. Instrum. and Methods, 94, 509 (1971).
6. V. P. Kovalev et al., At. Énerg., 32, No. 4, 342 (1972).
7. H. Frank, Z. Naturforsch., 14a, No. 247 (1959).
8. D. Rester and I. Derrickson, Nucl. Instrum. and Methods, 2, 86 (1969).
9. P. L. Gruzin and A. M. Rodin, Program and Abstracts of Papers of the XXV Conference on Nuclear Spectroscopy and Structure [in Russian], Nauka, Leningrad (1975), p. 490.
10. V. N. Kovalev, V. V. Gordeev, and V. I. Isaev, Abstracts of Papers of the V All-Union Coordination Conference on the Dosimetry of Intense Beams of Ionizing Radiation [in Russian], Moscow (1974), p. 33.
11. S. A. Vorob'ev and V. A. Kuz'minykh, Abstracts of Papers of the All-Union Science Conference on the Ionizing Radiation Protection of Nuclear-Industrial Installations [in Russian], Izd. MIFI, Moscow (1974), p. 42.
12. P. L. Gruzin and A. M. Rodin, op. cit. [9], p. 497.
13. A. P. Kalashnikov and V. A. Mashinin, Zh. Éksp. Teor. Fiz., 59, No. 6(12), 2025 (1970); Zh. Tekh. Fiz., 43, No. 11, 2229 (1973).
14. O. B. Firsov, Dokl. Akad. Nauk SSSR, Ser. Fiz., 169, No. 6, 1311 (1966); Fiz. Tverd. Tela, 9, 2145 (1967).
15. V. O. Vyazemskii et al., Experimental Instruments and Techniques [in Russian], Vol. 2 (1959).
16. H. Kanter, Ann. Phys., 20, No. 144 (1957).

MICRODOSIMETRIC DETERMINATION OF RADIATION QUALITY FACTORS

I. V. Filyushkin

UDC 535.23.08:621.014.481

The present maximum permissible levels of heavily ionizing radiation are based on the use of quality factors Q_j which indicate how many times the yield of adverse effects of a small dose D_j of heavily ionizing radiation of the j-th kind is greater than the effect of an identical dose D_γ of weakly ionizing x-ray or γ radiation. According to international recommendations [1] and Soviet norms [2], the quality factor depends only on the linear energy transfer (LET) of radiation and increases from 1 to 20 when LET increases from 3.5 to 200 keV/μ. The accepted quality factors have no firm radiobiological foundations and obviously need revision. For example, a radiobiological effectiveness (RBE) factor of about 100 has been experimentally obtained in radiation blastomogenesis with small radiation doses [3].

The main difficulty in obtaining valid quality factors lies in the necessity of far off extrapolation of the dose dependence of the yield of adverse effects caused by various kinds of radiations (or directly of RBE magnitudes) from the large doses used in radiobiological experiments to small doses [4]. Direct experimental determination of effects in maximum permissible doses is impossible without using vast numbers of experimental animals which can run into millions [5]. One possible way to overcome this difficulty is to establish a biophysical concept of radiation quality which would relate, for example, the dose dependence of RBE or the yield of effects per unit dose to physical parameters of radiation and to metabolic properties of mammalian cells whose damage causes the subsequent appearance of adverse radiation effects. The duality concept of the effect of radiation formulated by Kellerer and Rossi [6, 7] looks now most promising. However, the approach of Kellerer and Rossi contains several inadequately substantiated propositions so that their equations are essentially valid for the description of the yield of cellular effect only for small radiation doses with not too high LET [4]. Here we consider a more general approach to the description of the yield of radiation effects in mammalian cells which can be used to estimate the RBE of heavily ionizing radiations in small doses. Under certain specific assumptions, such estimates can serve as a basis for the derivation of radiation quality factors.

Model for Generation of Radiation Effects in Mammalian Cells

The duality concept of radiation effects [6, 7] in cells of mammals and higher plants is based on the analysis of the dose dependence of RBE of neutrons measured in several cellular effects. The results of this analysis indicate that the generation of many kinds of radiation effects in such cells can be formally associated with an injury and subsequent interaction of pairs of cellular subunits, loci, whose number in a cell is 10^6 to 10^7 and whose "size" is 10 to 100 Å. For an effect to take place, two biologically connected loci must be injured and these primary injuries must then interact at the biological stage of cell damage.

Mathematical formalization of the duality concept has resulted in a "linear-quadratic" equation which describes the yield of primary injuries $E(D_j)$ for small radiation doses with not too high LET [6, 7]:

$$E(D_j) = k(\zeta_j D_j + D_j^2). \quad (1)$$

where k is a factor independent of the kind of radiation, D_j is the dose of j-th radiation, and ζ_j is the average dose value of specific energy released in the crossing of a charged particle track through a sensitive area where biologically connected loci are located.

Translated from Atomnaya Énergiya, Vol. 40, No. 3, pp. 227-233, March, 1976. Original article submitted May 4, 1975.

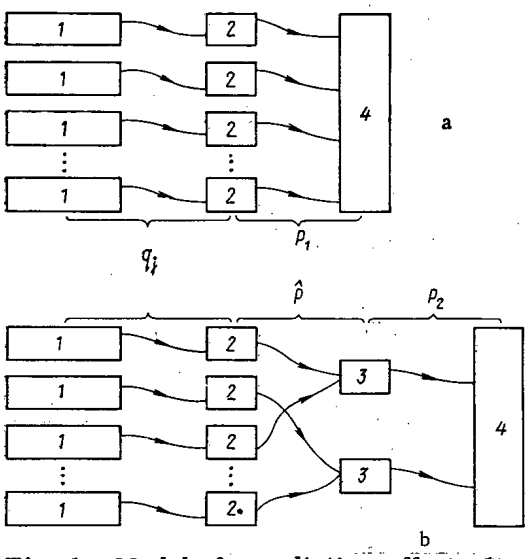

Fig. 1. Model of a radiation effect: 1) independent injury, restitution of loci at the chemical and preceding stages; 2) recovery of loci at the biological stage; 3) interaction of injured loci; 4) formation of radiation effect.

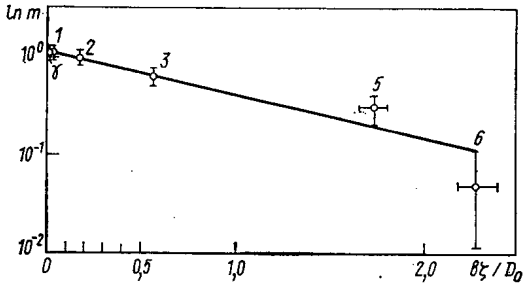

Fig. 2. Extrapolation number logarithms according to the data of Todd: 1/b = 1.15, d = 5.7 μ. The figures indicate ion charges, γ corresponds to 50-keV x-ray radiation.

Kellerer and Rossi [6, 7] took into account that the yield of loci damage at the primary stage of injury is proportional to the specific energy release in the region where loci are localized, including a factor independent of the kind of radiation.

The microdosimetric parameter ζ_j can be calculated for any kind of radiation if the diameter of the region where biologically connected loci are located is known. Thus, the diameter of this region determines the desired RBE at small doses. At the same time, the method of finding this diameter within the scope of the present concept is clearly unsatisfactory: to find it one has to know the RBE values corresponding to small doses, which in principle is the purpose of calculations. A more reasonable approach is to find this diameter from data concerning the effect of large doses. Thus, here we derive equations for cell survival curves based on a model which in several aspects is more exact than the one used in [6, 7].

The first refinement consists in taking into account the biological connections between loci. More general than in the model [6, 7], and not inconsistent with the duality hypothesis, is the removal of restrictions on the overlapping of regions in which interacting loci are located. We assume that primary injury of any one of K_0 loci of the cell can interact with the injury of one out of $K \leq K_0$ loci biologically connected to it. Loci, biologically connected to the given one, are localized in a microvolume containing the given locus. Primary injuries to the loci and their restitution (Fig. 1) take place at the chemical and preceding stages characterized by short times ($\leq 10^{-3}$ sec) and small possible product interaction lengths (≤ 100 Å) [8]. Microdosimetric estimates indicate that the probability of injury and nonrestitution of a locus can be considered to be proportional to the specific energy transferred to the microvolume but that the proportionality factor $\bar{q}_i$ can depend on the nature of radiation. At the biological stage, the injured locus may not recover with a probability $\hat{P}$ and may interact with some other injured locus connected with it (see Fig. 1b) forming a "double injury." With a probability P_2 each such double injury independently causes a radiation effect. Figure 1a shows an auxiliary model in which each primary injury does not recover with the probability P_1 and produces an effect without interacting with other injuries.

Derivation of Equations

It has been shown repeatedly [9] that models based, as the model in Fig. 1a, on the hypothesis of independent injury, recovery, and influence of unrecovered injuries on the yield of effects, lead to an exponential dependence of the survival N/N_0 on the dose of any kind of radiation:

$$N/N_0 = \exp(-D_j/D_{0j}). \quad (2)$$

According to model in Fig. 1a,

$$D_{0j} = (K_0 \bar{q}_j P_1)^{-1}.$$

For an effect to appear in an object which reacts to radiation in accordance with the hypothesis of duality (Fig. 1b), a double injury must be formed. The formation of a double injury (let this event be

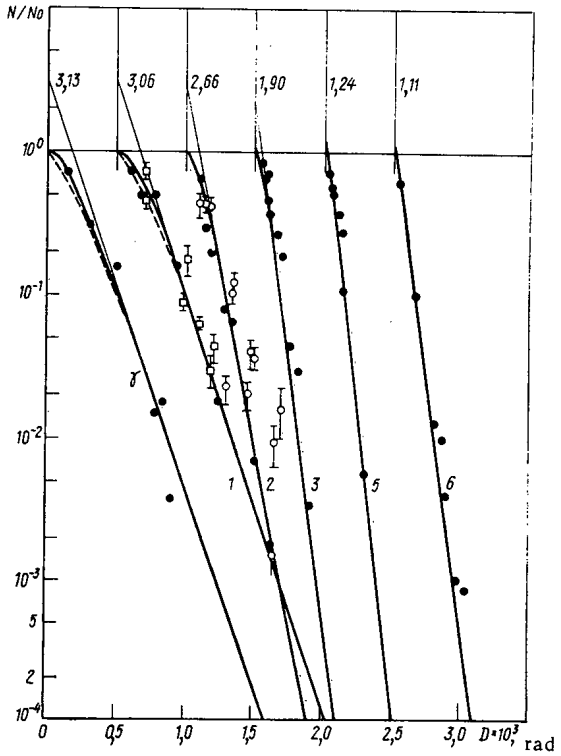

Fig. 3. Survival curves (●) measured by Todd and calculated from (16), —— and ---) $P_0 = 0$ and 0.3; ○ and □) adopted from Barendsen [14] (the remaining notation is the same as in Fig. 2).

TABLE 1. Characteristics of Heavy Ion Beams and Survival Curve Parameters

Ion species	L_j, keV/μ	$D_{0,j}$, rad	ζ for $\frac{d}{3.7}$ μ, rad	$b\zeta_j/D_{0,j}$	m_j exptl. data	m_j theor. values
^{1}H	6,4	140	4,5	0,027	3,1±0,4	3,06
^{2}He	25,1	93	17,8	0,16	2,7±0,3	2,66
^{7}Li	58	61	410	0,60	1,9±0,3	1,90
^{10}B	160	61	110	1,79	1,2±0,1	1,24
^{12}C	230	60	160	2,4	1,1±0,05	1,11

denoted by AB) as a result of application of an elementary dose dD_j following the dose D_j requires the occurence of two events.

Event A: injury due to the application of elementary dose and nonrecovery of some locus, say, α at all stages of the process [the probability of this event is P(A)].

Event B: injury due to the application of the dose $D_j + dD_j$ of some other locus connected with locus α and its interaction with the locus α. The conditional probability of the occurrence of such an event (under the condition that event A has taken place) is denoted by P(B/A).

Let the considered radiation produce in the medium a spatially noncorrelated (diffuse) ionization distribution. The absence of spatial correlation means that ionization (excitation) events are uniformly (to within fluctuations) distributed in the irradiated space. The probability P(B) can be obtained on the basis of the following considerations. From the point of view of continuation of the damage process of locus α injured by elementary dose dD, the interaction with any one of loci injured by the dose D,* in accordance with the model of Fig. 1b, includes exactly the same stages as the injury of some "one-stroke" object that reacts to radiation in accordance with the model of Fig. 1a. Thus, in case of "diffuse" radiation the probability P(B) agrees with the dose dependence of the injury of a "one-stroke" object in accordance with the model of Fig. 1a, except for the substitution of K for K_0 and the probability P for P_1:

$$P(AB) = [1 - \exp(-DK\bar{q}\hat{P})]. \tag{3}$$

The probability of an effect in the cell p_i due to a possible injury of locus i by an elementary dose dD is then given by

$$p_i = \bar{q}_i [1 - \exp(-DK\bar{q}\hat{P})]\, \hat{P}P_2\, dD. \tag{4}$$

The probability of injury of one cell, or the average number of cells injured by exposure to an elementary dose dD following the dose D is

$$\frac{dN}{N} = \sum_{i=1}^{K_0} p_i \approx K_0\bar{q}P_2P\,[1 - \exp(-DK\bar{q}\hat{P})]\, dD, \tag{5}$$

then

$$\frac{N}{N_0} = \exp\left\{-\frac{D}{D_0} + \frac{1}{b}\left[1 - \exp\left(-\frac{bD}{D_0}\right)\right]\right\}, \tag{6}$$

where $1/b = K_0P_2/K$;

$$D_0 = (K_0P_2\hat{P}\bar{q})^{-1}. \tag{7}$$

To derive an expression for a survival curve under the effect of any radiation it is only necessary to take into account the interactions at the biological injury stage caused by a single passage of a particle track through the sensitive area. The occurrence of event A, i.e., injury of a locus as a result of the

*Letters without subscripts denote quantities relating to "diffuse" radiation.

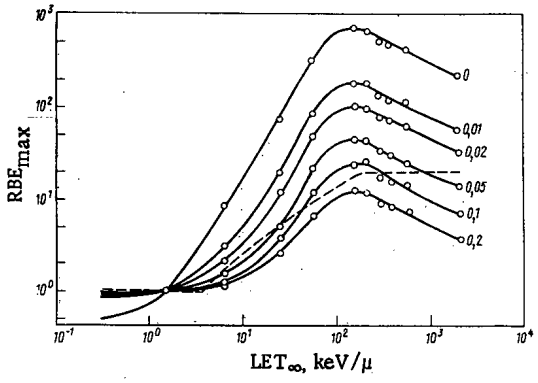

Fig. 4. Theoretical dependence of heavy ion RBE on LET with respect to 250 keV x-ray radiation for small radiation doses. The initial portion of curves correspond to ^{60}Co γ radiation. Figures at the curves are the assumed probabilities of the occurrence of an effect as a result of injury of a single locus; ---) recommended (1, 2) dependence of quality factor on LET.

track through the sensitive area. The occurence of event A, i.e., injury of a locus as a result of the application of an elementary dose dD_j, indicates that a track of ionizing particles passed through a locus and thus also through the microvolume containing other loci connected with it. Ionization events caused by this track can injure the connected loci. The argument of the dose dependence of the injury of "one-stroke" objects is the radiation dose D_j equal to the specific energy averaged over all microvolumes. Similarly, the argument of the function $P(B|A)$ should be the specific energy averaged over all loci injured by the elementary dose dD_j and transferred to the microvolumes connected with these loci. One part of this quantity is the dose D_j applied before (this part can be called the uncorrelated dose). The second part, the correlated dose $\bar{D}_j^{in}$, is the average specific energy imparted to the microvolume by the same track that caused injury of the locus connected with it. Assume that the spectrum of specific energies $f_j(z)$, produced by single passages of charged particle tracks of radiation j through the microvolume, is known. We wish to find the spectrum $\varphi_j(z)$ of energies released in microvolumes connected with injured loci. According to the Bayes inverse-probability theorem [10], $\varphi_j(z)dz$ is the posterior probability of the occurence of event C_i which consists of the transfer of specific energy in the range from z to z + dz from the charged particle track to the microvolume under the condition that the same track caused injury of the locus connected with this microvolume. Let this probability be $P(C_i|A)$. The a priori probability $P(C_i) = f_j(z)dz$. The probability of locus injury in case of transfer of specific energy in the range from z to z + dz is $P(A|C_i) = \bar{q}_j z$. Thus,

$$\varphi_j(z)\,dz = P(C_i|A) = \frac{P(C_i)\,P(A|C_i)}{\sum_{i=1}^{\infty} P(C_i)} = \frac{q_j z f_j(z)\,dz}{\bar{q}_j \int_0^{\infty} z f_i(z)\,dz} = z f_j(z)\,dz/\bar{z}.$$

Hence, the average correlated dose $\bar{D}_j^{in}$ is

$$\bar{D}_j^{in} = \int_0^{\infty} z\varphi_j(z)\,dz = \frac{\int_0^{\infty} z^2 f_j(z)\,dz}{\bar{z}} = \frac{\bar{z^2}}{\bar{z}} \equiv \zeta_j. \tag{8}$$

It turns out that the average correlated dose is identical to the radiation quality parameter introduced by Kellerer and Rossi [6, 7]. Thus, taking into account the effect of spatial correlation of ionization at the biological stage of injury gives the expression

$$\bar{p}(B|A) = 1 - \exp\{-(D_j + \zeta_j)\,\hat{P}\bar{q}_j K\}. \tag{9}$$

Substituting expression (9) into (5) we obtain the following expression for the survival curve for any kind of radiation:

$$\frac{N}{N_0} = \exp\left\{-\frac{D_j}{D_{0j}} + \frac{1}{b}\exp\left(-\frac{b\zeta_j}{D_{0j}}\right)\left[1 - \exp\left(-\frac{bD_j}{D_{0j}}\right)\right]\right\}, \tag{10}$$

which differs from expression (6) for "diffuse" radiation by the factor $\exp(-b\zeta_j/D_{0j})$ that decreases with increasing ζ_j. The theoretical survival curve varies thus from a sigmoid curve for weakly ionizing radiation, e.g., γ radiation, to an exponential curve for large LET values (corresponding to large ζ_j).

The magnitude of ζ_j depends on the kind of radiation and on the diameter of the microvolume where biologically connected loci are located. The microvolume diameter is governed by structural and metabolic properties of the cells, as is the parameter $b = K/K_0P_2$.

For a given kind of cells, these parameters, which depend on biological factors, can be found from a family of cell survival curves in the presence of various kinds of radiation. Expression (10) indicates that the extrapolation number of survival curve m_j (the y coordinate of the point of intersection of the continuation of the exponential portion of the curve with the y axis) is

$$m_j = \exp\left[\frac{1}{b}\exp\left(-\frac{b\zeta_j}{D_{0j}}\right)\right]. \tag{11}$$

If the cell is exposed to a beam of heavy ions which traverses it without stopping, then [7]

$$\zeta_{rad} = \frac{23L_j\ (\text{ueV}/\mu)}{d^2\ (\mu)}, \tag{12}$$

where L_j is the LET of the ion, and d is the microvolume diameter. Substitution of (12) into (11) and taking logarithms twice, gives

$$\ln(\ln m) = \ln\left(\frac{1}{b}\right) - \frac{b\,23L_j}{d^2 D_{0j}}. \tag{13}$$

Thus, on a semilogarithmic scale, the dependence of $\ln m_j$ on LET divided by D_{0j} should be represented by a straight line intercepting the y axis at a point with a coordinate 1/b. Figure 2 shows such a dependence obtained from survival curves of cells of human kidneys measured by Todd [11] (Fig. 3). This function corresponds to $1/b = 1.15 \pm 0.1$ and $d = 5.7 \pm 0.7\ \mu$. The x-axis scale in Fig. 2 takes into account these values. The heavy ions used by Todd, their LET, as well as the extrapolation numbers, theoretical and calculated from experimental survival curves, are listed in Table 1.

These data (Table 1 and Fig. 2) indicate that the dependence of the extrapolation number on radiation LET predicted by expression (13) holds to within experimental data accuracy. Consequently, the survival curves calculated from (10) on the basis of the above parameters are in good agreement with experimental data (see Fig. 3). Thus, expression (10), derived on the basis of the duality hypothesis which is true for small radiation doses, describes well the cell survival under the effect of large doses.

Yield of Cell Effects and RBE at Small Doses

Microdosimetric estimates indicate that for a γ radiation dose rate of 5 rad/yr, a cell 10 μ in diameter is traversed approximately once in several days by the track of recoil electron [9]. For heavily ionizing radiation, e.g., neutrons, the interception of secondary particle tracks by a cell is still less frequent. Because of recovery effects a cell can fully recover from sublethal injuries caused by preceding tracks before a next track traverses it. Thus, in case of small doses or low dose rates there is no interaction between primary injuries caused in the cell by different tracks, and the number of injured cells is proportional to the radiation dose. It can be shown [9] that the factor of proportionality is equal to the initial slope of the survival curve, i.e., to the angular factor of the tangent to zero dose. This quantity $(1/D_{1j})$ cannot be found experimentally with any acceptable accuracy but can be calculated from (10) using the parameters obtained before. Differentiation of the equation for $D_j = 0$ gives

$$\frac{1}{D_{1j}} = \frac{1}{D_{0j}}\left[1 - \exp\left(\frac{b\zeta_j}{D_{0j}}\right)\right]. \tag{14}$$

According to (14), when the dose of j-th radiation approaches zero, the RBE approaches its maximum value:

$$\text{RBE}_{max} = \frac{D_{0\gamma}\left[1-\exp\left(-\frac{b\zeta_j}{D_{0j}}\right)\right]}{D_{0j}\left[1-\exp\left(-\frac{b\zeta_\gamma}{D_{0\gamma}}\right)\right]}, \tag{15}$$

where quantities with the index γ refer to standard γ radiation.

Before proceeding to calculate these quantities it is necessary to make the following important reservation. Besides spatial correlation of ionization, which is responsible for the fact that ζ_j is not zero, the initial slope of the survival curve can be affected by biological factors. The most important of these are background sublethal injuries and nonsynchronism of cell populations. It is known, e.g., that in the mitosis phase the survival curve of mammalian cells is exponential even for weakly ionizing radiations [13]. Factors of biological origin can affect most strongly radiation sensitivity in case of small doses of weakly ionizing x-ray or γ radiation, when the role of the first factor is small.

To take into account biological factors it is necessary to introduce a certain probability P_0 of cell injury in case of an injury of a single noninteracting locus, i.e., without formation of a double injury. When this probability is taken into account Eq. (10) becomes

$$\frac{N^*}{N_0} = \exp\left\{-\frac{D_j}{D_{0j}} + \frac{1-P_0}{b}\exp\left(\frac{b\zeta_j}{D_{0j}}\right)\left[1-\exp\left(-b\frac{D_j}{D_{0j}}\right)\right]\right\}. \quad (16)$$

The initial slope for zero dose is then

$$\frac{1}{D_{1j}^*} = \frac{1}{D_{0j}^*}\left[1-(1-P_0)\exp\left(-b\frac{\zeta_j^*}{D_{0j}}\right)\right]. \quad (17)$$

The superscript * denotes quantities derived with the effect of biological factors on the initial slope taken into account. Theoretical survival curves shown in Fig. 3 as broken lines have been obtained assuming $P_0 = 0.3$. It is seen that the low accuracy of data on cell survival makes it impossible to choose between even quite different estimates ($P_0 = 0$ and $P_0 = 0.3$) on this basis alone.

Figure 4 shows the maximum RBE factors for heavy ions (17) with respect to 250 keV x-ray radiation for different assumed values of P_0. It is seen that without an initial slope of biological origin ($P_0 = 0$) the RBE factors reach very high values (up to 800) for LET ≈ 100 keV/μ. At the same time, the RBE of ^{60}Co γ radiation is found to be 0.5. On the contrary, when $P_0 = 0.2$ the maximum RBE factor does not exceed 12, while RBE of ^{60}Co γ radiation becomes unity for $P_0 = 0.01$. As an upper bound for P_0 for fast dividing cells one can take the mitotic index, i.e., the relative fraction of cells in the mitosis phase (~ 0.05). In this case the dependence of RBE on LET at small radiation doses becomes quite similar to the recommended dependence of the quality factor which with acceptable accuracy describes differences in injuries of cell systems characterized by fast regeneration (critical organs of the first group) by small doses of different radiations. However, the maximum value of RBE for LET = 100 keV/μ reaches up to 45. This value can be still higher in cell systems with a low mitotic index if other biological factors affecting the initial slope are insignificant. Finally, still higher values of RBE can be expected in exposure to small radiation doses of tissue in conditions of anoxia as a result of the fact that the final slope of the survival curve increases more rapidly with LET. Thus, RBE factors in excess of 100 have been obtained experimentally in [14] for the case of crystalline lens clouding. It should be taken into account that the high theoretical values of RBE at small radiation doses are associated exclusively with the decrease of the yield per unit of γ radiation which serves as a standard. Reduction of RBE with an increasing mitotic index is due to the corresponding increase of radiation sensitivity of cells at small doses of γ radiation.

We have shown here the basic possibility of a microdosimetric approach to the evaluation of the yield of cell effects under the action of small doses of various kinds of radiation, the evaluation being based on rules of cell injuries observed in cases of large radiation doses. The microdosimetric approach to a quantitative description of cell damage can serve as a basis for a subsequent derivation of more substantiated quality factors.

In conclusion the author expresses sincere gratitude to I. B. Keirim-Marcus for stating the problem, useful discussions, and constant interest, and to L. S. Andreeva for helping with the calculations and preparing the manuscript.

LITERATURE CITED

1. Radiation Protection. Magnitudes, Units, Methods, and Instrumentation [Russian translation], Recommendations 19 and 20 of the ICRU, Atomizdat, Moscow (1974).
2. Radiation Protection Norms of Bulgaria, 69 [Russian translation], Atomizdat, Moscow (1972).
3. C. Shellabarger et al., in: Biological Effects of Neutron Irradiation, IAEA, Vienna (1974), p. 391.
4. I. V. Filyushkin, Atominaya Tekhnika za Rubezhom, No. 5, 29 (1974).
5. G. Barendsen, in: Proc. of 3rd Symp. Microdosimetry, Vol. 2, Luxemburg (1972), p. 905.
6. A. Kellerer and H. Rossi, Radiation Res., 47, 15 (1971).
7. A. Kellerer and H. Rossi, Current Top. Rad. Res. Quat., 8, 85 (1972).
8. H. Dertinger and H. Jung, Molecular Radiobiology Biology, Springer-Verlag (1970).
9. O. Houg and A. Kellerer, Stochastic Radiobiology [Russian translation], Atomizdat, Moscow (1969).
10. M. Loew, Theory of Probability [Russian translation], Mir, Moscow (1972).
11. P. Todd, Radiation Res. Suppl., 7, 196 (1967).
12. G. Barendsen, Intern. J. Radiation Biology, 10, No. 4, 317 (1966).

13. W. Sinklar and R. Morton, Radiation Res., 29, 450 (1966).
14. A. Kellerer, Radiation Res., 56, 28 (1973).

THE DEVELOPMENT OF GAMMA-RESONANCE (MÖSSBAUER) SPECTROSCOPY IN THE SOVIET UNION

I. P. Suzdalev

UDC 539.184.2

Gamma-resonance (Mössbauer) spectroscopy (GRS) has found wide application in various areas of solid-state physics, chemistry, and biology. During the 17 years of its existence, GRS has helped establish the electronic and magnetic structures of many compounds and has made a significant contribution to the understanding of the nature of dynamical effects in solid bodies, such as the dynamics of the oscillations of atoms, the diffusion of atoms, spin relaxation, the dynamics of electrons, and electron exchange. The application of GRS has proven very useful also in geology and mineralogy, for example, for determining the tin content in ores. The achievements of GRS are reflected in a series of Soviet and foreign monographs and reviews [1-4] as well as in the proceedings of international conferences on GRS: Sacle (France) – 1961, Dubna (USSR) – 1962, Varna (Bulgaria) – 1967, New York (USA) – 1968, Tikhan' (Hungary) – 1969, Dresden (GDR) – 1971, Israel – 1972, Bratislava (Czechoslovakian SSR) – 1973, Bendor (France) – 1974, and Cracow (Poland) – 1975.

Great progress has been achieved in the Soviet Union in the area of the application of GRS to fundamental and applied research, in particular, to structural chemistry, biology, solid-state physics, the investigation of the dynamics of the crystalline lattice, magnetic relaxation phenomena, magnetism, and catalysis. It seems advisable to consider in the present review basic research from a number of the applied areas.

Study of Materials. The application of GRS to the study of materials has brought appreciable returns in the creation of alloys with the necessary strength and magnetic properties, magnetic materials for computer technology – ferrites, glasses, polymers, and so on.

The investigations of alloys having wide practical application have been carried out mainly at the I. P. Bardin Ferrous Metallurgy Central Scientific-Research Institute, the Moscow Engineering Physics Institute, the Institute of Chemical Physics of the USSR Academy of Sciences, and the Institute for the Physics of Metals of the Ural Scientific Center of the USSR Academy of Sciences (Sverdlovsk).

The application of GRS to the investigation of alloys permits characterization of the dynamics of the crystalline lattice of alloys, magnetization and its temperature dependence, and the electron states. For example, GRS has been applied [5] to the investigation of ferriferous zirconium alloys used in reactor construction for the purpose of establishing the redistribution of iron atoms upon corrosion. It was discovered that a significant variation occurs in the phase composition of the alloys investigated at a temperature of 750°C and an air pressure of 10^{-2} mm Hg during the oxidation process. A solid solution of oxygen in combination with Zr_2Fe and a solid solution of iron in combination with ZrH are formed, and also α-Fe and α-Fe_3O_4 are formed in ZrH.

Alloys of value as magnetic materials having special properties (high coercive force, magnetization, and so on) were investigated, e.g., in [6-8]. The alloys Ticonal, $SmCo_5$, Invar, and Permaloy were studied. It was shown that the special properties of alloys are often produced by nonuniformities in the crystalline and magnetic structure, which are reliably established by GRS with the help of the detection of superparamagnetic behavior of individual microregions.

Investigations of ferrites have received a lot of attention at the Crystallography Institute of the USSR Academy of Sciences, the Institute of Chemical Physics of the USSR Academy of Sciences, and Moscow and

Translated from Atomnaya Énergiya, Vol. 40, No. 3, pp. 234-239, March, 1976. Original article submitted June 23, 1975.

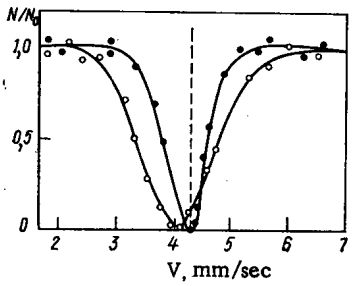

Fig. 1

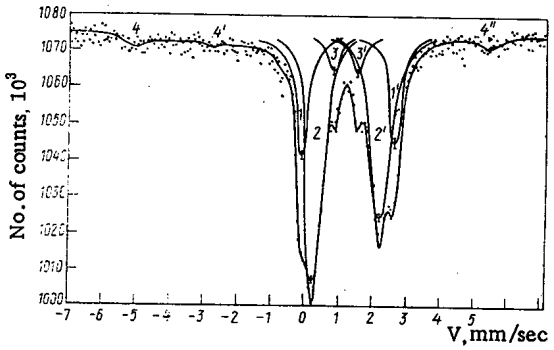

Fig. 2

Fig. 1. GR spectra of ^{119}Sn: ○) glass; ●) fiberglass.

Fig. 2. GR spectra of regolith returned by the Luna-16 spacecraft: 1, 1') olivine; 2, 2') pyroxene and pyroxenic glasses; 3, 3') ilmenite; 4, 4', and 4") metallic iron. The remaining spectral lines correspond to metallic iron and an alloy of iron with nickel.

Leningrad Universities. GRS is a very convenient and accurate method, since it permits determining the magnetization of individual sublattices and tracking down variations of the magnetic properties in the case of cation replacement. Chalcophile spinels and orthoferrites are very promising materials at present. Chalcophile spinels are observed to have a significant variation in their magnetic and electrophysical properties as well as a strong connection between them, which is important to the creation of materials having the correct properties. Gamma-resonance (GR) investigations of tin-substituted orthoferrites, which are widely applied in computer technology and magnetooptics [9] have shown that the nuclei of diamagnetic tin atoms are exceedingly sensitive to the local magnetic environment, the distortion of the crystalline structure, and alteration of the exchange interaction. Therefore, it is possible to use them as a unique measuring basis inside a ferrimagnetic matrix and control the variation of their properties upon replacement.

The structure of glasses is investigated with the aid of GRS mainly at the Institute of Physical Chemistry of the USSR Academy of Sciences and at the A. F. Ioffe Physicoengineering Institute of the USSR Academy of Sciences (Leningrad). The strong effect of modifying additives and the heat treatment conditions has been established in the study of oxide glasses with the aid of GRS. Since the production volume of oxide glasses is very large, even a small improvement in their mechanical properties as a result of heat treatment and the introduction of certain additives will have a large economic effect. One such additive is tin, which permits the application of GRS to ^{119}Sn nuclei. For example, it was established in [10] that the cooling rate depends strongly on the structure of the glass. Thus silicate and borosilicate glasses cooled at a slow rate have a polymeric structure and represent a two- or three-dimensional structure. Linear weakly branched structures are formed at a cooling rate of 10^4 deg/sec, which is attained in the drawing of a thin glass fiber. This results in the narrowing of the lines in the GR spectra (Fig. 1) due to a decrease in the scatter of the electric field gradients.

Chalcophile glasses have recently been widely applied in addition to the oxide glasses as special optical and semiconductor materials. A conclusion was drawn as to the transformation of the selenium in the glass from the crystalline state to an amorphous and a finely divided state in the course of a study of their properties with the help of GRS relative to a variation in the likelihood of the Mössbauer effect [11].

Mineralogical Phase Analysis. GRS is a very useful technique in the analysis of the phase composition of raw materials. A number of effective devices have been developed by the All-Union Scientific-Research Institute of Instrument Manufacture and the All-Union Scientific-Research Institute of Nuclear Geophysics and Geochemistry. A Mössbauer analyzer of cassiterite (MAK-1) which allows one to determine the tin content in ore to 0.1% under field conditions in a few minutes has, for example, received an extensive reputation. A GR analyzer of the phase composition of ferriferous ore (AZhM-1) has been developed which is intended for the quantitative determination of the content of iron phases (magnetite, hematite, etc.) [12]. For example, up to five ferriferous mineral components have been determined with an accuracy of 1% relative to iron for samples of iron ores from titanomagnetitic deposits. Quantitative relationships have been obtained between the system of undecomposed solid solution of titanium dioxide in magnetite and its decay products, which can characterize the technological value of ores, the quality of enrichment products, and the petrogenetic peculiarities of the deposit [13].

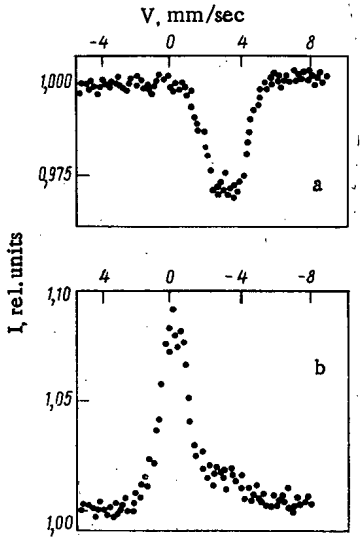

Fig. 3

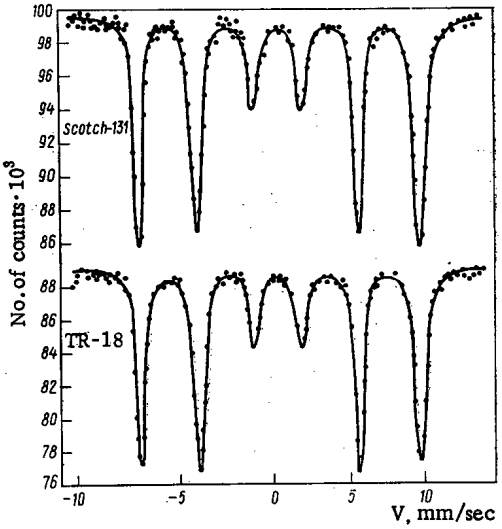

Fig. 4

Fig. 3. Adsorption (a) and emission (b) GR spectra of a frozen solution of $SnC_2O_4 \cdot 2H_2O$ in HCl.

Fig. 4. GR spectra of two kinds of magnetic recording tape with more highly oriented (TR-18) and less highly oriented (Scotch 131) γ-Fe_2O_3 particles.

GRS has been applied with success to the investigation of ore concentrates and the processes for their heat treatment. There has appeared in the course of investigation of the phase composition of iron-ore pourings and agglomerates the development in them of a significant amount of an amorphous phase which was not detected earlier by x-ray analysis, which increases the accuracy of the iron content determination. The investigation of the products of the autoclaved leaching out of pyrrhotine-containing concentrates has shown that mainly the oxide phases of iron – hematite, magnetite, and goethite – are formed during the decomposition of pyrrhotine (FeS_{1+x}). Quantitative relationships between these phases evidently depend upon the composition of the original concentrate and on the process conditions; the total amount of iron associated with these phases correlates well with the increase during the process of the amount of elemental sulfur. This provides for rapid indirect control of the leaching process, which is of great value in the extraction of nonferrous metals from the ores in question [14].

Geochemistry and Cosmochemistry. A new direction of GRS has developed in the area of geochemistry and cosmochemistry. There is great interest in the phase analysis carried out at the V. I. Vernadskii Institute of Geochemistry and Analytical Chemistry of the USSR Academy of Sciences [15] of the lunar regolith returned by the Luna-16 and Luna-20 spacecraft from mare and highland sites on the moon (Fig. 2). The following ferriferous minerals have been detected: pyroxenes and pyroxenic glasses, olivine, ilmenite, ulvospinel, and metallic iron. Fundamental differences have appeared between the mare and highland regolith: 1) there are more glasses in the pyroxenic component of the mare regolith; 2) the olivine of the mare regolith is more ferruginous; 3) there is more metallic iron in the mare regolith, and it is more dispersed; and 4) ilmenite predominates in the mare regolith, and ulvospinel replaces it in the highland regolith. The derived characteristics show that the minerals of the regolith from the lunar maria crystallized from a more reduced magma than did the minerals from the lunar highlands, which crystallized in an earlier process and at a greater depth.

A technique has been developed for applying a different kind of natural thermometer. A method of geothermometry based on determining the nature of the intracrystalline iron distribution (high-temperature diffusion in silicates) has been developed. A study of the kinetics of cation ordering has shown that the freezing temperature of cation exchange is very high in olivines (1100-1150°C), which makes the creation of an olivine thermometer promising. It has also been shown that a pyroxene thermometer may be applicable to the study of rapid geological processes, for example, explosive processes in kimberlite (diamond-bearing) pipes.

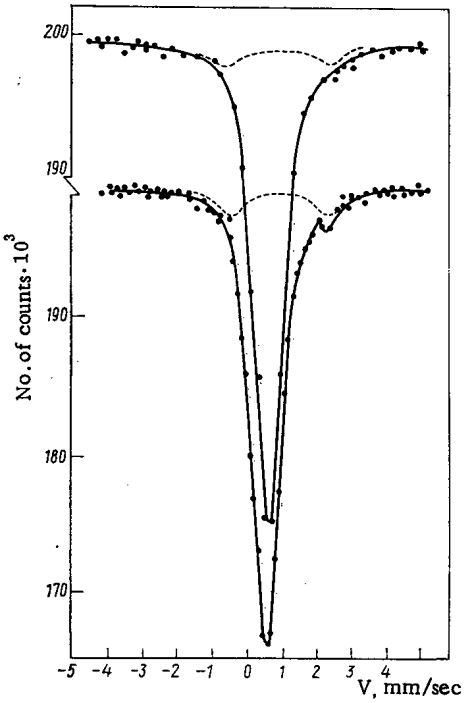

Fig. 5. GR spectrum of $CoMoO_4$-catalyzer prior to and after reaction (upper spectrum) and during the reaction (lower spectrum).

Chemical Results of Nuclear Transformations. GRS offers very interesting prospects, since it permits tracing the results of transformations and the stabilization forms of nuclei without destroying the material (for example, changing it into a solution). In addition, there is the possibility of tracing the processes occurring in a time of 10^{-7}-10^{-10} sec, which is comparable to the lifetime of the Mössbauer levels of nuclei. The practical and applied interest of such investigations is associated with the preparation of radiation sources and labelled compounds having the necessary properties, the enrichment of radioactive isotopes, and also the alteration of the properties of materials in response to radiation.

One of the promising trends in this area – the investigation of the stabilization forms of nuclei after radioactive transformations during 10^{-7}-10^{-10} sec – requires the inclusion of emission GRS, where the radiation source is used as the object being investigated. Mössbauer nuclei were investigated which undergo K capture, β decay, or take part in $n\gamma$, dp, pn, etc. reactions, in which the Mössbauer levels are populated after the radioactive transformations. This trend has been developed mainly at the Institute of Chemical Physics of the USSR Academy of Sciences and Leningrad and Moscow Universities.

A strong effect of the chemical bond has been observed on the nature of the atoms' stabilization after the radioactive transformations, along with a strong effect of the nature of the atoms' environment (its location in the crystalline lattice, in solution, or on the surface of adsorbents and ion-exchangers). Thus it was shown in [16] that the original structure is preserved with a probability of 90-40% in the case of an investigation of the results of K capture by ^{57}Co in groups having multidentate ligands (prophine groups of cobalt, groups of cobalt with the products of thiosemicarbazone), and in these cases one can judge from the emission GR spectra as to the structure of the original groups of cobalt. In the case of groups having unidentate ligands and the isolated structure of a crystal there occurred due to strong after-effects of K capture a powerful destruction of them, so that it is often difficult to ascertain the structure of the original compounds.

The effect of β decay and isomer conversion was studied in compounds of ^{125}Sb, ^{129}Te, and ^{121m}Sn [17]. A preservation was observed of the immediate surroundings of the atoms forming as a result of β decay. The daughter atoms ^{125}Te, ^{129}I, and ^{121}Sb were detected in valence states exceeding by one unit the valency of the parent atoms, which is responsible for the nature of nuclear transformation. Unusual states of the daughter atoms of ^{121}Sn were also observed in compounds of ^{121}Sn, which is probably associated with the result of single ionization due to a "shaking" effect.

The after-effects of the conversion isomeric transition of ^{119m}Sn were studied in frozen solutions of tin-containing salts [18]. The appearance of the results of nuclear transformations in these systems is shown in Fig. 3. The immediate surroundings strongly affect the stabilization form and the valence state of tin. Thus the addition of methyl alcohol results in a change in the valency of tin's stabilization forms from Sn^{4+} to Sn^{2+}.

Tapes for Video and Sound Recording. Compositions based on γ-Fe_2O_3 particles are the main coating on tapes used presently for video and sound recording. This situation permits the application of GRS to investigate the quality of magnetic recorder tapes, which is of great practical significance. An investigation has been carried out at the USSR Academy of Science's Institute of Chemical Physics on tapes allotted by the All-Union Television and Radio Broadcasting Scientific-Research Institute of the state of the γ-Fe_2O_3 particles on different kinds of tapes, and an attempt has been made to compare such parameters as the degree of magnetic orientation of the particles and the concentration of the coating particles determined by means of GRS with the results from other procedures [19]. These parameters are connected with the sensitivity and recording level of the tapes. It was discovered that GR spectra are very sensitive to the extent of the particles' orientation (Fig. 4). There is a possibility of determining the average inclination angle of the axes of particles having a needle-like shape with respect to the tape's plane from the

ratio of the strengths of the components of the spectrum's hyperfine structure. The average angle turned out to be in good agreement with the degree of magnetic orientation of the particles in the tape's plane determined from magnetic measurements. This characteristic is very important in the control of the magnetization level of the emulsion's particles during its deposition upon the base. The density of particle content is the second important characteristic of a tape, and it can also be determined with high accuracy by means of GRS. The result that paramagnetic layers are absent in the γ-Fe_2O_3 particles which form the tapes' coating has proven to be very interesting.

Catalysis. The important practical significance of catalysis has produced a heightened interest in the application of new procedures, and in particular, in GRS. Investigations of surface phenomena, started ten years ago, have now regenerated into investigations of catalytic reactions with the aid of GRS. Intense investigations in the area of catalysis are being carried out at the USSR Academy of Sciences' Institute of Chemical Physics and the Institute of Organic Catalysis and Electrochemistry of the Kazakhstan SSR's Academy of Sciences (Alma-Ata).

Recently, three basic approaches have been planned: 1) an investigation of the electronic state and structure of the catalyzer in the case of its modification and promotion (an increase in the catalytic activity with the help of additive-promoters); 2) a study of phenomena of atomic regroupings and topochemical transformations the cases of chemosorption and the action of reactive mixtures on the catalyzer; and 3) an investigation of the intermediate states which arise on the surface of the catalyzer in the actual course of the catalytic process.

The establishment of a correlation between the contact's activity and the physical and physicochemical properties of the system (point 1) is significant to the purposeful synthesis of new catalyzers with specified properties. The phenomena referred to in point 2 always accompany the actual catalytic process: The surface and surface layers of a crystal undergo in the course of the reaction significant rearrangements. It often happens that a catalyzer which is inactive at the start of a reaction is treated under the action of the reactive mixture and becomes active, and highly dispersed phases are formed. All of this can be very definitely traced with the help of GRS. Finally, the study of the intermediate states during catalysis (point 3) can result in a deeper understanding of the nature of the elementary catalytic event. For example, phase transitions and the rearrangement of the surface of a promoted iron catalyzer under the action of synthesis of high alcohols from Co and H_2 have been discovered with the help of GRS [20].

A macrocrystalline phase of ε-iron carbide is formed on the catalyzer during an extended synthesis. However, investigation of the formation of this new structure in the course of the catalyzer's "exploitation" is of special interest to catalysis. The catalyzer's activity during the initial period of its operation increases from zero to some constant value, which is accompanied (according to GRS data) by the formation of small clasts of ε-carbide ($\sim$50 Å).

As has already been noted, a new method – the combination of a GR-spectrometer with a catalytic reactor – has recently been applied in catalytic investigations [21]. The formulation of this procedure was accomplished at the USSR Academy of Sciences' Institute of Chemical Physics during the study of the oxidation reaction of propylene into acrolein, which is of great practical interest. It is shown in Fig. 5 how the spectrum of $CoMoO_4$ is changed with the addition of ^{57}Fe (3%) in the catalytic reaction process. The changes in the spectrum (the catalyzer's surface is 12 m^2/g) amounted to 5%, which is recorded with certainty and permits drawing conclusions as to the nature of the intermediate groups formed during catalysis. After the reaction's cessation, the catalyzer returned to its original condition, which corresponds to the initial spectrum.

Only a portion of those scientific-research institutes and groups at which GRS has been developed are mentioned in this review. There are presently 59 scientific-research institutes in the USSR at which GR research is being conducted in the area of solid-state physics, chemistry, and biology, and their number continues to increase. Significant progress in the area of the varied application of GRS in the Soviet Union, an increase in the breadth of coverage of the problems, inproving the accuracy of the spectroscopic data, and an increase in the proportion of quantitative results now place GRS on a par with such widespread spectroscopic methods as electron paramagnetic resonance, nuclear magnetic resonance, and so on, and based on certain indications they offer the possibility of surpassing these methods. All of this permits one to postulate that the rate of development of this comparatively new area of spectroscopy will not diminish in the future, and the areas of its application and popularity will grow.

LITERATURE CITED

1. V. I. Gol'danskii, The Mössbauer Effect and Its Application in Chemistry [in Russian], Nauka, Moscow (1963).
2. V. S. Shpinel', The Resonance of Gamma Rays in Crystals [in Russian], Nauka, Moscow (1969).
3. S. M. Irkaev, R. N. Kuz'min, and A. A. Opalenko, Nuclear Gamma Resonance [in Russian], MGU, Moscow (1970).
4. Chemical Applications of Mössbauer Spectroscopy [in Russian], Mir, Moscow (1970).
5. Yu. F. Babikova et al., At. Énerg., 38, No. 3, 138 (1975).
6. V. A. Makarov, Author's Abstract of Candidate's Dissertation, In-t Khim. Fiz., USSR Akad. Nauk SSSR, Moscow (1975).
7. V. A. Povitskii et al., Fiz. Metal. i Metalloved., 38, 1095 (1974).
8. L. Z. Men'shikov and E. E. Yurchikov, Zh. Éksperim. i Teor. Fiz., 63, 190 (1972).
9. I. S. Lyubutin, Author's Abstract of Doctoral Dissertation, In-t Kristollografii, Akad. Nauk SSSR, Moscow (1974).
10. G. M. Bartenev et al., Strukturnaya Khim., 14, 459 (1973).
11. P. P. Seregin et al., 5th International Conference on Mössbauer Spectroscopy, Theses. Bratislava, Sept. 3-7 (1973), p. 175.
12. V. I. Gol'danskii et al., Gamma-Resonance Methods and Devices for the Phase Analysis of Mineral Material, Atomizdat, Moscow (1974).
13. E. A. Ovsyannikov et al., op. cit. [11], p. 168.
14. A. G. Kitai et al., Tsvetnye Metally, No. 1, 11 (1975).
15. T. V. Malysheva, The Mössbauer Effect in Geochemistry and Cosmochemistry [in Russian], Nauka, Moscow (1975).
16. R. A. Stukan, Author's Abstract of Doctoral Dissertation, In-t Khim. Fiz., Akad. Nauk SSSR, Moscow (1974).
17. R. A. Lebedev et al., op. cit. [11], p. 162.
18. A. N. Murin et al., Khim. Vys. Énerg., 6, 494 (1972).
19. Yu. F. Krupyanskii et al., "An investigation of the structure and magnetic properties of tapes for video and sound recording on a γ-Fe_2O_3 base with the aid of GRS," Report from the USSR Academy of Sciences' Institute of Chemical Physics, Moscow (1974).
20. R. A. Arents, Author's Abstract of Candidate's Dissertation, In-t Khim. Fiz., Akad. Nauk SSSR (1974).
21. Yu. V. Maksimov et al., Dokl. Akad. Nauk SSSR, 221, 880 (1975).

NEW BOOKS FROM ATOMIZDAT*

V. E. Levin, Nuclear Physics and Nuclear Reactors [in Russian], Textbook for technical schools, 3rd edition, Atomizdat, Moscow (1975).

N. P. Galkin, V. A. Zaitsev, and M. B. Seregin, Collecting and Processing Fluorine-Containing Gases [in Russian], Atomizdat, Moscow (1975).

A. A. Moiseev and P. V. Ramzaev, Cesium-137 in the Biosphere [in Russian], Atomizdat, Moscow (1975).

K. A. Kapustinskaya and A. A. Makarenya, Metal from the "Stone of Hope" [in Russian], Atomizdat, Moscow (1975).

V. I. Davydov and S. B. Shikhov, Analytical Methods of Solution of Neutron Transport Equations [in Russian], Atomizdat, Moscow (1975), (The Physics of Nuclear Reactors [in Russian]).

P. A. Andreev, M. I. Grinman, and Yu. V. Smolkin, Optimization of the Thermal Energy Equipment of Atomic Electric Stations [in Russian], edited and with foreword by A. M. Petros'yanets, Atomizdat, Moscow (1975).

V. A. Sokolov, Generators of Short-Lived Radioactive Isotopes [in Russian], Atomizdat, Moscow (1975).

P. A. Andreev, M. I. Grinman, and Yu. V. Smolkin, Optimization of the Thermal Energy Equipment of Atomic Electric Stations [in Russian], A. M. Petros'yanets (editor), Atomizdat, Moscow (1975).

S. V. Serensen, The Resistance of Materials to Fatigue and Brittle Fracture [in Russian], Textbook for universities, Atomizdat, Moscow (1975).

R. S. Rezhnikov and Yu. P. Sel'dyakov, Industrial Semiconductor Detectors [in Russian], Atomizdat, Moscow (1975).

Plasma Chemistry [in Russian], Collection of articles, 2nd Issue, B. M. Smirnov (editor), Atomizdat, Moscow (1975).

A. B. Mikhailovskii, The Theory of Plasma Instabilities, Vol. I. Instability of a Uniform Plasma [in Russian], 2nd Edition, Revised and Supplemented, Atomizdat, Moscow (1976).

E. D. Lozanskii and O. B. Firsov, The Theory of a Spark [in Russian], Atomizdat, Moscow (1976).

Yu. Tel'deshi, T. Braun, and M. Kirsh, Analysis by the Method of Isotope Dilution (VNR, 1972), Translated from the English, edited by Yu. V. Yakovlev, Atomizdat, Moscow (1975).

R. M. Al'tovskii and A. S. Panov, Corrosion and the Compatibility of Beryllium [in Russian], Atomizdat, Moscow (1975).

R. F. Konopleva and V. I. Ostroumov, The Interaction of High-Energy Charged Particles with Germanium and Silicon, Atomizdat, Moscow (1975).

Problems in Reactor Protection Physics [in Russian], Collection of articles, 7th issue, edited by A.P. Veselkin, Yu. A. Egorov, S. G. Tsypin, et al. (editors), Atomizdat, Moscow (1975).

The Design and Construction of Radioisotope Radiation Chemistry Installations [in Russian], Handbook, E. E. Kulish (editor), Atomizdat, Moscow (1975). (Authors: E. E. Kulish, V. B. Osipov, B. M. Terent'ev, E. D. Chistov, A. V. Larichev, Yu. I. Bregadze, B. I. Ryabov, V. A. Gol'din, D. A. Kaushanskii, M. F. Romantsev, and I. F. Sprygaev).

*4th quarter of 1975.

Translated from Atomnaya Énergiya, Vol. 40, No. 3, p. 239, March, 1975.

DYNAMICS OF TRANSMISSION OF HIGH-FREQUENCY POWER DURING MAGNETOSONIC HEATING OF A PLASMA IN A TOKAMAK

N. V. Ivanov and I. A. Kovan

UDC 533.9:621.039.61

One promising method of auxiliary heating of a plasma in tokamak devices is the method of magnetosonic resonance. This method is based on the use of the characteristic magnetosonic oscillations of a plasma pinch ensuring effective introduction of high-frequency (hf) energy deep into the interior of a plasma. Oscillations are usually excited by means of loop exciters positioned in the shadow of the diaphragm and connected to a hf generator. Under resonance conditions in the circuit of the exciter loop there is inserted an active component of resistance, which determines the load of the hf generator, and depends on the plasma parameters. The present study is devoted to calculating this inserted resistance by the method of expansion in eigenfunctions of the plasma resonator with account of the inhomogeneity of its filling by a plasma and its nonstationarity in time, and also by a comparison of the calculation results with the experimental data obtained on a TO-1 tokamak.

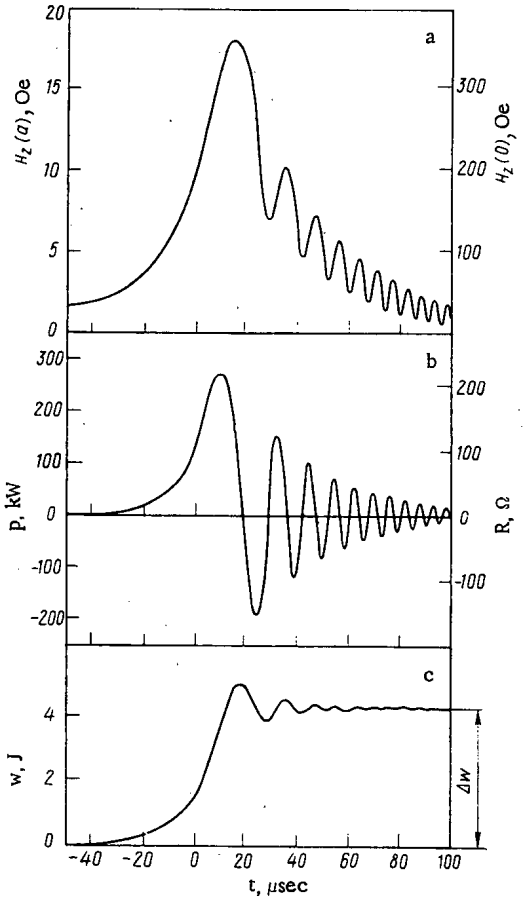

Fig. 1. Calculated dynamic characteristics of plasma resonator: a) amplitude of longitudinal hf magnetic field on the wall of the chamber $H_z(a)$ and on axis $H_z(0)$; b) hf power P and inserted active resistance; c) energy (w).

Calculations were carried out for three cases of resonance: for stationary resonance (the characteristic frequency of the plasma resonator does not vary with time), for quasistationary resonance (for the "time of established oscillations" $2Q/\omega$, the oscillation phase varies insignificantly), and for dynamic resonance (when the quasistationarity condition is not satisfied).

It is shown that whereas in the stationary case the hf power is proportional to the quality factor of the plasma resonator, in quasistationary and dynamic regimes the time-averaged hf power is independent of the quality factor, and increases in proportion to the density of the spectrum of the characteristic oscillations. In this case the transmission of energy in the plasma occurs by means of portions connected with successive excitation of different types of characteristic oscillations. The calculated dynamic characteristics of the plasma resonator obtained under the experimental conditions for the TO-1 tokamak are shown in Fig. 1.

In the present study we obtain analytical formulas for the inserted resistance, in which there enter numerical coefficients that depend on the form of the spatial distribution

Translated from Atomnaya Énergiya, Vol. 40, No. 3, pp. 240–243, March, 1976.

of the plasma density in the tokamak. The coefficients are calculated on a computer for the 30 lowest types of radial oscillations by means of integrating the spatial part of the wave equation with variable coefficients. Calculations were carried out for the model of a plasma cylinder with different axisymmetric forms of radial distribution of plasma density. The calculation results are shown graphically. Based on them we can conclude that for a bell-shaped profile of radial distribution of plasma density, the fields of the characteristic oscillations are concentrated towards the axis of the plasma pinch. In comparison with the homogeneous density distribution, this leads, on the one hand, to a decrease in the coupling between the resonator and the exciter, and on the other hand, to a reduction in the energy loss at the wall of the chamber and the peripheral regions of the plasma.

Original article submitted February 17, 1975.
Abstract submitted October 24, 1975.

APPLICABILITY OF THE METHOD OF MAGNETOSONIC HEATING FOR THERMONUCLEAR PARAMETERS OF A PLASMA IN A TOKAMAK

N. V. Ivanov and I. A. Kovan

UDC 533.9:621.039.61

In the present article we consider the applicability of the method of magnetosonic heating for thermonuclear parameters of a plasma in a tokamak. In order to do this we determine the limits within which the quality factor of the plasma should lie, in order to ensure introduction into the tokamak with the help of a single-turn exciter of hf power equal to the power of the loss of thermal energy from the plasma. As an example we consider a tokamak operating on a mixture of deuterium and tritium, having the following parameters: plasma temperature $T = T_e = T_i = 2 \cdot 10^4$ eV, charged-particle density $n = 10^{14}$ cm^{-3}, $n\tau = 2 \cdot 10^{14}$ cm$^{-3} \cdot$ sec, toroidal magnetic field $H_0 = 50$ kOe, and aspect ratio $R/a = 4$. It is assumed that the chamber wall of the tokamak and the exciting loop are made from a material having conductivity $\sigma = 5 \cdot 10^{16}$ cgse units. Although the selected plasma parameters can evidently be obtained only in apparatus of sufficiently large dimensions, in the study no constraints are placed on these dimensions and the limits within which the quality factor must lie are found as a function of the minor radius of the tokamak chamber. The criteria determining the quality factor are high efficiency of heating, sufficient electrical strength, and the possibility of cooling the exciter loop. In the article we consider weakly diagonal axisymmetric magnetosonic oscillations in the cylindrical approximation. They are excited in the plasma by a loop encompassing the plasma pinch and distributed in a special annular depression in the chamber wall.

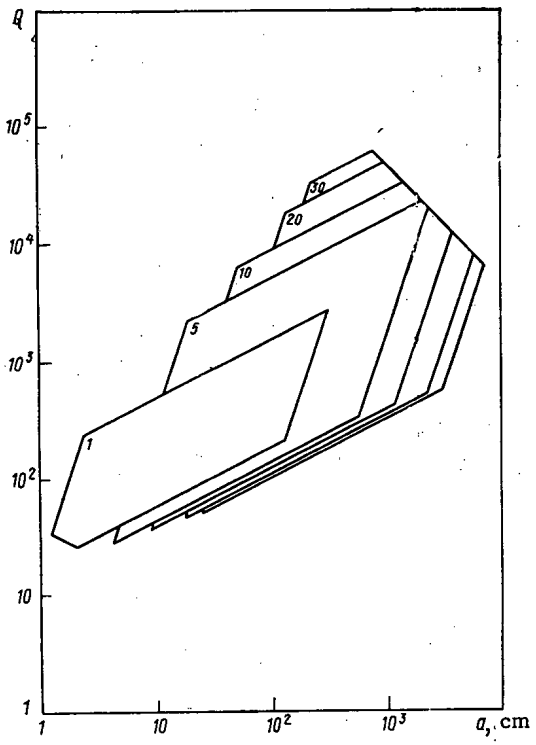

Fig. 1. Regions of admissible values of quality factor of the plasma suitable for heating. The numerals denote the number of the radial types of oscillations.

The obtained constraints on the quality factor of the plasma are shown in Fig. 1 for different types of oscillations for a parabolic profile of the radial distribution of the plasma density. We see from Fig. 1 that there are broad regions of values of quality factor and dimensions of the tokamak in which all the enumerated conditions are satisfied simultaneously.

The physical mechanisms of dissipation of energy of the magnetosonic oscillations, which have been investigated in a large number of theoretical and experimental studies,

are not discussed in the present article. As is shown by estimates, in the conditions under consideration it is entirely possible to use collisionless mechanisms such as cyclotron resonance and Cerenkov radiation. However, their exact account as applied to a tokamak requires additional investigation.

Original article submitted May 21, 1975.
Abstract submitted October 24, 1975.

METHOD OF CORRECTION OF MACROSCOPIC CONSTANTS OF FAST SYSTEMS BASED ON RESULTS OF INDIVIDUAL EXPERIMENTS

Yu. Yu. Vasil'ev, V. N. Gurin, and B. G. Dubovskii

UDC 621.039.51

At the present time in the field of reactor physics, experimental methods are used that enable us to obtain neutron-physical parameters of breeder systems without carrying out full-scale critical experiments. One of these methods is the substitution method which consists of the replacement of part of the reference critical system with an insert of the material being investigated [1-3]. A general shortcoming of the known modifications of the substitution method is the requirement that the spectra of the insert and the reference zone be close, and also the need for carrying out a series of experiments based on the substitution. The proposed method consists of the correction based on the least-squares method of the set of macroscopic constants of the insert for optimum description of a certain set of integral characteristics of the two-zone composition under investigation. The sensitivity coefficients, which determine the linear relation between the variations of the integral characteristics being described (in the present study – the effective multiplication constant of the neutrons) and the group macroconstants being corrected, are determined with the use of the generalized perturbation theory [4]. Experiments were analyzed by replacing with the MASURCA series [5]. Calculations were carried out in the diffusion three-group approximation for a one-dimensional cylindrical geometry. Values are obtained for the material parameter and the error in its prediction. We detect a weak dependence of the values of the predicted material parameter on the volume fraction of the insert, and good agreement with the experimentally measured value. Thus, for volume fraction of the insert 3% in the core, the divergence with the experiment is 4%.

An algorithm developed in the paper enables us, if necessary, to use very exact approximations of the kinetic equation.

LITERATURE CITED

1. R. Persson, in: Proc. IAEA Symp. Exponential and Critical Experiments, Vol. 3, Vienna (1964), p. 289.
2. In: Proc. Intern. Conf. on Fast Critical Experiments and Analysis, ANL-7320, Argonne (1966), p. 439.
3. F. Helm, Trans. Amer. Nucl. Soc., 11, 595 (1968).
4. L. N. Usachev, At. Énerg., 15, No. 6, 472 (1963).
5. A. Schmitt et al., in: Proc. IAEA Symp. Exponential and Critical Experiments, Vol. 1, Vienna (1964), p. 81.

Original article submitted March 17, 1975.
Revision submitted July 30, 1975.

OPTIMAL ELECTRON-POSITRON CONVERSION AT HIGH ENERGIES

V. A. Tayurskii

UDC 539.124.6

The positron beams for e^+-e^- colliding-beam experiments are obtained by electron conversion at 100 MeV or more in dense targets; the number of positrons taken up by the storage ring is governed by the conversion efficiency for electrons of energy E_-, the product being positrons of the required energy E_+, together with the acceptance factor, which is dependent on the radial and vertical acceptances ε_r and ε_z in the ring, together with the beam emittance ε_+.

Two methods of increasing the number of accepted positrons are considered for conversion from initial energies of $100 \leq E_- \leq 1000$ MeV, the positrons being of low energy. The first consists of raising the conversion efficiency for low-energy positrons ($E_+ \lesssim E_s$, where $E_s = 21$ MeV is the characteristic Coulomb-scattering energy). This involves using a thin cylindrical converter, in which repeated scattering allows a large fraction of the positrons having $E_+ \lesssim E_s$ to escape through the side walls. Estimates indicate that the positron spectrum for such a converter takes the form

$$\frac{dN_+}{dE_+} \approx 0.0023 \frac{E_-^{0,82}}{E_+^{1,82}} \ln (27E_+)\, T, \tag{1}$$

where $0.5 \gtrsim T/t_{max} \leq 2.5$, T is the converter length (in radiation units), and $t_{max} = 0.73 (E_-/E_+)^{0.38}$ is the position of the peak on the cascade curve for the photons [1]. For a converter in the form of a plate, the positron spectrum for an optimal thickness as regards positron yield takes the form:

$$\frac{dN_+}{dE_+} \approx 0.045 \frac{E_- + 37.5}{(E_+ + 12.8)^2};\ 1.5 \leqslant E_+ \leqslant 20 \text{ MeV}. \tag{2}$$

It follows from (1) and (2) that the yield of positrons having $E_+ \lesssim E_s$ from the cylinder is larger by a factor 2-3 than that from a plate. The second method consists of reducing the beam emittance for low-energy positrons by focusing the positrons directly in the cylindrical converter by means of an axially symmetrical magnetic field, which is produced by a heavy current pulse. It is found that the beam emittance is reduced in proportion to $1/\sqrt{B_0}$ by the focussing (B_0 is the field at the surface of the converter). Expressions (1) and (2) have been derived from formulas that approximate the $e^{-\gamma}$ shower characteristic for lead [1]. Monte Carlo calculations are presented based on the program of [2]. The estimates of [1] and [2] agree satisfactorily with the calculations, as do the focussing estimates.

LITERATURE CITED

1. H. Nagel, Z. Phys., 186, 319 (1965).
2. F. M. Izrailev et al., Preprint, Nuclear Physics Institute, SO Akad. Nauk SSSR, No. 63-73 (1973).

Original article submitted July 16, 1975.

CALCULATION OF RELEASED ENERGY AND TOTAL TRACK LENGTHS OF CHARGED PARTICLES IN SHOWERS IN XENON

M. Ya. Borkovskii and S. P. Kruglov

UDC 539.122.04

In this paper, the mean values of the total track lengths of charged particles and the energy released in the development of electron–photon showers in xenon are calculated by Monte Carlo methods, as are the rms spreads of those values. Xenon is used as a filling for bubble chambers and flash tubes by virtue of its shower properties (critical energy E_{cr} and radiation length X_0) with respect to TF-1, TF-5, and SF-1 heavy lead glass, CsI scintillators recording gamma rays, and iron employed to ensure radiation protection for accelerators.

In carrying out the calculations, use was made of a shower-modeling program with the aid of which showers in lead were calculated [M. Ya. Borkovskii and S. P. Kruglov, Yad. Fiz., 16, No. 8, 349 (1972)]. Charged particles were traced until their total energy had decreased to $E'_e = 7\ mc^2$, and gamma rays, to an energy of $E'_\gamma = 0.3\ mc^2$ (m is the electron mass and $mc^2 = 0.511$ MeV).

The mean value $\bar{L}$ of the total track length and the spread $\sigma(L)$ were found for the particles of a shower inside conical volumes with the cone axis in the direction of the primary gamma-ray momentum. It turned out that at angles of $\alpha > 15°$ (the angle formed by the cone with its axis) and a cone altitude of $l < 15X_0$ ($X_0 = 8.38$ g/cm^2), $\bar{L}$ and $\sigma(L)$ depend weakly on α. The magnitude of the rms spread $\sigma(L)$ of the track length increases at small l's, reaches a maximum, and then decreases, approaching some value [dependent on α and the primary gamma-ray energy $E(\gamma)$]. For $\alpha = 15$ to 90° and $E_\gamma = 50$ to $2 \cdot 10^3$cm^2, the value of $\sigma(L)$ proves to be 1.1 to 3 times greater at the maximum than as $l \to \infty$ (l is reckoned from the point of interaction of the primary gamma ray). For $\alpha = 90°$ and $l = 30X_0$, the value of $\bar{L}$ and $\sigma(L)$ are well described by the simple equations $\bar{L} = aE_\gamma$ and $\sigma(L) = b\sqrt{E_\gamma}$, with an error of 1 and 8%, respectively, where

$$a = 0.0236X_0mc^2; \quad b = 0{,}036X_0/\sqrt{mc^2}.$$

The mean values $\bar{E}_b$ of the released energy and their rms spread $\sigma(E_b)$ were obtained for cylindrical volumes of various sizes; the primary gamma ray travels along the cylinder axis. If the point of conversion of the primary gamma ray is fixed on the basis of a cylinder, then $\sigma(E_b)/\bar{E}_b$ proves to be smaller than when it is not fixed. In all cases $\sigma(E_b)$ has a maximum at some depth and thus tends to zero as l increases. The energy distribution with depth for large l and $R = 15X_0$ is well described by an exponential curve with exponent $0.3\,l$ (l is expressed in radiation lengths X_0).

Original article submitted October 10, 1975.

LETTERS

MOMENTS OF NEUTRON DENSITY DISTRIBUTION FUNCTIONS

A. A. Kostritsa and E. I. Neimotin

UDC 621.039.51.12:539.125.52

In [1], the second spatial moment $\langle x^2(t)\rangle$ of the time-dependent neutron density distribution function is found by the random walk method. The appearance of this paper initiated a discussion during the course of which a number of researchers [2] showed how to obtain the moments of a distribution function directly from the one-velocity Boltzmann equation. A simple method for calculating the moments was utilized in [3], where $\langle x^2(t)\rangle$ was also found. In a note [4], the question of obtaining the moments of a spatial distribution of particles undergoing n collisions with the atoms of the medium from the linear transport equation was asked. For the special case of the stationary problem (with isotropic scattering) this question has been answered previously [5] by the method proposed in [6]. We shall cite similar arguments for the nonstationary case, taking into consideration the anisotropy of the scattering and the possible anisotropy of the neutron source. The medium is assumed to be homogeneous and infinite.

Utilizing the method of successive collisions for solving the transport equation and the Fermi–Marshak method for calculating the moments of the functions satisfying the kinetic equation, one can obtain detailed information concerning the evolution of the neutron momentum in space and time. Knowledge of the moments of the distribution functions for particles undergoing a fixed number of collisions is useful in practice for calculations using the Monte Carlo method, for the appropriate generalization to multigroup problems, and for comparison with experimental results.

Let us write the kinetic equation for a two-dimensional geometry in the form:

$$\frac{\partial N}{\partial t}+v\mu\frac{\partial N}{dx}+v\Sigma N=\frac{v\Sigma_s}{2}\sum_{i=0}^{\infty}c_iP_i(\mu)\int_{-1}^{+1}P_i(\mu')\,N\,d\mu'+S, \tag{1}$$

where $N(x, \mu, t)$ is the neutron density function; Σ_S and Σ are the scattering and total cross sections, respectively; v is the neutron speed; c_i are the coefficients of expansion of the scattering function in a series of Legendre polynomials $P_i(\mu)$[$c_0 = 1$; $c_1 = 3\bar{\mu}$, where $\bar{\mu}$ is the mean cosine of the scattering angle]; $S = S(\mu)\delta(x)\delta(t)$ is the local momentum neutron source. Let us denote the density function for the number of particles undergoing k collisions by $N^{(k)} = N^{(k)}(x, \mu, t)$. Then, one can obtain the mean-square of the departure from the source for particles undergoing k collisions from the formula

$$\langle x_k^2(t)\rangle=\frac{\int_{-\infty}^{+\infty}dx\,x^2\int_{-1}^{+1}N^{(k)}\,d\mu}{\int_{-\infty}^{+\infty}dx\int_{-1}^{+1}N^{(k)}\,d\mu}=-\frac{\int_{-1}^{+1}d\mu\left[(\partial^2/\partial q^2)\int_{-\infty}^{+\infty}N^{(k)}\,e^{-iqx}\,dx\right]_{q=0}}{\int_{-1}^{+1}d\mu\left[\int_{-\infty}^{+\infty}N^{(k)}\,e^{-iqx}\,dx\right]_{q=0}}. \tag{2}$$

In order to find the moments of the distribution function, it is sufficient to know the value of the Fourier transform and its derivatives at the origin of the coordinate plane of the complex variable q, the parameter of the Fourier transform.

Let us introduce the notation:

$$F=\int_{-\infty}^{+\infty}dx\,e^{-iqx}\int_{-\infty}^{+\infty}N\,e^{-i\omega t}\,dt; \tag{3}$$

$$\psi=\int_{-\infty}^{+\infty}dx\,e^{-iqx}\int_{-\infty}^{+\infty}S\,e^{-i\omega t}\,dt. \tag{4}$$

Translated from Atomnaya Énergiya, Vol. 40, No. 3, pp. 244-245, March, 1976. Original article submitted May 23, 1974.

Let us proceed from Eq. (1) to the system of equations for the Fourier transform of the function $N^{(k)}$:

$$(i\omega + iqv\mu + v\Sigma)\, F^{(0)} = \psi; \tag{5}$$

$$(i\omega + iqv\mu + v\Sigma)\, F^{(k)} = (v\Sigma_s/2) \sum_{i=0}^{\infty} c_i P_i(\mu)\, F_i^{(k-1)}, \tag{6}$$

where

$$F_i^{(k-1)} = \int_{-1}^{+1} F^{(k-1)} P_i(\mu)\, d\mu. \tag{7}$$

Integrating Eqs. (5) and (6) term by term with respect to $d\mu$, it is easy to find

$$[F_0^{(k)}]_{q=0} = \left(\frac{v\Sigma_s}{i\omega + v\Sigma}\right)^{k+1} \frac{\psi_0}{v\Sigma_s}, \tag{8}$$

where

$$\psi_i = \int_{-1}^{+1} \psi P_i(\mu)\, d\mu. \tag{9}$$

Let us find the second derivative of $F_0^{(k)}$ with respect to dq at q = 0. Performing term by term differentiation in Eq. (6) and integrating with respect to $d\mu$, we obtain

$$(i\omega + v\Sigma)\left[\frac{\partial^2 F_0^{(k)}}{\partial q^2}\right]_{q=0} + 2iv\left[\frac{\partial F_1^{(k)}}{\partial q}\right]_{q=0} = v\Sigma_s\left[\frac{\partial^2 F_0^{(k-1)}}{\partial q^2}\right]_{q=0}. \tag{10}$$

For the second term in Eq. (10), we construct the equation

$$(i\omega + v\Sigma)\left[\frac{\partial F_1^{(k)}}{\partial q}\right]_{q=0} + iv\int_{-1}^{+1} \mu^2 F_{q=0}^{(k)}\, d\mu = \frac{v\Sigma_s}{3} c_1 \left[\frac{\partial F_1^{(k-1)}}{\partial q}\right]_{q=0}. \tag{11}$$

We obtain the second term in Eq. (11) with the aid of Eqs. (5) and (6):

$$\int \mu^2 F_{q=0}^{(k)}\, d\mu = \left(\frac{v\Sigma_s}{i\omega + v\Sigma}\right)^{k+1} \frac{\psi_0 + 2(c_2/5)^k \psi_2}{3v\Sigma}. \tag{12}$$

Substituting this result into Eq. (11), we obtain

$$\left[\frac{\partial F_1^{(k)}}{\partial q}\right]_{q=0} = -\frac{i}{3v\Sigma_s^2}\left(\frac{v\Sigma_s}{i\omega + v\Sigma}\right)^{k+2}\left(\frac{c_1}{3}\right)^k\left[\psi_0 \sum_{j=0}^{k}\left(\frac{3}{c_1}\right)^j + 2\psi_2 \sum_{j=0}^{k}\left(\frac{3c_2}{5c_1}\right)^j\right]. \tag{13}$$

Substituting Eq. (13) into Eq. (10), after simple algebraic transformations we find

$$\left[\frac{\partial^2 F_0^{(k)}}{\partial q^2}\right]_{q=0} = -\left(\frac{v\Sigma_s}{i\omega + v\Sigma}\right)^{k+3} \frac{2\psi_0 Q}{3v\Sigma_s^2}, \tag{14}$$

where

$$Q = 1 + \frac{k}{1-\bar{\mu}} - \frac{\bar{\mu}^2[1-(\bar{\mu})^k]}{(1-\bar{\mu})^2} + \frac{2\psi_2}{\psi_0}\frac{1}{1-\frac{c_2}{5\bar{\mu}}}\left[\frac{1-(\bar{\mu})^{k+1}}{1-\bar{\mu}} - \frac{c_2}{5\bar{\mu}}\frac{1-(c_2/5)^{k+1}}{1-\frac{c_2}{5}}\right]. \tag{15}$$

In Eqs. (8) and (14) we make an inverse Fourier transformation for the dependence on time and substitute the results obtained into Eq. (3). The mean-square departure from the source (as a function of time) for particles undergoing k collisions with atoms of the medium is equal to

$$\langle x_k^2(t)\rangle = \frac{2v^2t^2}{3(k+1)(k+2)} Q. \tag{16}$$

For an isotropic neutron source $\psi_2 = 0$ and Eq. (16) corresponds to Eq. (18) in [1].

From Eq. (16) there follows the obvious conclusion that at a given moment of time the mean-square of the distance of the neutrons from the source is greater for those neutrons which underwent fewer collisions. The effect of the anisotropy of the source basically reduces to an increase in the moments, which is easily seen from the quantity $\langle x_k(t)\rangle$:

$$\langle x_k(t)\rangle = \frac{vt}{k+1}\frac{\psi_1}{\psi_0}\frac{1-(\bar{\mu})^{k+1}}{1-\bar{\mu}}. \tag{17}$$

The finding of higher-order moments encounters some basic difficulties.

Knowing Eqs. (8) and (14) and integrating them over the period of influence of the sources, one can find the formula for a stationary distribution:

$$\langle x_2^k \rangle = \frac{2}{3\Sigma^2} Q. \tag{18}$$

Utilizing the technique presented, one can investigate the moments of a distribution function satisfying the transport equation with an energy dependence for certain special cases involving velocity-dependent cross sections [7].

LITERATURE CITED

1. C. Barnett, Nucl. Sci. and Engng., 50, 398 (1973).
2. G. Pomraning, Nucl. Sci. and Engng., 52, 144; E. Cohen, 280; E. Canfield, 53, 137; B. Ganapol, 350 (1973).
3. T. E. Zima et al., At. Énerg., 31, No. 2, 154 (1971).
4. C. Barnett, Nucl. Sci. and Engng., 52, 281 (1973).
5. T. E. Zima et al., Izv. Akad. Nauk KazSSR, Ser. Fiz.-Mat., No. 6, 77 (1970).
6. I. G. Dyad'kin, Zh. Éksperim. i Teor. Fiz., 34, 1504 (1958).
7. T. E. Zima et al., At. Énerg., 33, No. 2, 700 (1972).

EFFICIENCY OF A SCINTILLATION GAMMA DETECTOR IN AN ISOTROPIC RADIATING MEDIUM

Yu. A. Sapozhnikov, V. A. Lopatin, and V. P. Ovcharenko

UDC 539.107.43

The activity of gamma emitters in isotropic radiating–absorbing media is identified and estimated quantitatively from the total absorption peaks of primary gamma radiation recorded by gamma spectroscopic equipment.

The purpose of the present paper is to estimate the magnitude of the total absorption peak of primary gamma radiation of a given energy. This quantity can be determined by calculating the gamma flux incident on the detector and the probability of its total absorption in the crystal.

Graphical integration for point isotropic sources showed that the efficiency of commonly used cylindrical crystals of diameter and height d is only slightly different from that of spherical detectors having the same volume with a radius given by the relation [1]

$$R^3=\frac{3}{16}d^3. \tag{1}$$

In the present paper we make the calculation in spherical geometry using spherical coordinates r, θ, φ with the origin at the center of the crystal. The medium is characterized by the linear absorption coefficient μ_1 (cm^{-1}) and the source density A (photons/$cm^3 \cdot$ sec); the crystal has a linear absorption coefficient μ_2 (cm^{-1}) and a radius R (Fig. 1).

The gamma flux incident on the crystal from an element of volume $dV = r^2 \sin\theta d\theta d\varphi dr$ of the surrounding medium is

$$d\Phi_0 = A\,(4\pi)^{-1}\,e^{-\mu_1 x}\,dV\,d\Omega, \tag{2}$$

where $A/(4\pi)$ is the number of photons emitted from a unit volume of the medium per unit solid angle per unit time, $d\Omega$ is an element of solid angle, and x is the distance from the volume element dV to the element of area $d\sigma$ (Fig. 1).

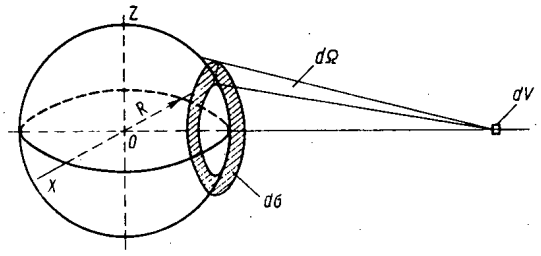

Fig. 1. Derivation of formula for calculating flux of primary gamma radiation incident on a spherical crystal.

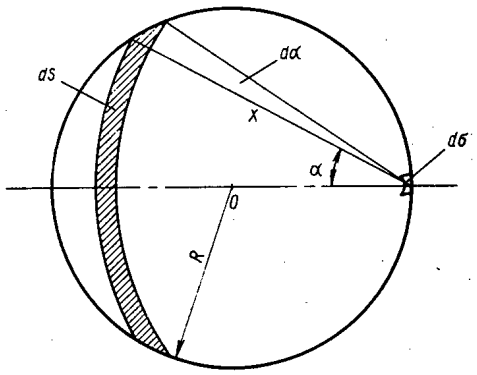

Fig. 2. Derivation of formula for calculating the efficiency of a spherical scintillation crystal.

Translated from Atomnaya Énergiya, Vol. 40, No. 3, pp. 246-247, March, 1976. Original article submitted October 24, 1974.

After substituting the expressions for dV and $d\Omega = \pi(r^2-R^2-x^2)(x^2r)^{-1}dx$ into Eq. (2) we obtain

$$d\Phi_0 = A(r^2-R^2-x^2)\, r\,(4x^2)^{-1}\, e^{-\mu_1 x} \sin\theta\, d\theta\, d\varphi\, dr\, dx. \tag{3}$$

The total gamma flux is determined by integrating Eq. (3) over the volume of the medium and over x from $x = r-R$ to $x = \sqrt{r^2-R^2}$:

$$\Phi_0 = 4^{-1}A \int_0^{\pi} \sin\theta\, d\theta \int_0^{2\pi} d\varphi \int_R^{\infty} dr \int_{r-R}^{(r^2-R^2)^{1/2}} (r^2-R^2-x^2)\, rx^{-2}\, e^{-\mu_1 x}\, dx. \tag{4}$$

The integration over θ and φ gives 4π, and Eq. (4) becomes

$$\Phi_0 = \pi A\left[\int_R^{\infty} dr \int_{r-R}^{(r^2-R^2)^{1/2}} r^3x^{-2}\, e^{-\mu_1 x}\, dx - \int_R^{\infty} dr \int_{r-R}^{(r^2-R^2)^{1/2}} R^2 rx^{-2}\, e^{-\mu_1 x}\, dx - \int_R^{\infty} dr \int_{r-R}^{(r^2-R^2)^{1/2}} re^{-\mu_1 x}\, dx\right]. \tag{5}$$

The terms in square brackets are denoted by J_1, J_2, and J_3 respectively. Making the substitutions $\nu = \mu_1 R$ and $\tau = x/R$ and changing the order of integration gives the following expressions:

$$J_1 = R^3\left(\nu^{-2}+\nu^{-1}+\int_0^{\infty} e^{-\nu\tau}\tau^{-1}\, d\tau\right); \quad J_2 = R^3\int_0^{\infty} e^{-\nu\tau}\tau^{-1}\, d\tau; \quad J_3 = R^3\nu^{-2}. \tag{6}$$

The integrals for J_1 and J_2 diverge logarithmically as $\tau \to 0$, but because of the compensation of the divergences a finite expression is obtained from (5) for the number of photons incident on the spherical crystal per unit time:

$$\Phi_0 = \pi R^2 A \mu_1^{-1}. \tag{7}$$

Equation (7) for the total gamma flux agrees with the expression given in [2], where Φ_0 was found by calculating the effective volume of the medium from which radiation enters the counter. However, the counting efficiency was not computed in [2].

The counting efficiency ε is defined as the ratio of the number of photons Φ interacting with the material of the crystal to the total number of photons Φ_0 incident on the crystal per unit time. The flux density of the gamma radiation incident on the surface of a spherical crystal is $I = \Phi_0/(4\pi R^2)$. The number of photons passing through the element of area $d\sigma$ on the surface of a spherical crystal (Fig. 2) into the solid angle $d\omega$ within the crystal per unit time is $d\Phi_0 = I(4\pi)^{-1}d\sigma d\omega$.

The fraction of this flux which interacts with the material of the crystal is:

$$d\Phi = (1-e^{-\mu_2 x})\, d\Phi_0. \tag{8}$$

Using Eq. (8) the efficiency ε of a spherical detector becomes

$$\varepsilon = 1-(1-e^{-2\lambda})\,(2\lambda)^{-1}, \tag{9}$$

where $\lambda = \mu_2 R$.

Reference 3 gives

$$\varepsilon = 1-2(\lambda+1)\lambda^{-2}e^{-\lambda},$$

which for $\lambda \ll 1$ has the physically wrong asymptotic behavior $\varepsilon = -2\lambda^{-2}$, and if only for this reason cannot be considered correct. Equation (9) shows physically reasonable asymptotic behavior for $\lambda \ll 1$ (weak gamma absorption in the detector) and for $\lambda \gg 1$ (strong absorption): if $\lambda \ll 1$, $\varepsilon = 2^{-1}\lambda$, and if $\lambda \gg 1$, $\varepsilon = 1-\lambda^{-1}$.

By using Eqs. (7) and (9) the specific activity of an isotropic emitting–absorbing medium can be calculated from readings of a detector embedded in the medium and tabulated values of the linear absorption coefficients of the crystal μ_2 and the medium μ_1.

LITERATURE CITED

1. C. Sybesma, Measurements of Continuous Energy Distributions of Gamma Rays in a Scattering Medium, Amsterdam (1961).
2. G. I. Kosourov, Pribory i Tekh. Éksperim., No. 5, 95 (1962).
3. Yu. A. Egorov, Scintillation Methods in Gamma and Fast Neutron Spectrometer [in Russian], Gosatomizdat, Moscow (1963).

SINGLE-CHANNEL ALPHA SPECTROMETER FOR MEASUREMENT OF RADON DAUGHTER PRODUCT CONCENTRATIONS

N. I. Antipin, Yu. V. Kuznetsov, and L. S. Ruzer

UDC 621.039-78

Measurement of the concentrations q_A, q_B, and q_C of radon daughter products in air are important for monitoring radiation safety in mines and other industrial installations, in meteorology and medicine, and in the performance of scientific research. The aerosol radiometers RANag-1, RV-alpha, IZV-1 and others are used for these purposes. In this case, the air activity of radon daughter products is determined by measurement of the total α activity of isotopes on a filter with subsequent calculation of q_A, q_B, and q_C by well-known formulas [1-3]. Considerable error is attached to this method since the contribution of each isotope to the total activity turns out to be different for different sample holding times, particularly for significant shifts in the equilibrium value of $(q_A : q_B : q_C)$. A higher accuracy in the determination of isotopic activity is given by the method of α spectrometry [4], which is based on individual measurement of isotopic activities characterized by a considerable difference in α-particle energies (5.998 and 7.680 MeV, respectively).

The practical use of spectrometry for measurement of radon daughter product concentrations in air is not new. Such an instrument has been described [5], but the equipment developed has not been widely accepted because of large size and high cost resulting mainly from the use of a multichannel analyzer.

A portable alpha spectrometer (Figs. 1 and 2) is described in this paper. This instrument is characterized by small size and weight because of the employment of spectrometric nonemanating sources in it [6] which are used for the establishment of the appropriate discrimination levels. Such sources are issued at the present time under TU No. I-118-69 (the isotopes ^{226}Ra, ^{239}Pu, ^{238}Pu, $^{233}U + ^{238}Pu + ^{239}Pu$).

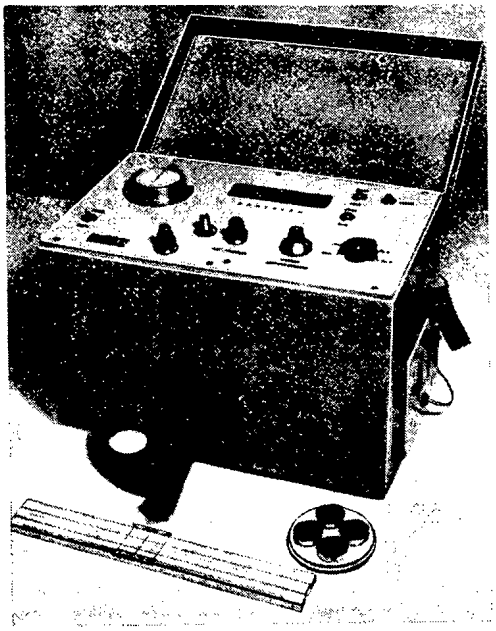

Fig. 1. General view of instrument.

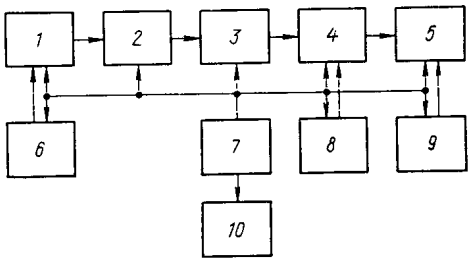

Fig. 2. Structural diagram of single-channel alpha spectrometer: 1) detection unit; 2) amplifier; 3) discriminator; 4) anticoincidence circuit; 5) scaler; 6) high-voltage transformer (1200 V); 7) power supply; 8) test oscillator (60 Hz); 9) transformer (220 V); 10) PRV-1M blower.

Translated from Atomnaya Énergiya, Vol. 40, No. 3, pp. 247-248, March, 1976. Original article submitted January 14, 1974.

The alpha spectrometer is constructed in the form of an assembly consisting of a measurement panel, detection unit, functional units, air intake system, and two power-supply units – a line supply and a built-in supply (STsS-3 storage battery). With discriminator operation in the integral mode (switch position RaC'), α particles from ^{214}Po (RaC') are detected. To determine RaA, RaB, and RaC concentrations in air, samples are collected on an AFA-RSP-10 spectrometric filter installed in the filter holder. The filter is then placed underneath the detector and the number of pulses from RaA and RaC' are successively measured. The quantities q_A, q_B, and q_C are determined from the number of pulses recorded by means of the following expressions,

$$q_A = \frac{2N_A(\theta, t_1)\,C_1}{v\varepsilon\eta a};$$

$$q_B = \frac{2}{v\varepsilon\eta a}[C_2N_C(\theta, t_3) - C_3N_C(\theta, t_2) - C_4N_A(\theta, t_1)];$$

$$q_C = \frac{2}{v\varepsilon\eta a}[C_5N_C(\theta, t_2) - C_6N_C(\theta, t_3) - C_7N_A(\theta, t_1)],$$

where q_A, q_B, and q_C are the RaA, RaB, and RaC concentrations in air; $N_A(\theta, t_1)$, $N_C(\theta, t_2)$, and $N_C(\theta, t_3)$ are the number of pulses recorded per minute from RaA and RaC' at the times t_1, t_2, and t_3 after pumping; θ and v are time and rate of aerosol pumping through the filter; ε is the efficiency of α-particle detection; η is the efficiency of aerosol collection; a equals $2.22 \cdot 10^{12}$ dis/min-Ci; C_1-C_7 are coefficients which take into account the radioactive transformations of short-lived radon daughter products on the filter as a function of pumping time θ and of the times of measurement t_1, t_2, and t_3 after pumping [7].

The energy resolution of the alpha spectrometer for the RaC' peak is no worse than 5%; the α-particle detection efficiency over an angle of 2π is not less than 8.5%; the nonlinearity of the spectrometer channel over the energy range from 4.791 to 7.680 MeV does not exceed 1%; the root-mean-square errors in measurements of q_A, q_B, and q_C over the measured concentration range from $2 \cdot 10^2$ to $4 \cdot 10^5$ $\text{sec}^{-1} \cdot \text{m}^{-3}$ are no more than 10, 20, and 10% respectively; the aerosol pumping rate through the filter is 20 liters/min; the maximum power demand from the line is no more than 25 W; size of the instrument is 320 × 190 × 265 mm and the weight is 11 kg.

The instrument was tested and certified with the State special standard for the unit of concentration of artificial and natural radioactive aerosols [8].

LITERATURE CITED

1. K. P. Markov, N. V. Ryabov, and K. N. Stas', At. Énerg., 12, 315 (1962).
2. K. P. Markov et al., in: Trudy SNIIP, No. 2, Atomizdat, Moscow (1965), p. 183.
3. N. P. Kartashov, At. Énerg., 20, 444 (1966).
4. L. S. Ruzer and V. G. Labushkin, Byull. Izobret., No. 11 (1966).
5. E. Dowell et al., Health Phys., 17, No. 1, 131 (1969).
6. V. G. Labushkin and L. S. Ruzer, At. Energ., 19, 24 (1965).
7. L. S. Ruzer, Radioactive Aerosols [in Russian], Izd. Komiteta Standartov, Moscow (1968).
8. N. I. Antipin et al., Izmeritel'. Tekh., No. 12, 24 (1973).

ALGORITHM FOR MONTE CARLO SIMULATION OF COMPTON SCATTERING INCLUDING GAMMA-RAY POLARIZATION

N. L. Kuchin, K. K. Popkov, and I. N. Trofimov

UDC 539.12.172

The solution of the problem of γ-ray transport in matter by the Monte Carlo method is associated with repeated simulation of Compton scattering. In calculations of γ-ray transport, Compton scattering is ordinarily taken into account by the introduction of the differential cross section for the process, assuming the absence of polarization. As is well known [1], however, the actual scattering process leads to partial polarization of the γ rays even if they were not previously polarized. Inclusion of this effect makes subsequent scattering nonrandom with respect to the azimuthal scattering angle, which is important in γ-ray transport problems associated with the reflection of γ rays from the structural surfaces of shadow and labyrinth shielding.

In a description of γ-ray polarization, one uses, in addition to the usual Cartesian coordinates XYZ, the coordinates l, m, and n associated with the direction of motion of a quantum; the direction of the n axis is chosen along the direction of the quantum, the m axis is in the XOY plane, and the l axis is in a plane with the OZ axis and is directed upwards at an angle θ to that axis.

The degree of polarization is conveniently described by the Stokes parameters ξ_1, ξ_2, and ξ_3 [1], with the parameter ξ_3 characterizing the degree of linear polarization relative to the axes l and m, the parameter ξ_1 characterizing the degree of polarization along the direction at an angle of 45° with respect to the l and m axes, and the parameter ξ_2 characterizing the degree of circular polarization. The range of variation of the parameters ξ_1, ξ_2, and ξ_3 is from -1 to $+1$.

Upon rotation of the coordinates l, m, and n by an angle φ required, for example, for alignment with the scattering plane, the polarization parameters are converted [2] by means of the expressions

$$\begin{aligned} \xi_1(\varphi) &= \xi_1 \cos 2\varphi - \xi_3 \sin 2\varphi; \\ \xi_2(\varphi) &= \xi_2; \\ \xi_3(\varphi) &= \xi_1 \sin 2\varphi + \xi_3 2\varphi. \end{aligned} \tag{1}$$

The dependence of the cross section for scattering of polarized γ rays by an unpolarized electron into the scattering plane on the polarization parameters of the scattered γ ray is given by [1]

$$\frac{d\sigma}{d\Omega} = \frac{r_0^2}{4}\left(\frac{E'}{E}\right)^2 \{F_0 + F_3(\xi_3 + \xi_3') + F_{11}\xi_1\xi_1' + F_{22}\xi_2\xi_2' + F_{33}\xi_3\xi_3'\}, \tag{2}$$

where

$$\left.\begin{aligned} F_0 &= \frac{E}{E'} + \frac{E'}{E} - \sin^2\theta_0; \quad F_3 = \sin^2\theta_0; \\ F_{11} &= 2\cos\theta_0; \quad F_{22} = \left(\frac{E}{E'} + \frac{E'}{E}\right)\cos\theta_0; \\ F_{33} &= 1 + \cos^2\theta_0. \end{aligned}\right\} \tag{3}$$

Here, θ_0 is the scattering angle, i.e., the angle between the n and n' axes.

Translated from Atomnaya Énergiya, Vol. 40, No. 3, pp. 249-250, March, 1976. Original article submitted March 24, 1975; revision submitted September 15, 1975.

The scattering cross section summed over the polarization parameters of the final photon is given by

$$\frac{d\sigma}{d\Omega}=\frac{r_0^2}{2}\left(\frac{E'}{E}\right)F, \tag{4}$$

where

$$F=F_0+\xi_3(\varphi)F_3. \tag{5}$$

The dependence of the scattering cross section on the azimuthal angle is shown by $\xi_3(\varphi)$ in Eqs. (1). The scattering cross section integrated over the polarization parameters of the initial photon transforms into the Klein–Nishina–Tamm formula with no dependence on φ, which makes it possible to select the scattering angle θ_0, and consequently the energy E' of the scattered quantum, at random in the Monte Carlo method and usually independently of the random selection of the angle φ [3].

The azimuthal angle φ is randomly selected for known θ_0 and E' in accordance with Eq. (4) by the Neumann method [4] with a resultant determination of the scattering plane. Then the polarization parameters of the initial photon in the scattering plane, $\xi_1(\varphi)$, $\xi_2(\varphi)$, $\xi_3(\varphi)$, can be calculated from Eqs. (1), and those of the final photon in the scattering plane can be calculated from the following expressions:

$$\begin{aligned}\xi_1'(\varphi')&=\frac{F_{11}}{F}\xi_1(\varphi);\\ \xi_2'(\varphi')&=\frac{F_{22}}{F}\xi_2(\varphi);\\ \xi_3'(\varphi')&=\frac{F_3+F_{33}}{F}\xi_3(\varphi).\end{aligned} \tag{6}$$

Conversion of the polarization parameters of the scattered photon from the scattering plane to a selected frame of reference is easily accomplished by rotation of the coordinates of the polarization frame by an angle $(-\varphi')$ in accordance with Eqs. (1) with

$$\begin{aligned}\sin(-\varphi')&=\frac{\omega_1\omega_2'-\omega_2\omega_1'}{\sin\theta\sin\theta'};\\ \cos(-\varphi')&=\frac{\omega_1'\cos\theta-\omega_3}{\sin\theta\sin\theta'},\end{aligned} \tag{7}$$

where ω_1, ω_2, ω_3 and ω_1', ω_2', ω_3' are the direction cosines of the incident and scattered photons; θ and θ' are the angles between the OZ axis and the direction of flight of the incident and scattered photons.

Six special cases are observed instead of two in the conversion of the direction cosines [4]. Additional special cases appear at $\theta = 0$ (there is no frame of reference for the azimuthal angle of the incident photon) and at $\theta' = 0$ (there is no frame of reference for the azimuthal angle of the scattered photon). These indeterminancies are easily eliminated if one introduces in the special cases measurement of the azimuthal angle from the OX axis, for example.

The proposed algorithm is sufficiently simple and differs from the algorithm proposed in [5] by virtue of greater generality. The algorithm was realized in a program coded for an M-220 computer. The Neumann method used for the simulation has a high efficiency, which ensures short computing time for γ-ray histories.

LITERATURE CITED

1. V. B. Berestetskii, E. M. Lifshits, and L. P. Pitaevskii, Relativistic Quantum Theory [in Russian], Pt. 1, Nauka, Moscow (1968).
2. U. Fano, L. Spencer, and M. Berger, Gamma-Ray Transport [Russian translation], Gosatomizdat, Moscow (1963).
3. S. M. Ermakov, Monte Carlo Method and Related Problems [in Russian], Nauka, Moscow (1971).
4. N. P. Buslenko et al., Methods of Statistical Testing [in Russian], Fizmatgiz, Moscow (1962).
5. W. Vesely and A. Chilton, Trans. Amer. Nucl. Soc., 10, 410 (1967).

SEMICONDUCTOR RADIOMETER – SPECTROMETER FOR MEASUREMENT OF SURFACE CONTAMINATION BY ALPHA-RADIOACTIVE MATERIALS

V. A. Manchuk and A. A. Petushkov

UDC 539.1.074+539.853.22:621.039.76

An important problem in the control of the radiation environment is the measurement of contamination by α-radioactive materials of the surfaces in working areas, of the surface of the skin, etc. Furthermore, the problem is often not limited to measurement of specific surface activity alone but also requires rapid differentiation of the activity with respect to the individual α-radioactive components.

This paper discusses the possibility of constructing an alpha radiometer–spectrometer for contamination in working areas. Similar detectors have been used extensively in recent years in various fields of nuclear physics and of applied sciences including the resolution of radiation safety problems [1, 2].

The nature of the measurement of the degree of contamination of working surfaces requires the use of a detector having a sensitive surface of relatively large area (~100 cm^2). The energy resolution of individual silicon detectors with such an area and of mosaic detectors is unsatisfactory at normal temperature. The limit of achievable energy resolution for nonuniform silicon detectors can be calculated on the basis of the premises given in [3, 4] from

$$\Delta E_{Si} = \left[0{,}5ZA^{8/3} + 1{,}5E + \left(2{,}35\,\frac{\omega}{e}\right)^2 kTC\right]^{1/2},$$

where Z, A, and E are the atomic number, atomic mass, and energy of an α particle; ω is the average energy expended in the formation of a pair of charge carriers in silicon; e is the charge of an electron; T is absolute temperature; k is the Boltzmann constant; C is the electrical capacitance of the detector. The first term determines line broadening because of nuclear collisions, the second term, the fluctuation in the amount of pairs of charge carriers formed, and the third term of the sum reflects the deterioration of resolution because of thermal noise generated in an electron-hole junction detector.

According to the formula, the energy resolution of an actual detection system with a sensitive surface area of 100 cm^2, a specific resistance of 500 Ω-cm for the original detector material, and a working voltage in the neighborhood of 50 V is found to be $\Delta E_{Si} > 400$ keV, which is clearly unsatisfactory for the identification of the natural α-radioactive isotopes. However, this difficulty can be resolved to a known extent if one uses a mosaic structure of several detectors connected in parallel such that it is possible to disconnect one of the detectors from all the others in order to make spectrometric measurements. In such a case, the advantages of a mosaic system, which provides an opportunity to construct a detector with the required area of sensitive surface (100 cm^2 and more) for efficient search for contamination, are combined with the spectrometric properties of an individual detector with an area (5-8 cm^2) small in comparison with the area of the mosaic but with an energy resolution that provides spectrometry.

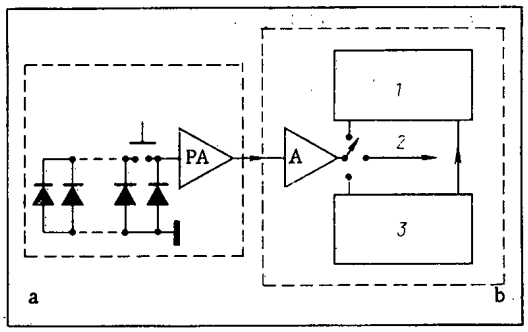

Fig. 1. Structural diagram of semiconductor radiometer–spectrometer: 1) electromechanical counter; 2) output to multichannel analyzer; 3) single-channel analyzer.

Translated from Atomnaya Énergiya, Vol. 40, No. 3, pp. 250-251, March, 1976. Original article submitted March 27, 1975.

Based on this principle, a model of an alpha radiometer–spectrometer for contamination of working surfaces was constructed (see Fig. 1). Mounted in the detection unit (Fig. 1a) is a mosaic detector, the charge-sensitive preamplifier PA, and a switch makes it possible to disconnect from the input of the preamplifier all detectors except the spectrometer detector when it is necessary to perform spectrometric measurements. The charge-sensitive preamplifier is made up of a cascade circuit and has a high dynamic input capacitance. The main amplifier A, the single-channel analyzer circuit, and the system for recording pulses are located in the recording unit (Fig. 1b) together with the electric batteries which provide power for all the electronic circuits in the instrument.

The mosaic detector with a working area of 130 × 95 mm consists of 12 commercially produced DKP-500 detectors connected in parallel. The area of the sensitive surface of an individual detector is 5 cm^2 and the energy resolution is in the neighborhood of 70 keV. Detectors suitable for the mosaic were selected mainly for the magnitude of the maximum permissible working voltage. The demand for identity of optimal working voltage values for all detectors proved to be less important since the dependence of energy resolution on voltage does not have a sharp maximum for such detectors as a rule. Seventy percent of the detectors in a single qualification group were suitable for use in the mosaic, which is evidence of the accessibility of this principle and the possibility of its broad application.

The mosaic detector is fitted with two interchangeable adapters intended for the spectrometric and radiometric modes of operation. The radiometric adapter covers the surface of the detectors with a metallized Mylar film 4 μm thick, which protects against contamination and ensures optimal geometric conditions for measurement. Detector efficiency depends on the size of an active spot, its separation from the sensitive surface, and the location of the source within the limits of the sensitive area. On the average, the efficiency is 37% when measured at the distance between detector surface and surface monitored provided by the adapter (6 mm), and is a function of the location of a source 10 mm in diameter. The energy resolution of the instrument in the spectrometer mode is 140 keV when measuring the radiation spectrum from a ^{239}Pu source in air. Separation of the detector from the surface monitored during spectrometry is no more than 1.5-2 mm. The dependence of the degree of spectrum smearing on thickness of source or of inactive absorber has been analyzed [5]. One can conclude from the data in that paper that absorption of radiation in a layer of contamination up to 0.1-0.2 mg/cm^2 thick does not introduce marked deterioration of energy resolution. The width of the window of the single-channel analyzer is 280 keV and its position is smoothly controlled over the energy range from 4 to 9 MeV. The background counting rate in the single-channel mode is less than 0.5 counts/h.

LITERATURE CITED

1. R. Parker, Phys. Medicine and Biology, Vol. 15, No. 4 (1970), p. 605.
2. V. Manchuk et al., Rep. SZD-148, Berlin, DDR (1973), p. 112.
3. Yu. K. Akimov et al., Semiconductor Detectors of Nuclear Particles and Their Application [in Russian], Atomizdat, Moscow (1967).
4. J. Dearnley and D. Northrop, Semiconductor Counters for Nuclear Radiations [Russian translation], Mir, Moscow (1966).
5. I. E. Konstantinov and V. F. Baranov, Methods of Spectrometry for Ionizing Radiation [in Russian], Moscow (1971).

AN APPARATUS FOR ASSAYING HELIUM IN CONSTRUCTIONAL MATERIALS

A. I. Dashkovskii, A. G. Zaluzhnyi,
D. M. Skorov, O. M. Storozhuk,
and M. V. Cherednichenko-Alchevskii

UDC 621.039.548.343

Neutron irradiation affects the mechanical properties of constructional materials because helium and hydrogen are produced by nuclear reactions, which means that research on the formation and behavior of these products in reactor materials is very important.

Here we describe a mass spectrometer system for assaying helium in reactor materials (steels), the main parts shown in Fig. 1 being as follows: the working volume, the measuring volume, the pumping system consisting of the ÉRA-100-2 discharge system together with the GIN-05M-1 ion-getter pump, and the analytical system, which is based on an IPDO-1 omegatron, with a RMO-4S tube as the transducer. The entire equipment, apart from the working volume and the transducer, is made of stainless steel, while the vacuum seals are made of copper. The working volume is a glass bulb with a ground joint. The walls of the bulb are cooled by water.

The system operates as follows: The etched specimen (oxide film removed) of exactly measured mass 30-40 mg is placed in the center of the heater on a refractory ceramic substrate. The heater is a tungsten wire spiral. The working and measuring volumes are evacuated by the discharge pump to about 10^{-6} mm Hg. Then this pump is disconnected from the system, and the measuring and working volumes are evacuated by the GIN-05M-1 pump, which works in the sorption mode without removing the inert gases [1], as was confirmed in a series of tests on the system. The helium background was determined in this way. The working volume is then disconnected from the measuring volume by a DU-2 needle valve, and strong heating for about 5 min is used to evaporate the material completely. The vacuum deteriorates considerably in the working volume during the heating, so this volume is evacuated by the GIN-05M-1 pump via the DU-2 valve in such a way that the pressure in the measuring volume remains around 10^{-6} mm Hg (the optimum pressure for the IPDO-1). When the pressures in the two volumes have equalized, the amount of helium released by the evaporation is determined.

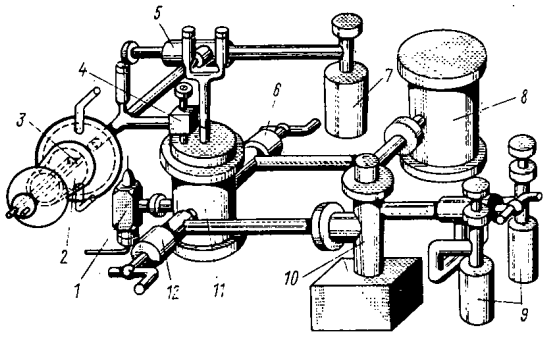

Fig. 1. Apparatus for determining helium content in a material: 1) RMO-4S omegatron; 2) working volume; 3) heater; 4) needle valve; 5, 6, 12) high-vacuum valves; 7, 9) TsVN-1 sorption pumps; 8) ion-getter pump; 10) ÉRA-100-2 electrical discharge system; 11) measuring volume.

The limit of detection in partial pressure is about $3 \cdot 10^{-10}$ mm Hg, while the total working volume of the apparatus is about 10 liters. The overall error in determining the amount of helium is composed of errors in weighing, determining the measuring volume, and in measuring the partial pressure. The overall value does not exceed ~20%.

The system was checked out using 0Kh16N15M3B steel (foil thickness about 100 μ), which has been exposed to 70 keV α particles at about 70°C in an ILU-100 magnetic separation system to a dose of about $3 \cdot 10^{16}$ particles per cm^2. Calculations indicated that a sample of mass about 30 mg contained about $1.2 \cdot 10^{16}$ helium

Translated from Atomnaya Énergiya, Vol. 40, No. 3, pp. 251-252, March, 1976. Original article submitted September 1, 1975.

atoms. The mean measured amount of helium in a series of five specimens was $1.0\text{-}1.1 \cdot 10^{16}$ atoms.

LITERATURE CITED

1. A. F. Francio and R. N. Jensen, in: Residual Gases in Electronic Tubes, Énergiya, Moscow (1967), p. 196.

SURFACE BLISTER BURSTING

B. A. Kalin, N. M. Kirilin,
A. A. Pisarev, D. M. Skorov,
V. G. Tel'kovskii, S. K. Fedyaev,
and G. N. Shishkin

UDC 533.924:539.12.17

Gas-filled cavities (blisters) are produced when materials are exposed to helium ions [1]. The mode of failure of these is dependent on the physicomechanical properties of the target, and it determines the erosion of the material to a considerable extent [1, 2].

We have examined the mode of failure of blisters on niobium, VN-2AÉ niobium alloy, and 1Kh18N9T steel using 20 keV helium ions at 700-800°K.

The specimens were irradiated with a mass monochromator [3, 4] at 10^{-6} mm Hg with a current density of 0.2-0.6 A/m^2; the targets were made of electrically polished steel of thickness $1\text{-}2 \cdot 10^{-4}$ m. The irradiated specimens were examined with a UÉMB-100K electron microscope using one-step carbon replicas.

The electron micrographs showed that $4 \cdot 10^{21}$ ion $\cdot$ m^{-2} always produced blisters, some of which are burst (Figs. 1-3). The modes of failure are essentially of two types: at the periphery (Fig. 1b) and central

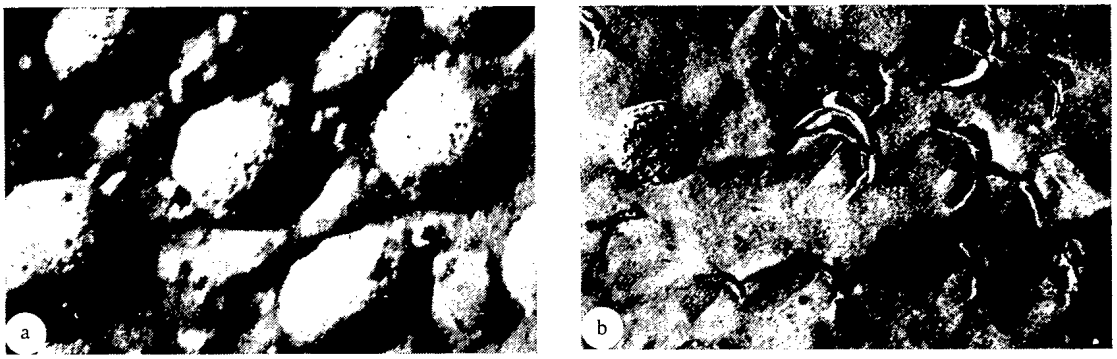

Fig. 1. Blisters produced by $9 \cdot 10^{21}$ ion $\cdot$ m^{-2} (both pictures 4 × 6 μm) on: a) 1Kh18N9T steel; b) niobium.

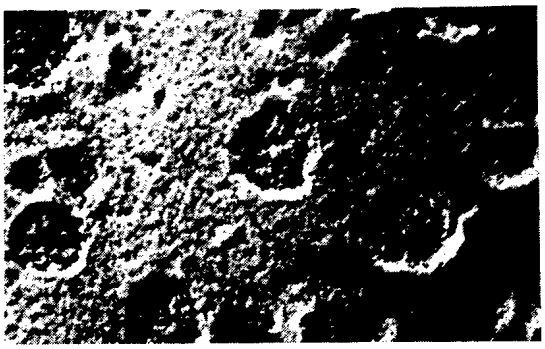

Fig. 2. Blisters on VN-2AÉ alloy at $6 \cdot 10^{12}$ ion $\cdot$ m^{-2}.

Fig. 3. Blisters on niobium at $4 \cdot 10^{21}$ ion $\cdot$ m^{-2}.

Translated from Atomnaya Énergiya, Vol. 40, No. 3, pp. 252-253, March, 1976. Original article submitted May 29, 1975.

(Fig. 3). In the peripheral case, there are sometimes radial cracks (Fig. 1b). The central failure can occur along one direction or along three or four (Fig. 3).

Peripheral failure often leads to complete detachment, i.e., flaking and pitting (Fig. 2). In the central case, flaking still occurs at high doses, when the density of the blisters is so high that the formation and rupture of adjacent cavities causes complete detachment. Then the erosion due to peripheral failure may be more extensive than that due to central. Also, the shedding tends to affect the heat transfer adversely, which may result in local overheating and accentuates the erosion.

The form of failure is governed by many factors, of which the plasticity appears to be important. Blisters on 1Kh18N9T steel, the most plastic of these three materials, show very little failure and have a regular convex shape, which indicates that the stresses arising in a blister due to the helium are absorbed mainly via the plasticity. The niobium and alloy usually showed a failure. Figures 1b and 2 show that completely detached blisters occur more quickly with VN-2AÉ, which is the less plastic material in the working temperature range.

We thus conclude that plastic materials can withstand higher helium-ion doses without appreciable erosion, and consequently that 1Kh18N9T steel has the highest resistance to surface damage on exposure to helium ions up to $9 \cdot 10^{21}$ ions $\cdot m^{-2}$ at 700-800°K.

LITERATURE CITED

1. M. Kaminsky and S. Das, Nucl. Technol., 22, No. 3, 373 (1974).
2. S. Das and M. Kaminsky, J. Vac. Sci. Technol., 10, No. 1, 273 (1973).
3. V. A. Kurnaev, V. M. Sotnikov, and V. G. Tel'kovskii, in: Plasma Physics [in Russian], Atomizdat, Moscow (1967), p. 65.
4. V. G. Tel'kovskii et al., Abstracts for the All-Union Conference on Engineering Aspects of Controlled Fusion Research [in Russian], Izd. NIIÉFA, Leningrad (1974), p. 272.

TEMPERATURE DEPENDENCE OF EROSION OF STAINLESS STEELS UNDER IONIC BOMBARDMENT

A. D. Gurov, B. A. Kalin,
N. M. Kirilin, A. A. Pisarev,
D. M. Skorov, V. G. Tel'kovskii,
S. K. Fedyaev, and G. N. Shishkin

UDC 533.924:539.12.17

Stainless steels are regarded as promising materials for the first thermonuclear units [1]. It is therefore of interest to investigate the behavior of stainless steels under ionic bombardment. Our aim is to investigate the temperature dependence of erosion of steels Kh18N9T and 0Kh16N15M3B under bombardment by helium and hydrogen ions with energies of 20 and 25 keV, respectively, at 300-1000°K and an irradiation dose of $(1-50)\cdot 10^{21}$ ion $\cdot$ m^{-2}.

Experimental Procedure. Specimens of both types of steel were obtained by electropolishing from foil $(1-2)\cdot 10^{-4}$ m thick. Steel 0Kh16N15M3B was subjected to preliminary austenization at 900°K for 30 min; steel Kh18N9T was investigated in the rolled state. The specimens were subjected to ionic bombardment in a mass-monochromator under the conditions described in a previous communication [2]. The topography of the irradiated steels was investigated by means of carbon replicas under a UÉMV-100K electron microscope. Erosion was assessed from the electron micrographs by measuring the geometric dimensions of the disintegrated blisters and by calculating the number of atoms in the split-off steel blister caps from the equation

$$n = N_A(\rho V/A),$$

where N_A is Avogadro's number, ρ is the density, V is volume of the split-off blister caps, and A is the atomic weight of the material. The overall error in the determination of the erosion coefficient was ~50%.

Results and Discussion. Figures 1-4 show typical electron micrographs of replicas of the surfaces of steels bombarded with helium ions. An analysis of the results of an investigation of blister formation revealed that the steel behavior markedly depends on the bombardment temperature and the integral dose of helium ions. Formation of dome-shaped undamaged gas-filled blister cavities in a wide temperature

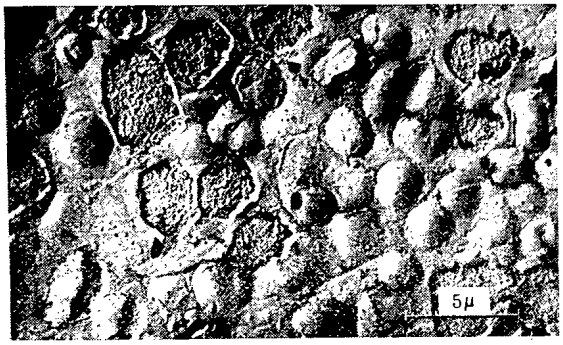

Fig. 1. Electron micrographs of carbon replicas of the surface of steel Kh18N9T bombarded with helium ions (dose $3\cdot 10^{22}$ ion $\cdot$ m^{-2}) at 375°K.

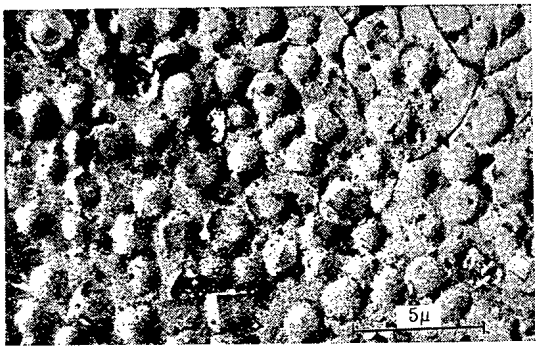

Fig. 2. Blisters on the surface of steel Kh18N9T bombarded with helium ions (dose $8\cdot 10^{21}$ ion $\cdot$ m^{-2}) at 675°K.

Translated from Atomnaya Énergiya, Vol. 40, No. 3, pp. 254-255, March, 1976. Original article submitted May 29, 1975.

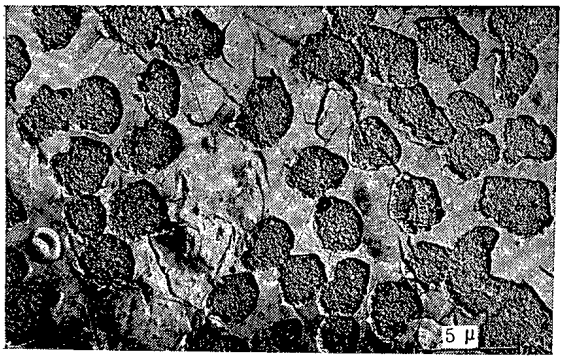

Fig. 3. Surface of steel 0Kh16N15M3B with disintegrated blisters after bombardment with helium ions (dose $4.3 \cdot 10^{22}$ ion $\cdot m^{-2}$) at 375°K.

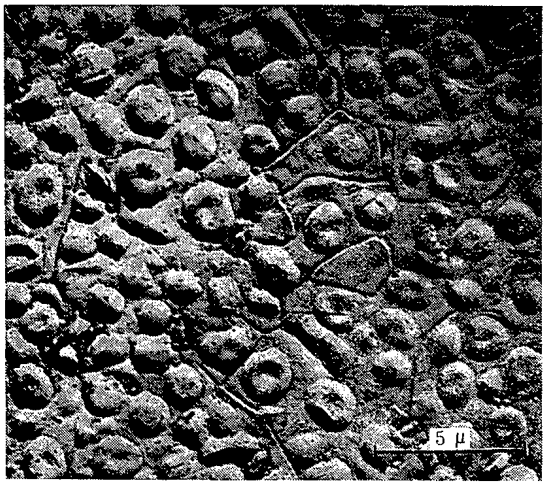

Fig. 4. Blisters on the surface of steel 0Kh16N15M3B bombarded with helium ions (dose $5.2 \cdot 10^{21}$ ion $\cdot m^{-2}$) at 775°K.

range is typical of steel Kh18N9T. It was established that the critical dose of helium ions, i.e., the dose at which we observe blister disintegration, leading to scaling of the steel by cap detachment, increases with the bombardment temperature. For the range 300-400°K the critical dose is $2 \cdot 10^{22}$ ion $\cdot m^{-2}$ (see Fig. 1); maximum steel erosion is observed in this range. At 300°K the erosion coefficient of steel Kh18N9T is 0.08 ± 0.04 atom/ion. An increase in the bombardment temperature sharply reduces scaling of the steel. With bombardment in the range 650-900°K, undamaged blisters are observed at doses higher than $8 \cdot 10^{21}$ ion $\cdot m^{-2}$ (Fig. 2). With an increase in the bombardment temperature (above 900°K) the number of blisters per unit surface decreases and the surface acquires the relief typical of cathodic etching.

For steel 0Kh16N15M3B an important factor is the presence of a wide temperature range (300-800°K) in which bombardment was accompanied by intense erosion owing to blister disintegration by cap detachment (Fig. 3). Maximum erosion is observed at 550-750°K with a dose of $1 \cdot 10^{22}$ ion $\cdot m^{-2}$ or above. At 670°K and a dose of $1.1 \cdot 10^{22}$ ion $\cdot m^{-2}$ the erosion coefficient of steel 0Kh16N15M3B is 0.65 ± 0.32 atom/ion, and at 300°K it is 0.40 ± 0.20 atom/ion. Like a decrease in the radiation dose, a decrease or increase in the radiation temperature of steel 0Kh16N15M3B outside the critical range (550-750°K) was accompanied by a decrease in its erosion. At relatively low doses ($4-5 \cdot 10^{21}$ ion $\cdot m^{-2}$) the blisters remain dome-shaped throughout the temperature range investigated (Fig. 4). At fairly high doses (more than 10^{22} ion $\cdot m^{-2}$) an increase in the radiation temperature to 950-1000°K reduces the number of disintegrated blisters: The irradiated steel 0Kh16N15M3B surface acquires the relief typical of cathodic etching. Thus we have shown that steels Kh18N9T and 0Kh16N15M3B behave quite differently during bombardment by helium ions under comparable conditions: Steel 0Kh16N15M3B undergoes intense erosion at 300-800°K, whereas erosion of steel Kh18N9T is observed only at 300-400°K. The difference in the behavior of the steels, particularly the tendency of the blisters on steel 0Kh16N15M3B to brittle fracture by cap detachment in a wide temperature range, is largely attributable to the difference between the physicomechanical properties of the materials, for example, the plasticity, and the variation of these properties with temperature [3, 4]. Being the most plastic one, steel Kh18N9T is less subject to erosion by disintegration of the gas-filled cavities. This means that after bombardment with helium ions up to $5 \cdot 10^{22}$ ion $\cdot m^{-2}$, preference from the viewpoint of the use of steels as the primary wall of thermonuclear units must be accorded to steel Kh18N9T.

An analysis of the results of the electron-microscopic investigation of steel Kh19N9T bombarded with helium atoms and protons at 300°K also enabled us to distinguish a number of regularities. Irradiation of the steel only with protons led to formation of blisters at a dose above $6 \cdot 10^{21}$ ion $\cdot m^{-2}$. It was noted that formation of blisters on mechanically polished specimens takes place preferentially on scratches and their intersections.

Combined successive bombardment of steel Kh18N9T with helium ions and protons revealed that distention of the steel is not observed up to overall doses of order $1 \cdot 10^{21}$ ion $\cdot m^{-2}$. Nor did annealing at 1000°K after bombardment lead to the appearance of blisters. An increase in the overall dose to $1.5 \cdot 10^{21}$ ion $\cdot m^{-2}$ has little effect on the topography of the bombarded surface, but annealing after bombardment for

30 min leads to formation of blisters with a fairly high density (10^{12} m^{-2}). For comparison we bombarded the steels only with helium ions (dose $5 \cdot 10^{20}$ ion $\cdot m^{-2}$) followed by annealing under similar conditions. It was established that with combined bombardment the blister density is double that observed for bombardment only with helium. This is apparently due to the fact that at the depth of helium ion penetration the gas cavities are traps for the hydrogen ions diffusing to the surface from a greater depth. Hydrogen capture in the region of helium atom accumulation probably leads to an increase in the overall gas pressure in the bubbles, and therefore to blister formation when the critical total irradiation dose is attained.

Thus we have established that combined bombardment of steel with protons and helium ions intensifies blister formation.

LITERATURE CITED

1. G. Kulcinski et al., Nucl. Technol., 22, 20 (1974).
2. V. G. Tel'kovskii et al., in: Abstracts of Reports to the All-Union Conference on Engineering Problems of Thermonuclear Synthesis Control [in Russian], Izd. NIIÉFA, Leningrad (1974), p. 272.
3. F. F. Khimushin, Heat-Resistant Steels and Alloys [in Russian], Metallurgiya, Moscow (1969), p. 660.
4. Norms for Calculating the Strength of Components of Reactors, Steam Generators, Vessels, and Pipelines of Atomic Power Plants, Experimental and Research Nuclear Reactors and Units [in Russian], Metallurgiya, Moscow (1973), p. 19.

DIFFUSION COEFFICIENTS AND SOLUBILITY OF VANADIUM, NIOBIUM, AND CERIUM IN BERYLLIUM

V. M. Anan'in, V. P. Gladkov, A. V. Svetlov, D. M. Skorov, and V. I. Tenishev

UDC 539.219.3:546.45.546.881: 546.882:546.655

We have investigated the diffusion mobility and solubility of V, Nb, and Ce in beryllium by means of radioactive indicators, using layerwise analysis with measurement of the integral activity of the residue of the specimen.

The diffusion coefficient D was determined by comparing the experimental curves of the integral activity vs penetration depth with a set of theoretical curves specially tabulated for certain cases. This method is used for constant and instantaneous diffusion sources and enables us to greatly reduce the error of determination of the diffusion coefficient.

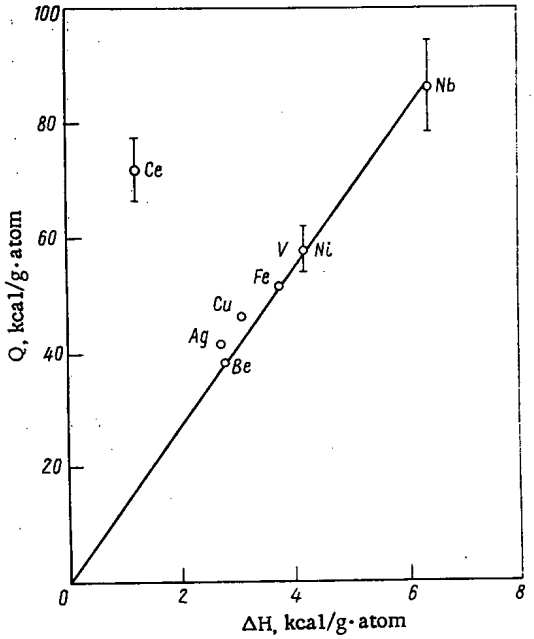

Fig. 1. Activation energy of diffusion Q vs the heat of melting of the diffusing elements ΔH_{me}.

With a constant diffusion source, the solubility of the diffusing element was determined from the ratio of the specific activities of the solid solution and the diffusion source layer [2]. The composition of the latter on the specimen surface was determined by x-ray phase analysis.

The material for the investigation was distilled beryllium, remelted in an arc furnace on a water-cooled copper hearth in purified helium. The chemical composition of the cast beryllium was as follows (wt. %): Si 0.003, Fe 0.031, Mg 0.001, Mn 0.004, Ni 0.003, Al 0.003, Cu 0.005, Ca 0.005, O 0.160, and C 0.090. On the polished surfaces of the beryllium specimens were deposited radioactive isotopes of V, Nb, and Ce as vanadium nitrate (^{48}V), niobium oxalate (^{95}Nb), and cerium chloride (^{141}Ce). Diffusion annealings were performed in the range 1170-1540°K in a TVV-5 furnace in purified helium; the preliminary vacuum was not less than $1 \cdot 10^{-5}$ mm.

During diffusion annealings a layer of a compound forms on the specimen surface. In the case of diffusion of niobium and cerium, x-ray phase analysis revealed that this compound is $NbBe_{12}$ and $CeBe_{13}$, respectively. The composition of the layer on the surface during diffusion of vanadium was not established.

TABLE 1. Coefficient of Diffusion and Solubility of Vanadium in Beryllium

T, °K	D, cm^2/sec	S, rel. units	T, °K	D, cm^2/sec	S, rel. units
1173±5	$(5,8\pm1,5)\ 10^{-10}$	$(5,5\pm0,8)\ 10^{-3}$	1323±5	$(9,7\pm1,9)\ 10^{-9}$	$(8,5\pm1,4)\ 10^{-3}$
1273±5	$(1,3\pm0,3)\ 10^{-9}$	—	1373±5	$(1,6\pm0,3)\ 10^{-8}$	$(1,2\pm0,2)\ 10^{-2}$
1223±5	$(2,5\pm0,5)\ 10^{-9}$	$(5,6\pm1,1)\ 10^{-3}$	1423±5	$(3,9\pm0,7)\ 10^{-8}$	$(1,3\pm0,2)\ 10^{-2}$

Translated from Atomnaya Énergiya, Vol. 40, No. 3, pp. 256-257, March, 1976. Original article submitted June 25, 1975.

TABLE 2. Coefficient of Diffusion and Solubility of Niobium in Beryllium*

T, °K	D, cm²/sec	S, at.%	T, °K	D, cm²/sec
1173±5	—	0,015±±0,003	1473±5	(3,4±0,7) 10⁻⁹
1318±5	(1.3±0,3) 10⁻¹⁰	—	1493±5	(3,9±0,8) 10⁻⁹
1393±5	(6,3±1,2) 10⁻¹⁰	—	1513±5	(9,0±2,0) 10⁻⁸
1423±5	(1,7±0,3) 10⁻⁹	0,039±±0,008	1538±5	(5,5±1,1) 10⁻⁶

*Right-hand column for values of S were omitted in the Russian original – Publisher.

TABLE 3. Coefficient of Diffusion and Solubility of Cerium in Beryllium

T, °K	D, cm²/sec	S, at.%	T, °K	D, cm²/sec	S, at.%
1223±5	(4,8±0,8) 10⁻¹¹	—	1513±5	(1,1±0,8) 10⁻⁸	(0,30±0,05) 10⁻²
1273±5	(1,2±0,2) 10⁻¹⁰	—	1518±5	(4,2±0,8) 10⁻⁸	—
1323±5	(4,0±0,8) 10⁻¹⁰	(0,16±0,03) 10⁻²	1523±5	(6±2) 10⁻⁸	(0,45±0,13) 10⁻²
1423±5	(2,6±0,5) 10⁻⁹	—	1528±5	(3,0±0,8) 10⁻⁷	—
1456±5	(4,8±0,9) 10⁻⁹	(0,25±0,05) 10⁻²			

Analysis of the concentration curves indicates observance of the conditions of a constant diffusion source, which enables us to determine the solubility of these elements in beryllium for several temperatures (for vanadium the temperature dependence of the solubility was determined in relative units).

Tables 1-3 list the values of the diffusion coefficient D and the solubility S for various temperatures.

The temperature dependence of the diffusion coefficient of V, Nb, and Ce in beryllium is expressed by the following equations:

$$D_V = 29^{+8}_{-17} \exp\left[-\frac{58.0 \pm 4.0}{RT}\right], \text{ cm}^2/\text{sec at } T = 1173 - 1423 \text{ T, °K}$$

$$D_{Nb} = (2.0^{+46.0}_{-1.9}) \cdot 10^4 \exp\left[-\frac{85.9 \pm 8.1}{RT}\right], \text{ cm}^2/\text{sec at } T = 1318 - 1513 \text{ T, °K}$$

$$D_{Ce} = (3.1^{+8.0}_{-2.4}) \cdot 10^2 \exp\left[-\frac{72.5 \pm 4.5}{RT}\right], \text{ cm}^2/\text{sec. at } T = 1223 - 1513 \text{ T, °K}$$

For niobium and cerium we obtained the values of the diffusion coefficients in α and β beryllium, i.e., in hcp and bcc lattices. The mobility in the bcc lattice was higher than in the hcp lattice.*

From published reports [3, 4] and the experimental data we plotted the activation energy of diffusion vs the heat of melting of the diffusing elements (Fig. 1); from this graph we see that the points corresponding to the transition elements lie close to a straight line of the form

$$Q = 13.8\,\Delta H_{me}.$$

The marked deviation of the point corresponding to cerium enables us to postulate that the rare earths obey a different dependence to that observed for transition metals.

LITERATURE CITED

1. P. L. Gruzin, Problems of Metallography and the Physics of Metals [in Russian], Metallurgizdat, Moscow (1952).
2. V. M. Anan'in et al., in: General Laws in the Structure of Phase Diagrams of Metallic Systems [in Russian], Nauka, Moscow (1973), p. 184.
3. I. I. Papirov and G. F. Tikhinskii, Physical Metallurgy of Beryllium [in Russian], Atomizdat, Moscow (1968).
4. V. M. Anan'in et al., At. Énerg., 29, 3, 220 (1970).

* For comparison the values of the diffusion coefficients in the hcp lattice were extrapolated to the corresponding temperatures.

DIFFUSION AND SOLUBILITY OF ALUMINUM IN BERYLLIUM

V. P. Gladkov, A. V. Svetlov, D. M. Skorov, V. I. Tenishev, and A. N. Shabalin

UDC 539.219.3:546.45:546.621

Published reports have dealt with self-diffusion of Be [1, 2], and with diffusion of Ni [3], C [4], Fe, Ag, Cu, H, and He [5] in beryllium. Data on the diffusion mobility and solubility of aluminum in beryllium are necessary because aluminum is one of the principal impurities of the commercial metal and has a marked effect on its properties. Diffusion of aluminum in beryllium has not been previously investigated. Electron local analysis of binary alloys shows that its solubility in beryllium is 0.02 at. % at 630°C [6].

We have investigated distilled beryllium, remelted in an arc furnace on a water-cooled copper hearth in purified helium (Table 1). To investigate the diffusion mobility we used the method of layerwise analysis and determination of the integral radioactivity of the residue of the specimen. A layer of $AgCl_3$ containing the isotope ^{26}Al was deposited onto the specimen surface. During diffusion annealing the isotope ^{26}Al diffused from the Al_2O_3 layer. The gamma-radiation intensity was determined by means of a USD-1 scintillation detector, the information being transferred to an AI-128-2 pulse analyzer. An amplitude analyzer was used to increase the ratio of the useful signal to the background and to eliminate the error due to the possible presence of other radioactive impurities in the isotope solution. For a constant diffusion source, from the graph of the integral activity of the specimen residue I_n vs the depth of penetration of the diffusing substance x we can determine the solubility S of the diffusing element (Table 2) in the specimen matrix. In this connection we use the known equation for determining the concentration in a solid solution [7]:

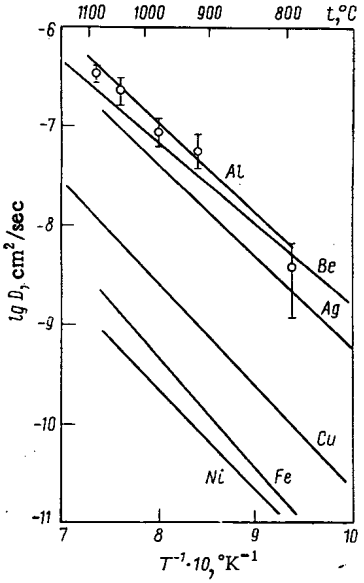

Fig. 1. Temperature dependence of diffusion coefficients of various elements in beryllium. (The data on diffusion of Ag, Cu, Fe, Ni, and self-diffusion are taken from [5].)

TABLE 1. Impurity Content of Cast Beryllium

Element	C·10⁻³, at.%	Element	C·10⁻³, at.%
C	75,2	Cr	0,5
Al	4	Cu	0,2
Fe	3,4	Mn	1,6
Si	1,0	Ni	0,5

TABLE 2. Diffusion Mobility and Solubility of Aluminum in Beryllium

T, °K	D, cm²/sec	S, at.%
1356±5	(3,3±0,5) 10⁻⁷	—
1313±5	(2,3±0,7) 10⁻⁷	0,10±0,06
1248±5	(8,7±2,5) 10⁻⁸	0,075±0,028
1191±5	(5,4±1,7) 10⁻⁸	0,069±0,029
1068±5	(3,7±2,6) 10⁻⁹	0,034±0,015

Translated from Atomnaya Énergiya, Vol. 40, No. 3, pp. 257-258, March, 1976. Original article submitted June 25, 1975.

$$C_{\text{sol.s}} = \frac{\left[-\frac{\partial I(x)}{\partial x}\Big|_{x_0} + \mu I(x)\Big|_{x_0}\right]_{\text{sol.s}}}{\left[-\frac{\partial I(x)}{\partial x}\Big|_{x_0} + \mu I(x)\Big|_{x_0}\right]_{\text{la}}} C_{\text{la}}, \quad (1)$$

where μ is the linear absorption coefficient of the radiation, x_0 is the coordinate of interface of the layer of diffusant and the specimen matrix. The temperature dependence of the coefficient of diffusion of aluminum in beryllium in the range 795-1083°C is represented by the equation

$$D = 1.0^{+2.1}_{-0.9} \exp\left[-\frac{40200 \pm 4300}{RT}\right], \text{ cm}^2/\text{sec}. \quad (2)$$

The temperature dependence of the solubility, obtained from the experimental data, has the form

$$S = 13^{+18}_{-12} \exp\left[-\frac{12600 \pm 2500}{RT}\right], \text{ at. \%}. \quad (3)$$

Equations (2) and (3) are given with the rms errors and were calculated by the method of least squares.

The experimental results indicate that aluminum has a higher diffusion mobility than the other elements investigated; it is comparable with the mobility of beryllium during self-diffusion in the range 795-1083°C (Fig. 1). The solubility data obtained by extrapolation of the experimental results to 630°C agree with the literature data [6].

LITERATURE CITED

1. I. Dypouy, I. Mathie, and Y. Adda, Mem. Sci. Rev. Metal., 63, No. 5, 481 (1966).
2. L. V. Pavlinov, G. V. Grigor'ev, and Yu. G. Sevast'yanov, Fiz. Metall. i Metallov., 25, No. 3, 565 (1968).
3. V. M. Anan'in et al., At. Énerg., 29, No. 3, 220 (1970).
4. V. S. Zotov et al., in: Proc. 4th Republican Conference on the Preparation of Pure Metals and Investigation of Their Properties [in Russian], Vol. 2, Izd. FTI Akad. Nauk SSSR, Khar'kov (1970), p. 59.
5. I. I. Papirov and G. F. Tikhinskii, Physical Metallurgy of Beryllium [in Russian], Atomizdat, Moscow (1968).
6. F. A. Shank, Structures of Binary Alloys [in Russian], Metallurgiya, Moscow (1973).
7. V. M. Anan'in et al., in: General Laws in the Structure of Phase Diagrams of Metallic Systems [in Russian], Nauka, Moscow (1973), p. 184.

RELATIVE MEASUREMENTS OF THE SPECTRAL CHARACTERISTICS OF NEUTRON DISTRIBUTIONS BY THE ACTIVATION RATIOS METHOD

R. D. Vasil'ev, E. I. Grigor'ev, and V. P. Yaryna

UDC 621.039.51

Obtaining experimental information on the neutron spectrum in a reactor is a complicated and time-consuming problem. This is particularly so in measuring the spectrum over the whole reactor and not at just one point. Sometimes there is one point in a reactor at which precise measurements of the spectrum can be made by several methods. In other cases conditions are such that the neutron spectrum at some point corresponds closely to the calculated value. Such points can be used as reference points.

We describe a method of making relative measurements of the characteristics of a neutron field, by a neutron activation method, which serve as input for determining the spectrum by using precise data at a reference point. The differential spectrum $\varphi(E)$ is recovered from the results of neutron activation measurements by using the activation integrals R_i (where i is the type of detector) which are related to the spectrum by the integral equations

$$R_i = k \int_0^\infty \sigma_i(E)\, \varphi(E)\, dE, \tag{1}$$

where $\sigma_i(E)$ is the activation cross section and k is a scale factor taking account of the differences in the neutron flux density at the detector locations, for example at various power levels. The activation integrals are determined from the measured activity of the detectors:

$$R = (n/\varepsilon)\,(1/N)\,[e^{-\lambda t_b}/(1-e^{-\lambda t_0})], \tag{2}$$

where ε is the efficiency of the counting apparatus relating the rate of counting pulses n to the activity of the detectors, N is the number of nuclei of the target isotope in the detector, λ is the decay constant of the reaction product, t_0 is the duration of the irradiation, and t_b is the time interval between irradiation and the measurement of the activity of the detector.

We introduce the concept of the activation ratio C_i, defining it as the ratio of the counting rates for two detectors of the same type i. The counting rates are measured with a comparator (a counting arrangement for comparing detector activities) for identical detector conditions, conditions of measurement on the comparator, irradiation times, and cooling times. The activation ratios are obviously equal to the ratios of the corresponding activation integrals.

Over a wide range of energies the reactor neutron spectrum does not depend on power. Therefore the irradiation can be performed in a regime which is optimum for each type of detector. In this case the integral equations (1) will have different scale factors k and a relative normalization is required to solve the equations. The most frequently employed normalization method is based on the simultaneous irradiation of the i-th detector and a detector–monitor. An activation detector which has a broad dynamic range of measurement of neutron flux density and the most suitable activity in the measurement is chosen as a monitor. The activation integrals are normalized to a unit reading of the monitor, transforming the system of integral equations (1) to the form

Translated from Atomnaya Énergiya, Vol. 40, No. 3, pp. 259-260, March, 1976. Original article submitted August 14, 1975.

$$R_i^* = \frac{R_i}{R_M} = \int_0^\infty \sigma_i(E)\,\varphi'(E)\,dE, \tag{3}$$

where the spectrum $\varphi'(E)$ differs from $\varphi(E)$ only by the constant factor $[1/\int_0^\infty \sigma_M(E)\varphi(E)dE]$. This method of normalization takes account not only of the effect of irradiation of the detectors at different reactor power levels, but also the effect of the gradient of the neutron flux density due to the error in placing a detector at a definite point. The system of normalized integral equations (3) does not contain different scale factors and can be solved simultaneously for $\varphi'(E)$.

With the normalization method described, making relative measurements of spectral characteristics of the neutron distribution consists in simultaneously irradiating detectors of type i and detector–monitors at the reference point (0) and the point under investigation (j) and subsequently determining the activation ratios:

$$\left.\begin{aligned} C_i &= (n_{ij}/n_{i0}) = (R_{ij}/R_{i0}); \\ C_M &= (n_{Mj}/n_{M0}) = (R_{Mj}/R_{M0}), \end{aligned}\right\} \tag{4}$$

where n is the counting rate.

We consider examples of the use of the activation ratios C_i and C_M to solve specific measuring problems.

Example 1. The normalized activation integrals R_{i0}^* for a certain set of detectors are measured precisely at point 0. Transforming Eqs. (4) we obtain

$$R_{ij}^* = R_{i0}^*\,(C_i/C_M). \tag{5}$$

This is a system of integral equations for determining the differential spectrum at point j.

Example 2. The differential neutron spectrum $\varphi_0(E)$ is measured precisely or is known a priori at reference point 0. Using $\varphi_0(E)$ and the activation cross sections $\sigma_i(E)$ the activation integrals R_{i0} and R_{M0} and the normalized activation integrals R_{i0}^* are calculated from Eq. (1). Then the problem is solved as in the first example except that the calculated values of R_{i0}^* are used instead of the measured values. In this example the following favorable features should be noted: The true activation cross sections can be used in the calculations without taking account, for example, of self-shielding and other effects characteristic of real samples; the accuracy requirements of the cross sections $\sigma_i(E)$ are lowered significantly; it is important only that the cross sections be single-valued in calculating R_{i0} and recovering the spectrum at point j.

Example 3. The integral spectrum $\Phi_0(E) = k\int_E^\infty \varphi_0(E)dE$ is precisely measured or known a priori at point 0. This problem commonly arises in fast neutron measurements. In this case threshold activation reactions are used in the measurements. We normalize the integral spectrum to the integral neutron flux density measured by the detector–monitor, and denote the normalized spectrum by $g_0(E)$:

$$g_0(E) = \frac{1}{\Phi_M}\Phi_0(E). \tag{6}$$

In accordance with the method of effective threshold cross sections the integral neutron flux density measured by the i-th detector is

$$\Phi_i \equiv \Phi(E_{effi}) = \frac{R_i}{\sigma_{effi}} \tag{7}$$

or in normalized form

$$g_i = R_i^* \frac{\sigma_{effM}}{\sigma_{effi}}. \tag{8}$$

Using the activation ratios C_i and C_M we obtain

$$g_{ij} = g_{i0}\frac{C_i}{C_M}. \tag{9}$$

The values found for the normalized integral neutron flux density are input data for recovering the integral spectrum at point j.

The method of activation ratios appreciably simplifies the procedure for measuring neutron spectra while maintaining high reliability of the results characteristic of the reference points. We employ this method to certify standard neutron sources for nuclear physics installations such as reactors, neutron generators, etc.

MONTE CARLO SOLUTION OF GAMMA – GAMMA LOGGING PROBLEMS FOR LARGE DISTANCES FROM THE SOURCE

R. T. Khamatdinov

UDC 519.283:550.3

Monte Carlo techniques are widely used in research on gamma–gamma borehole logging [1, 2]. However, results presently available relate only to relatively small distances from the source to detector (probe length), namely up to 30-40 cm. The probability of a γ ray entering the detector becomes much smaller at larger distances, and the computer program run time increases correspondingly. When such a job is handled by Monto Carlo methods, the run time may be represented by

$$t_A = t_{l_0} \exp[k(l-l_0)](\delta/\delta_0), \quad (1)$$

where t_{l_0} is the time needed to attain a preset accuracy for a given probe length l_0, k is the factor representing the fall in the γ-ray flux density along the probe length in cm^{-1}, l is probe length in cm, and δ is the error in % for a probe length l.

About 1 h of M-220 computer time is required for such a job for a probe of length 10 cm with a rock density of 2.3-2.5 g/cm^3 and a specified error of 10%. The use of (1) for a probe of length 40 cm under the same conditions would require over 100 h. Correspondingly, the run time increases by an order of magnitude if the acceptable error is reduced by a factor 3. It is therefore quite unrealistic to handle such jobs by Monte Carlo methods for probes of lengths more than 35-50 cm, whereas in fact systems are in use with probes of length more than 40-50 cm, in particular in relation to high-power controlled γ-ray sources [3].

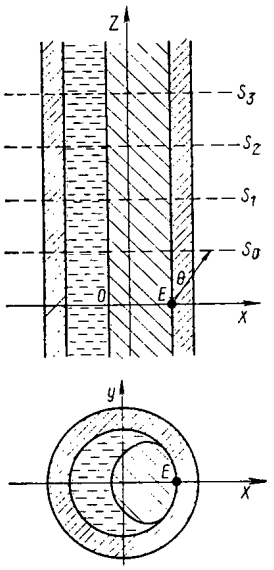

Fig. 1. Scattering geometry.

The algorithms of [2] are not intended for large probes; the following recommendations are made in the literature [4, 5]: local computation, exponential transformation, and path subdivision; however, all of these need testing and adaptation for borehole physics. Here we report results on the splitting method [5]. The job was handled as follows: In a borehole of diameter 200 mm filled with a fluid there lies a logger in the form of an elliptic cylinder (Fig. 1), and at the surface of the instrument pressed to the wall there lies a γ-ray source containing ^{60}Co with a collimation angle relative to the axis of the instrument of 45°. The clay encrustation on the borehole wall is simulated. The borehole passes through a sandstone bed, whose density was taken as 2.0,

TABLE 1. Run Time as a Function of Probe Length

l, cm	t_A, h	t_p, h	l, cm	t_A, h	t_p, h
10	1	1	60	1800	6
20	4,5	2	70	—	7
30	20	3	80	—	8
40	90	4	90	—	9
50	400	5			

Translated from Atomnaya Énergiya, Vol. 40, No. 3, pp. 260-262, March, 1976. Original article submitted July 28, 1975.

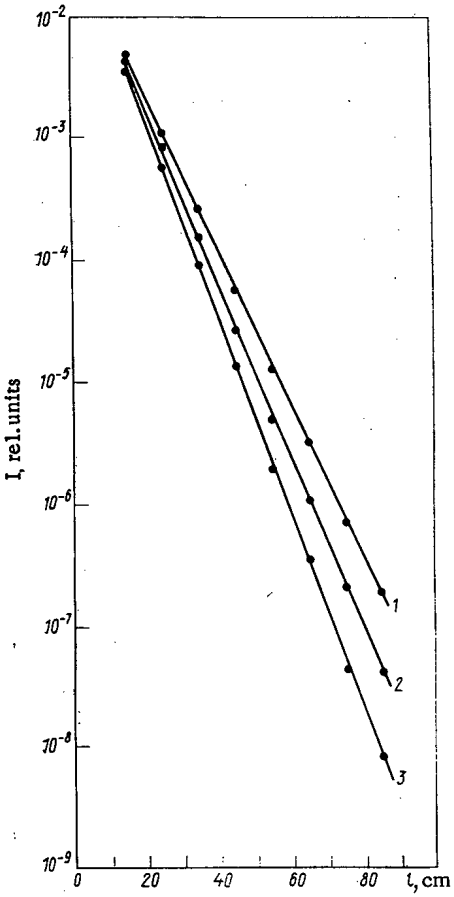

Fig. 2. Scattered γ-ray intensity as a function of probe length. Curves 1-3 are for rock densities (g/cm^3) of 2.0, 2.325, and 2.650, respectively.

2.325, and 2.65 g/cm^3 (corresponding porosities 40, 20, and 0%). The back-scattered γ rays are recorded. The program envisages scope for generating histograms in terms of coordinate, energy, and recording angle.

The calculations for all three rock densities were performed simultaneously by dependent-test methods; the basic medium was taken as a rock of density $\rho_0 = 2.0$ g/cm^3. Statistical weights $p(\rho_j)$ [6] were introduced for the other densities ρ_j. Fictitious multiplication planes S_i (Fig. 1) were introduced to realize the splitting method; when a γ ray intersects a surface S_i, the phase point for the intersection is taken as a radiation source, and paths q_i for the γ rays are generated. The mass of the recorded quantum is here multiplied by q_i^{-1}. If a quantum intersects several surfaces, its statistical mass is multiplied by $(q_1 \cdot q_2 \cdot q_3 \ldots q_n)^{-1}$, where the factors are the multiplication coefficients for the corresponding planes. The final mass of the γ ray is put as

$$Q = p(\rho_j) \prod_{i=1}^{n} q_i^{-1}.$$

A distinctive feature of the algorithm is as follows. The multiplication is performed immediately after intersecting the nearest plane on the source size, during the randomization of the free path. In this method, a quantum cannot intersect several planes without multiplication at each of them. In the exponential-transformation method [4], the multiplication occurs only after collision. Therefore, some random quantum with a long range directed towards the detector can introduce a very large distortion into the result.

The number of planes was chosen on the basis of the required probe length and calculation time; the distances between the surfaces and the multiplication coefficients were selected from experiment so that the flux attenuation on attaining surface S_i was balanced by the multiplication at that surface. Previously available evidence indicated that a layer of rock of thickness 10 cm and density 2.3-2.5 g/cm^3 attenuates a γ-ray flux by a factor 10, so the distances between the planes were taken as 10 cm and the q_i as 10.

We now consider the run time required with this method. For convenience, we take t_0 as the time needed for calculation in the scheme mentioned at the start with an error δ_0 for $l = l_0$, $l_i - l_{i-1} = l_0$, and $\delta = \delta_0$; in that case, the calculation time for the splitting scheme with $l = l_n$ is the sum

$$t_p = e^{kl_0} + e^{k(l_1 - l_0)} + \ldots + e^{k(l_n - l_{n-1})}.$$

As $l_i - l_{i-1} = l_0$, we have $t_p = e^{kl_0} n = t_0 n$.

Consider the ratio $t_A/t_P = t_0 e^{k(l-l_0)}/t_0 n = n^{-1} e^{k(l-l_0)}$; as l increases up to l_n, the run-time economy in our scheme by comparison with the other scheme increases exponentially.

Table 1 gives the run time needed for calculations with an error of 10% in relation to probe length for both schemes; the advantage of the latter scheme increases rapidly with the probe length, and for lengths of 50-60 cm the factor of advantage is 100-300. The program was written in FORTRAN.

Figure 2 shows the scattered γ-ray intensity as a function of probe length for various rock densities.

This method enables one to realize the Monte Carlo method for the entire realistic range of probe lengths in a fashion appropriate to the conditions of petroleum, ore, and coal boreholes. If the geometry is modified appropriately, the method can also be used for other problems involving long-distance γ-ray transport.

LITERATURE CITED

1. Yu. A. Gulin, The Gamma–Gamma Method of Borehole Logging [in Russian], Nedra, Moscow (1975).
2. I. G. Dyad'kin (editor), Monte Carlo Methods in Physics and Geophysics [in Russian], Ufa (1973).
3. A. P. Grumbkov et al., Trudy VNII Yad. Geofiz. Geokhim., Issue 17, Moscow (1974), p. 22.
4. Yu. A. Gulin, V. A. Velizhanin, and I. G. Dyad'kin, in: Monte Carlo Methods in Computational Mathematics and Mathematical Physics [in Russian], G. I. Marchuk (editor), Nauka, Novosibirsk (1974).
5. G. A. Mikhailov, Theory of Monte Carlo Methods [in Russian], Nauka, Novosibirsk (1974).
6. G. D. Varvarin, E. M. Filippov, and A. I. Khisamutdinov, in: Nuclear Geophysics Methods [in Russian], Nauka, Novosibirsk (1972), p. 46.

SYMPOSIUM ON "THE DRAWING-UP OF APPARATUS SYSTEMS OF NUCLEAR INSTRUMENT MAKING FOR LABORATORY AND INDUSTRIAL APPLICATIONS"

A. S. Tuchina

The symposium took place September 16-17, 1975 in Dubno (USSR) in compliance with the plan of operation of the PKIAÉ SÉV. The purpose of the symposium was to acquaint specialists with the present state of development and production of apparatus for instrument making in the member countries of COMECON, and their introduction into the national economy. At the same time, an exhibition was organized showing the apparatus that formed the theme of the symposium. Seventy five specialists from the member countries took part in the symposium, together with members of the COMECON secretariat and a representative of MAGATE. During the two days of the symposium, 28 papers were read.

The greatest number of papers was concerned with the development and production of apparatus for scientific investigations and for use in industry, including the development of apparatus complexes for the nuclear power stations. The papers showed that apparatus permitting wider use of radioisotope methods in the control of chemical processes in metal-mining and light industry, in medicine, during geophysical investigations, and in the production of radioisotopes, have been developed and brought into quantity production within the COMECON countries. A great deal of interest has been shown in the creation and industrial development of complexes of apparatus for radiation monitoring in manufacturing processes, and for monitoring personnel and the environment of the nuclear power stations and the surrounding regions, in the systematization of questions arising out of the development of the individual subsystems for these complexes, in order to prepare material for COMECON Standards covering the design of apparatus for nuclear power stations. These papers showed a further growth in the development of apparatus for scientific research and industrial uses based on the "Vector"–KAMAK concept. The convenience of working with systems based on the "Vector"–KAMAK modules is confirmed by experimental workers, together with the mobility of such systems, the ability to change their structure and function, the use of a computer for data transmission, and automatic control of the experiment. The use of similar modules is considered for the control of the generator units in a power station, for the creation of complexes of apparatus for medical research, activation analysis, for the construction of Mössbauer spectrometers, and in other fields of scientific research and industry. Such questions as the unification of the design of the "Vector" –KAMAK systems, assembly of the elements of these systems, the ergonomics and aesthetic aspects of the design, and especially the problems of organizing quantity productive of the "Vector"–KAMAK units in the factories of the various COMECON countries were also discussed. Papers were read on the further improvement of the design of the scheme, on increasing the quality of the measurement characteristics of the apparatus, particularly their stability and the rate of processing of the analog data received; metrological questions relating to the design of the third-generation apparatus, based on a whole-system approach, were also covered.

An outstanding feature of the symposium was the discussion of questions relating to the design of system apparatus operating under computer control. This illustrates the appearance of a qualitatively new stage in nuclear-instrument design and at the same time underlines the need to concentrate the resources of the COMECON countries on the development of a programmed method of system planning. The symposium also showed the advisability of developing within the COMECON countries work on metrological implementation of newly developed and already manufactured apparatus as a way of increasing the accuracy and stability of its parameters, work on ergonomic and aesthetic aspects of the design, illustrating

Translated from Atomnaya Énergiya, Vol. 40, No. 3, pp. 263-264, March, 1976.

the need for closer attention to the question of unifying within the COMECON framework the individual items of equipment and the elements of the design.

The exhibition showed 35 exhibits of new pieces of apparatus representing the Republic of Cuba, Poland, Rumania, and the USSR. The Soviet Union exhibited apparatus developed in the Union instrument-making research institute and manufactured at mass-production factories in the USSR; electronic apparatus for monitoring, controlling and protecting nuclear power reactors, instruments and units of the "Vektor" system, universal designs of the "Chereshnya" type, complete field and laboratory-pattern radiometers, and unified detection units were all represented in the Soviet exhibits. Specialists from Poland demonstrated the products of the "Polon" nuclear instrument factory group, exhibiting a rack cubicle of KAMAK, a KAMAK frame with units, an electrodynamic vibrator for Mössbauer measurements, a self-contained 130 processor, a punched-tape reader and punch, and an erection stand type MS-2. The Republic of Cuba showed two instruments for analyzing the phase composition of steel, providing a high degree of accuracy in analysis. Rumania showed five modern instruments of the unit type based on the KAMAK design. About 200 specialists visited the exhibition. The participants of the symposium and the visitors to the exhibition had the opportunity of discussing the exhibits, and obtaining the necessary designs and pamphlets.

The symposium and exhibition demonstrated the marked successes achieved in nuclear instrument making in the COMECON countries since the last symposium held in Warsaw in 1973, as well as the need for periodically taking such measures. The results of the symposium and exhibition were discussed and approved in detail by the working group on nuclear instrument making of the PKIAÉ SÉV (Dubna, September 17-20, 1975).

COMECON COLLABORATION NOTES

The 6th Meeting of the RS (Radiation Safety) Section of the Scientific Collaboration Commission Was Held September 8-12, 1975 in Usti na Labe (Czechoslovakia). Suggestions and agreed working plans on 25 topics were considered. Agreement was also reached on a draft of recommendations on methods and instruments for determining the radiation environment at nuclear power stations, and preliminary reports were heard from a conference "Problems in Radiation Safety in Operating Nuclear Power Stations," which was held on the initiative of the Council of September 8-12, 1975 in Usti nad Labem, together with information on the finalized details for a collaboration program and steps taken towards realization. General technical specifications for instruments for recording radioactive substances in air, water, and flowing liquids were discussed and agreed upon; suggestions were considered on collaboration with the International Atomic Energy Agency as regards radiation safety, and decisions were taken on various other topics.

A Conference of Representative of COMECON Member Countries. This conference on isotope production (SOP-75) was held September 22-25, 1975 in Budapest. Means of coordinating plans for isotope production in the member countries in 1976-1980 were considered and discussed. Information was reported on researches within the framework of the scientific collaboration plan for 1971-1975. A research plan for 1976-1977 was discussed and agreed upon, together with standardization projects for 1976-1980.

The Second Conference of Representatives of the Convention on Multilateral International Specialization and Cooperation in Isotope-Component Production. This was held September 25-27, 1975 in Budapest. There were participants from ministries, institutes, and foreign-trade organizations of the members. Information was presented on progress in realizing the convention.

Conference of COMECON Specialists on Radiation Shielding and Radiation Technology. This was held from September 30 to October 3, 1975 in Torun (Poland). The meeting was attended by specialists from the member countries, members of the COMECON secretariat, and representatives of the Interatom instruments organization. The following were discussed and agreed upon: a COMECON draft standard for general technical specifications for laboratory furnishings for work with radioactive substances, and a draft of recommendations for standardizing laboratories for work with ionizing-radiation sources, including classification and general technical specifications; also, working plans on scientific collaboration for 1976-1980 on unifying and specializing packaging equipment for shipping radioactive substances, unifying holders, chambers, and extraction hoods, including manipulators, viewing windows and so on, the drafts for the working plans of the standing commission of COMECON on atomic energy for 1976-1977, and a plan of researches on standardization in radiation protection and radiation technology. A decision was taken to adopt a basic document in the definition of standards: a general base set of parameters and indices for radiation-protection components; in addition, the range of components for use in radiation technology was discussed.

The 10th Meeting of the Radiation Technology Section of the Council on Scientific Collaboration was Held October 7-10, 1975 in Minsk. Participants were members of this section, experts from COMECON member countries, observers from Cuba, and members of the COMECON secretariat. In the discussions and exchanges of views on the topics it became clear that the Cuban representatives were interested in the radiation treatment of food and agricultural products, and in strengthening their relationships with the section.

Conference of COMECON Specialists on Radiation Sterilization of Medical Materials and Components and Unification of Standardization Documents. This conference was held October 21-24, 1975 in Leningrad. Reports were heard from the symposium of specialists from the COMECON member countries on the radiation sterilization of medicinal substances (Brno, Czechoslovakia, April 1975). Agreement was reached

Translated from Atomnaya Énergiya, Vol. 40, No. 3, p. 264, March, 1976.

on a list of rules governing the performance of radiation sterilization for medicinal substances in COMECON members; other items agreed upon were gas-chromatographic determination of styrene, aromatic hydrocarbons, and dioctyl phiholate in aqueous extracts; medical specifications for polymer and composite materials for primary packing of disposable medical items for radiation sterilization, and other techniques. Information was reported on some studies made to draw up documents and plans for future scientific collaboration in 1976-1980; also, proposals were prepared on the sequence and timing of the studies.

INFORMATION

50 YEARS OF CORRESPONDING MEMBER OF THE ACADEMY OF SCIENCES OF THE SSSR, A. M. BALDIN

N. N. Bogolyubov, A. A. Kuznetsov,
and I. N. Semenyushkin

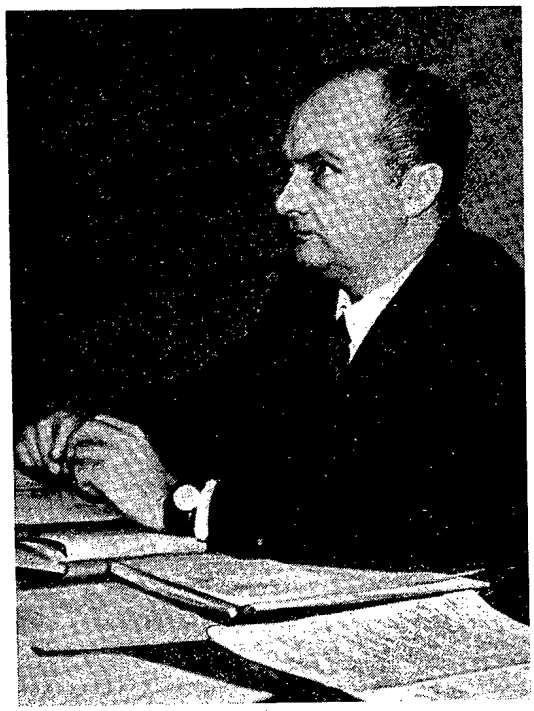

Corresponding Member of the Academy of Sciences of the SSSR, Aleksandr Mikhailovich Baldin is a well-known scientist and a specialist in the field of nuclear physics and the physics of elementary particles and accelerators. He was born on February 26, 1926. The scientific activity of A. M. Baldin started 26 years ago in the P. N. Lebedev Institute of Physics of the Academy of Sciences of the SSSR, after completing the development of the theory of cyclic accelerators at the Moscow Engineering-Physics Institute. In his first papers, he (jointly with V. V. Mikhailov and M. S. Rabinovich) proposed a method for investigating betatron oscillations, given the title of "The method of envelopes," which at the present time is used widely in calculations of the parameters of strong-focussing accelerators. A. M. Baldin is one of the authors of the physical basis of the 10-GeV synchrophasotron in Dubna. Recent papers by A. M. Baldin in this field have been devoted to the redesign of the synchrophasotron in an accelerator of nuclei, on which beams of relativistic deuterons and α particles are being produced at the present time.

The talent of A. M. Baldin as a scholar–physicist was manifested particularly fully in his investigations on nuclear physics and the physics of elementary particles. The results of these works brought international fame to him and introduced him into the ranks of the most eminent specialists of the Soviet Union. Here, first and foremost, the cycle of papers on the photocreation of ions should be mentioned, for which A. M. Baldin together with his colleagues was honored with the State Prize of the Soviet Union.

Translated from Atomnaya Énergiya, Vol. 40, No. 3, pp. 265-266, March, 1976.

The papers on the theory of the photocreation of mesons by deuterons and complex nuclei were a great contribution, and had a decisive influence on the development of research into photomeson processes in both the Soviet Union and abroad.

An important series of papers by A. M. Baldin and his students is devoted to theoretical investigations of the photodisintegration of nuclei and the properties of small-nucleon systems. The predictions and conclusions of the theory developed by them subsequently were confirmed by experiments carried out in the USA, and they received international recognition.

In addition to these main routes, A. M. Baldin was occupied with other problems of theoretical physics, in particular the systematics of elementary particles. He put forward and developed the idea of creation according to the isotopic spin of systems with zero hypercharge. In 1971, A. M. Baldin, on the basis of generalization of the principle of scaling invariance, predicted a new effect – the cumulative formation of particles in interactions of relativisitc nuclei with nuclei. By his initiative, experiments were set up which were of great fundamental importance.

Among recent papers, mention should be made of the experimental investigations on the creation and decay of vector mesons at high energies and on the cumulative formation of particles of different nature in nuclear–nuclear collisions. A. M. Baldin was not only the initiator, but also the scientific director and most active participant in these tasks. For the first time, the electron–positron decays of vector mesons were successfully detected experimentally. This phenomenon was recorded in 1971 as a discovery. Somewhat later, A. M. Baldin with coworkers for the first time also detected and investigated in detail the effect predicted by him – the cumulative formation of mesons and baryons. These investigations were of a fundamentally new field of physics – relativistic nuclear physics.

In 1968, A. M. Baldin was selected for the post of Director of the High Energy Laboratory of the Joint Institute of Nuclear Research. He paid great attention to the organization of international scientific collaboration, set up within the framework of the Joint Institute of Nuclear Research. He is a member of the Committee on High-Energy Physics of the European Physical Society, the organizer of a number of international symposia, seminars and schools. In addition, A. M. Baldin is one of the organizers and the vice-chairman of the Scientific Soviet of the Academy of Sciences of the SSSR on the problem of "Electromagnetic Interactions," and the deputy to the editor-in-chief of the scientific periodical "Problems of the Physics of Elementary Particles and Atomic Nuclei." He carries out active work in the training of scientific personnel. Under his direction, a large number of highly qualified specialists have been trained, many of whom have become well-known scientists.

The merits of A. M. Baldin have been highly recognized by government and by other awards.

SEMINAR ON THE VARIABLE OPERATING CYCLES OF NUCLEAR POWER STATIONS

B. B. Baturov, O. M. Glazkov,
and R. R. Ionaitis

In October 1975, the trade seminar "Engineering and Economic Aspects of Nuclear Power Generation" was held in Moscow, at which the problems of using atomic electric-power stations as a variable part of the plot of energy-system loadings were discussed. More than 100 specialists from scientific and planning-construction organizations, occupied with the development of plant for nuclear power stations, representatives of power and mechanical engineering and exploitationists participated in the work of the seminar. Opening the seminar, Corresponding Member of the Academy of Sciences of the SSSR I. Ya. Emel'yanov stressed that the increasing role of nuclear power stations in the energy supply of the Soviet Union, the placing into operation of powerful energy installations based on organic and nuclear fuel, and the continued tightening-up of the plot of energy-system loadings are changing the operating conditions of thermal and atomic electric-power stations. Even more rigorous demands are being made on adjustability of technological plant, which compels the designers and planners to assess more carefully the maneuverability of nuclear power station plant and to bring it into conformity with the requirements of the power systems.

In the reports heard at the seminar, such problems were dealt with as the requirements of the power systems on technological plant, the possibilities of using domestic reactors in variable cycles, the special features of reactor physics during operation in power systems, corrosion of structural materials and the demands on them for conditions of durability in variable operating cycles of nuclear power stations, etc.

In the first group of papers (Academician L. A. Melent'ev, A. V. Bakanov, et al.), the prospects were shown for the formation of power systems for the Soviet Union and the main requirements were formulated on maneuverability of the power units during their expected operation in an even more irregular load chart. Among the main requirements of power systems on the technological plant of nuclear power stations in 1980 and later, the following were mentioned: nightly shutdowns for 5 to 8 h with subsequent setting of the load at a rate of not less than 1.2% per min; shutdowns on nonworking days of 24-32 or 40-55 h with subsequent setting of the load at a rate of not less than 0.7% per min; change of load after prolonged operation within the limits of the controllable range (30-100% of nominal power) at a rate of not less than 4% per min without limiting the number of such cycles, etc. The nonfulfillment of these and certain other demands reduces significantly the operating efficiency of power systems and may lead to the nonprovision of the electric power requirements, for example, because of the lag of the power setting of the power units behind the load required according to the chart.

The second group of papers showed how completely the existing designs of reactors of the RBMK, VVÉR, and BN types satisfy the requirements of the power systems and what are the possibilities for improving their maneuvering characteristics.

RBMK reactors (K. K. Polushkin and A. Ya. Kramerov) permit the power to be varied over the range 100-50% of nominal with rates of ~0.1% per sec and to operate for a long time over this range of power without falling into the "iodine well." The thermomechanical cycle of the principal structural elements of the reactor, the coolant circuit, and the steam tubes are almost independent of the power and do not impose restrictions during operation in variable cycles. At the same time, the efficiency of the fuel elements and the stabilization of the energy release field during variable cycles require special consideration and further study.

Translated from Atomnaya Énergiya, Vol. 40, No. 3, pp. 266-267, March, 1976.

VVÉR reactors (V. P. Spasskov, et al.) possess excellent controllable characteristics – pickup, fast response of the operative control organs, absence of limitations over the range of loads of normal control which are unacceptable according to the conditions of thermocyclic durability. The disadvantage of the VVÉR – the reduction of the controllable range at the end of the run – is relatively simply eliminated for nuclear power stations with several energy-generating units, when recharging of the fuel into the reactor can be carried out at a different time. The efficiency of the fuel elements in the case of multicyclic load changes also requires further studies.

Experience in the operation of fast sodium reactors confirmed that they have excellent dynamic characteristics and can function stably over a wide range of loads and rates of change (V. S. Danilovskii); however, economic considerations and the specific characteristics of these reactors compel their use in the basic part of the power system load chart.

The construction of the multichannel RBMKP reactor in sectional-modular form and with nuclear steam superheating (O. M. Glazkov) shows that during the development of the project the main requirements of power systems have been taken into consideration, and there is a basis for assuming a completely real operation of the power unit with such a reactor under variable conditions. The special features of the RBMKP reactor which enlarge its maneuverable characteristics are sectionalization of the core and of the circulatory loop, the cooled metal structure, the absence of large-diameter, thick-walled plated collectors, vertical separators, the use of superheated steam turbines, etc.

The report by P. A. Kruglikov et al. was concerned with the extension of the maneuverable capabilities of a power unit with an RBMKP reactor. The paper was devoted to the special features of a power unit thermal system which permits temperature regulation of the superheated steam at the outlet from the reactor during variable cycles.

Experience in the operation of the reactors of the Bilibinsk nuclear and thermal power stations under the complex conditions of an isolated power system (A. V. Bondarenko) confirmed the high operating reliability of channel reactors.

In the interesting paper by Yu. I. Mityaev, the physical aspects of the operation of reactors of the RBMK type under variable cycles are analyzed in detail. It shows how to use in the best way the available reserve of reactivity, taking into account the physical and economic limitations. Weekly shutdowns of the reactor on nonworking days of 40-55 or 24-32 h do not produce additional limitations on the conditions of leaving the "iodine well." On the contrary, daily shutdowns of 5-8 h are more unfavorable and are economically unprofitable. It is mentioned also that the neutron-physical characteristics of reactors of the RBMK type do not limit the required rate of change of power, with the exception of the rate of rise of power over the range 80-100% of nominal. Before building up sufficient operating experience, it is advantageous to carry out a power increase over this range carefully, taking account of stabilization and the formation of energy-release fields.

The discussions on stabilization of neutron fields in the VVÉR-100 reactor (A. S. Dukhovenskii and V. N. Semenov) and the behavior of the reactivity of the VVÉR-440 under the operating conditions of a nuclear power station in a variable load cycle (V. F. Gorokhov) were interesting.

When using stainless austenitic steels, perlite class steels and zirconium alloys as structural materials for nuclear power stations with VVÉR and RBMK reactors, no reduction of their corrosion resistance should be expected during periodic shutdowns of several days also including depressurization of the circuit (V. V. Gerasimov). During shutdowns of longer duration, in the case of the use of perlite steels, inhibiting agents must be introduced into the circuit.

The large number of papers devoted to the requirements for materials and plant according to the conditions of endurance and resource of their operation in variable cycles (T. P. Karzov), and analysis of the thermally stressed state of the main turbine elements (A. Sh. Leizerovich et al.), confirms the possibility of using the main technological plant during the operation of nuclear power stations with controlled loading.

The discussion which took place at the seminar enables the following conclusions to be drawn:

1. The existing designs of reactors can be used in variable cycles and satisfy the majority of the power system requirements.

2. Certain requirements on reactors by the power system, such as the necessity for a daily shutdown, an unlimited number of power changes by ±100% at a rate of 2% per sec and a number of others, are excessive, economically unjustified, and must be provided by other means.

3. During the development of prospective reactor and thermomechanical plant designs, it will be essential to take into account fully the requirements of the power systems.

4. The efficiency of the fuel elements in a multicycle change of load requires further serious study and experimental verification.

INTERNATIONAL SYMPOSIUM ON GAS-COOLED REACTORS

I. Kh. Ganev

An international symposium on Gas-Cooled Reactors, organized by the IAEA and the Nuclear Energy Agency (NEA) of the OECD, was held from October 13-17, 1975 at the Center for Nuclear Research, Julich (Federal German Republic). The symposium concerned all reactors with helium cooling: high-temperature power reactors (HTR) with steam turbines (HTR-ST) and helium-turbine cycles (HTR-HT or HHT), ultra-high-temperature reactors UHTR for the production of heat and electric power, high-conversion reactors HTR-HC and the helium breeder-reactor GCFR.

The trend considered in reactor construction has been developed during 20-25 yr. The experimental reactors "Dragon," "Peach Bottom," and AVR have operated successfully during 8-10 yr. Recently, the reflector has been replaced on the "Dragon" reactor (similar operations are being considered on the HTR, in consequence of the high fast neutron fluences). The first unit of the Peach Bottom nuclear power station has been shut down for a careful study of the facility after eight years of operation. A year ago, the outlet temperature of the helium in the AVR reactor was increased from 850 to 950°C, which led to an increase of output of fission products from the fuel elements (R/B): ^{133}Xe by a factor of three; and ^{135}Xe by a factor of one and one-half. The predominantly γ-active isotopes in the primary circuit of AVR were ^{65}Zn, ^{110m}Ag, ^{137}Cs, and ^{134}Cs. The total increase of γ activity of all the noble gases amounted to 30-50% and the level of contamination of the helium by carbon monoxide increased by a factor of three to five.

During many years, the main problem in the development of HTR reactors was the building of a commercially competitive HTR-ST for entry into the market of nuclear power stations. This is still the principal goal in the West but difficulties have been encountered recently on the path to its achievement. Despite the well-understood and positive qualities of the HTR, which still remain in force, it is felt that nuclear power generation probably could have managed even without the widespread introduction of nuclear power stations with HTR-ST because of the use of well-exploited light-water reactors (LWR) and breeders (LMFBR or GCFR in the case when unforseen complications arise with LMFBR). The HTR-HT has somewhat better odds in competition with the LWR, but this type of HTR is still insufficiently developed and its future depends in many respects on the success of HTR-ST. The situation which has been created is explained in part by the difficulties encountered in the construction of semiindustrial HTR-ST, and also by the noncompletion of the thorium fuel cycle, on which the majority of HTR are dependent, in particular the construction of facilities for reprocessing the fuel.

Delivery to commercial operation at the Fort St. Vrain nuclear power station (planned in March 1972) is expected in June 1976. This nuclear power station has built up considerable positive experience of cold and hot physical startups, which took place at the end of 1974 and in May 1975 when it reached the power level of 2% of nominal. However, together with this, unfortunately, a considerable experience has already been built up of various breakdowns and troubles. One of the most recent of these events occurred in January 1975: during shutdown of the reactor, in not very clear circumstances, a considerable quantity of water (several tons) from the gas blower water system reached the primary circuit. In May, leakage of hot helium was detected through the upper inner containment structures and also failure of part of the electric cables. Startup of the station and arrival at the power generation level is expected at the end of 1975 and the beginning of 1976. In view of the circumstances established, the company General Atomics (GAC) curtailed plans for the construction of large-scale nuclear power stations with HTR-ST down to a single demonstration nuclear power station "Summit," with two units of up to 770 MW (el). It is proposed to introduce the first unit in 1981 under the sponsorship of ERDA.

Translated from Atomnaya Énergiya, Vol. 40, No. 3, pp. 267-269, March, 1976.

A second semiindustrial THTR nuclear power station, built in the Federal German Republic, will be started up in 1978. Constructional work has been completed to a considerable degree and in 1976 it is planned to carry out stressing of the cables and to test the concrete pressure vessel under pressure. In view of the position of the firm of Krupp, having concluded an alliance with GAC on the further improvement of an HTR-ST with an electrical capacity of 1160 MW (HTR-1160), the development has started in the Federal German Republic on the route to the construction of an HTR-ST with spherical fuel elements. The construction of AVR and THTR reactors has been discontinued and large-scale nuclear power stations with HTR-1160 and helium turbine HHT with a capacity of 1170 MW (el) are being planned, with cores of lumped fuel elements.

The HTR-1160 reactor is accepted as the main reactor in France also, and at present it is planned for further improvement, taking into account the local conditions, in conjunction with GAC. It has been decided to increase the outlet temperature of the helium in the French version from 750 to 1000°C by the use of lumped fuel elements with a more homogeneous arrangement of the fuel for the application of this reactor in the chemical and metallurgical industries. A similar leaning toward the development primarily of VHTR has been adopted also in Japan. In the Japanese experimental reactor, it is proposed to use lumped fuel elements of the British type with tubular rod elements arranged directly in the openings of the graphite blocks for passage of the coolant. The capacity of the reactor is 50 MW (th) with a helium outlet temperature of 1000°C. The question of construction of this reactor still has not been resolved. In conjunction with GAC, the possibility also is being studied of building a seismic-stable HTR-ST.

The most extensive and important work on VHTR has been evolved in the Federal German Republic. The main items of research are the heat exchangers, which are gradually increasing in size, in which the heat from the hot helium entering them at 950°C is utilized for gasification of coal and also for producing and heating up the reducing gases (hydrogen alone or in mixtures with carbon monoxide). The most recent type of heat-exchanger, the steam converter (SC), is being studied on the electrically heated EVA facility with a power of 1 MW, which has been operating in KFA since 1972. The SUPER-EVA facility, with a power of 10 MW, will be started up in 1978. Work on the investigation of the gasifiers and steam converters is proposed for completion by the construction in the 1980's of semiindustrial and industrial facilities with VHTR reactors with thermal outputs 750 and 3000 MW and with spherical fuel elements for a single passage of the core. The concept of the VHTR reactor developed in the paper by R. Schulten et al. is interesting. A facility of the loop-type is proposed, with a reactor in a vessel of prestressed cast steel (PSRV) and with external pressurization. The loops of the steam converter (700-950°C) and the steam generators (SG) (250-700°C) are arranged around the vessel and right up against it. The hot helium is fed to the steam converters through the central tube (with a thin internal heat insulation) of a coaxial heat tube and is returned to the reactor after passing through the steam generators along the coaxial gap. The steam converters are composed of the Field tubes of a centrifugal casting with a diameter of 100 mm and a wall thickness of 15 mm, with an outlet for the hot reducing gas from the steam converters through an inner tube. An intermediate heat exchanger is not planned for the facility; however, a study of such a heat exchanger, made in the form of coaxial tubes with a gap of 0.1 to 1 mm, is planned on the EVA facility. These tubes will be produced by the firm of General Electric (GE), having started from 1974 in conjunction with GAC and the firm of Westinghouse (WG) on a study of VHTR in the USA. The General Electric studies are based on spherical fuel elements developed in the Federal German Republic and Westinghouse's studies are based on lumped fuel elements of the type used in the NERVA project.

The Federal German Republic, USA, and Switzerland are also conducting joint work on coordinated projects of HTR-HT and GCFR. The basis for the development of the HHT reactor are the gas-turbine test benches in the Federal German Republic: HHV, built in KFA (startup planned in 1977), and EVO in Oberhausen (at the present time, being brought into operation). The merit of the pilot HHT, with an efficiency of 37%, is the capability of discharging the heat into dry air cooling towers, which will facilitate the choice of site for a nuclear power station. In the USA an HTR-HT is being developed, designed on the use of an additional circuit with ammonia coolant (for removal of residual heat of the water) which will enable the efficiency to be raised to 42% and even 50% (with increased heating of the helium in the reactor from 816 to 982°C).

The three-dimensional artificial roughness applied to the fuel elements of the loop assembly and intended for reactor tests in BR-2 in 1976 is new in the papers on the GCFR (D. Donne, Karlsruhe). This type of roughing permits approach to the theoretical limit for intensifying the removal of heat by the helium. Reports on the experimental work carried out in the USA on ventilated fuel elements were interesting, as were

the proposals of the European Association of Gas Breeders (J. Sherman), recommending a return to consideration of the problem of building a prototype GCFR with a capacity of 600 MW (el). The report spoke about the long-time studies on the GFCR (GBR-4), which showed that its operating reliability and breeding properties are better than the LMFBR. P. Kasten et al. (USA), in a paper on the priority of developing different types of gas-cooled reactors, placed GCFR in second place after HTR-ST, in view of the high value of breeders in the economy of uranium sources: however, the GCFR is considered only as a reserve version in the case of failure with the sodium breeder.

As alternatives in the case of delay in the introduction of breeders, E. Toichert et al. (Federal German Republic) suggest the operation of any type of HTR in the high-conversion range (breeding coefficient = 0.76), and subsequently in an almost breeding cycle (breeding coefficient = 0.97), using the thorium fuel cycle. The HTR-HC cycle leads to a reduction of the specific power to 5 MW/m^3 and a burnup of 20-30 MW · d per 1 kg of fuel.

Considerable attention was paid to the problems of exploitation of materials: insulation, weakly diffusing graphite, nonmetallic blades for helium turbines, high-temperature alloys with the addition of aluminum oxides to NK-40 steel (25% Cr, 20% Ni), increased breaking strength from 1 to 8 kg/mm^2 at 900°C (G. E. Vasilevskii et al., the USA), etc. Great efforts are being devoted to the study of mechanisms of escape of fission products from the fuel elements, and their deposition in the circuit, and also on the improvement of fuel and the completion of the fuel cycle. In 1976 alone, ERDA assigned to this work 20 out of 30 million dollars intended for completing the HTR-ST. Completion of the work is planned in 1986. In 1977, in KFA the "Jupiter" facility will be started up, for the reprocessing of AVR fuel elements. Improvement of the microfuel is proceeding by the route of replacing the SiC cladding with ZrC claddings and adding oxides of Al, Si and other elements to the fuel kernel in order to stabilize the "Amoeba" effect (displacement of the fuel kernel). The number of countries participating in the development of HTR is expanding (Brazil, Austria, etc.). The national program of Austria consists of the design and improvement of the individual plant units of the HTR. At the Austrian Nuclear Center, Seibersdorf, large-scale test benches have been built for testing pressure vessels of stressed concrete (PCRV) and other plant at pressures in the circuit of up to 100 bar. An interesting feature of the Austrian PCRV is the use of a heated (300°C) internal pressurizing vessel, located in front of the thermal insulation of the pressure vessel, which facilitates its inspection and maintenance. Austrian specialists do not see any obstacles for increasing the pressure in the PCRV up to 150-200 bar.

A paper by A. P. Aleksandrov et al., from the Soviet Union, on the structure of nuclear power stations in the process of development of nuclear power generation, was presented at the symposium.

The symposium, by gathering about 300 delegates from 21 countries and five international organizations, demonstrated the wide front of scientific researchers and experimental-constructional work on the technology of gas-cooled reactors and confirmed (despite some difficulties with the HTR-ST) the necessity for further development of the HTR (especially VHTR).

THE SOVIET – FRENCH SEMINAR ON WATER-COOLED WATER-MODERATED POWER REACTORS

V. P. Denisov

From the September 17-23, 1975 a Soviet–French seminar was held at the Center for Nuclear Studies, Saclay (France), on the theme "Steam Generators, Structural Materials and Manufacturing Technology of the Primary Circuit Components of Water-Cooled/Water-Moderated Reactors." A second theme of the program of cooperation between the State Committee on Atomic Energy (GKAE) of the Soviet Union and the Commisariat a l'Energie Atomique (CEA) of France in the field of developments for nuclear power stations with water-cooled reactors, agreed to in 1974, was discussed. The first theme of the program, "Physics, Hydraulics, and Heat Exchange of Water-Cooled/Water-Moderated Reactors" was discussed at a seminar in October 1974 in the I. V. Kurchatov Institute of Atomic Energy.

Six Soviet and eight French papers were presented at the seminar in Saclay. The Soviet papers covered the problems of development of water-cooled/water-moderated power reactor facilities, steam generators for them, structural materials for the basic plant of reactor installations, and also demonstrations of the durability of the principal components of the primary circuit. The French papers considered the individual problems of vertical steam generators of the firm Westinghouse used in nuclear power stations constructed with water-cooled/water-moderated reactors in France, the development of a new design for straight-through vertical steam generators, the results of an investigation of the embrittlement of steel pressure vessels under irradiation, the feasibility of electron-beam welding of the primary circuit components, the results of development of quality control systems for the equipment of the primary circuit during operation. The main part of the discussion was occupied by the problem of steam generators for nuclear power stations with water-cooled/water-moderated reactors. The Soviet specialists in their reports, based on a decade of experience in the operation of steam generators in the first unit of the Novovoronezh nuclear power station and many years of experience in the operation of the steam generators of the second to fourth units of this station, and also the steam generators of the Kol'sk nuclear power station, the "Nord" nuclear power station and "Kozlodun," showed the correctness of the choice of the horizontal construction of steam generators with vertical cylindrical tubular collectors, which ensure a reliable operating capability of the heat-exchanger surface, made from normal austenitic 0Kh18N10T steel. Corrosion resistance is ensured in that under the conditions of the horizontal arrangement of the tube bundle and the vertical tubes of the collectors, there is no possibility of the continued buildup of corrosion-active impurities due to the provision of a stable circulation of "boiler" water and the maintenance of the water cycle rate. The French specialists presented the results of numerical–experimental investigations aimed at the improvement of operation of the vertical steam generators with U-shaped bundles. The disadvantages of these steam generators are the corrosion defects of the heat-exchanger tubes at sealing points in the tube plates. In one of the reports, the circulation of boiler water in the U-shaped tube bundle was discussed and it was proposed to use built-in jet pumps in order to intensity the circulation, in particular in the region of the plane tube plate of the steam generator, and thereby prevent the continued buildup of corrosion impurities at the tube plate.

In a report on the study of steam separators in the steam generators, the use in models of a mixture of water and freon as the working medium, and the measurement of the humidity of the steam by various sensors, is interesting. Another report of the French specialists was devoted to the corrosion resistance of the heat-exchanger surface tubes of the vertical steam generators, in which, according to the results of the investigations, the inadequate corrosion resistance of tubes of nickonel-600 is shown, and preference is given to nickolo-800; it is recommended that the alloy Sanicro-30 be used for new designs of steam

Translated from Atomnaya Énergiya, Vol. 40, No. 3, pp. 269-270, March, 1976.

generators. The Soviet specialists expressed a positive opinion on vertical steam generators, but in their reports the working conditions achieved at the points of sealing of the tubes in the tube plates are similar to the working conditions in horizontal steam generators.

From the reports presented by the French specialists and according to the results of a visit by the Soviet delegation to a number of laboratories in Saclay, it can be seen that in France great attention is being paid to the problems of structural materials, quality control of the equipment of the primary circuit of nuclear power stations with water-cooled/water-moderated reactors of the Bugy and Fessenheim type both during manufacture and in operation, to studies of the irradiated pressure-vessel steel of the reactors and to the embrittlement resistance of the structural materials on samples with a simulated crack. It should be mentioned that considerable success has been achieved in the Saclay laboratories on the problems enumerated. Thus, in equipment for the quality control of the metal of the main elements of the reactor pressure vessel during operation, a system has been fully developed using methods of ultrasonic monitoring, magnetopowder defectoscopy, eddy currents, and acoustic emission. The French specialists demonstrated the operation of all the main equipment on full-size models of the units of the reactor pressure vessel. The distinguishing feature of the ultrasonic defectoscopy equipment is the use of sensors with adjustable focussing, having a high sensitivity and resolution, and also the use of an attachment with a system of grouped sensors. The technological development of a number of solutions for the equipment of the primary circuit is being undertaken in the Saclay laboratories, for example, welding of the branch pipes to the reactor vessel is being improved by means of electron-beam welding. The use of the method of local evacuation of the weld sections should be mentioned here; an equipment has been developed and adapted for welding longitudinal and annular seams, and also for welding branch pipes with dimensions in excess of 1 m in external diameter. The Saclay laboratories are equipped with quite a large inventory of modern equipment.

The seminar took place in a business-like, friendly atmosphere and, in the opinion of the Soviet and French specialists, brought a definite practical benefit for both countries in the development of nuclear power stations with water-cooled/water-moderated reactors. After concluding the work of the seminar, the Soviet specialists were received by the Director of the French Atomic Energy Commission (CEA) and acquainted with the long-term construction of nuclear power stations with water-cooled/water-moderated reactors in France over the next ten years.

SYMPOSIUM ON THE TRANSPLUTONIUM ELEMENTS

K. Shvetsovii

The work of the 4th International Symposium on the Transplutonium Elements (September 1975 in Baden-Baden, Federal German Republic) was devoted to the systematization of properties, chemistry of separation, preparative chemistry, physical and coordination chemistry and the applied use of the actinide elements, and the synthesis and stability of the transactinide elements. More than 50 papers were presented.

In the first section, on the Systematization of the Properties of the Actinide Elements, nine papers were given concerned with the establishment of mechanisms in the properties of the actinide elements due to their electron structure. For example, in the paper by H. Hill and E. Kmetko (USA), an attempt was discussed to interpret the electron structure of the actinide metals from the aspect of the valence bond theory. V. Ward and H. Hill (USA) suggested a method of calculating the normal entropy of the metals, taking into account the nonmagnetic and magnetic components.

A number of reports were devoted to the systematics of recent experimental data on the thermodynamic properties of ions of the actinide elements, by determining the mechanisms in their changes and by estimating the oxidation potentials for different pairs on the basis of the ratios obtained.

In the reports on the Chemistry of Separation, high-speed methods of separation and identification of the transactinide elements in a gaseous sphere were discussed. V. Bruckl et al. (Federal German Republic), investigated the extraction of analogues of elements 108-116 by diethyldithiophosphates into an organic diluent from hydrochloric and sulfuric acid solutions. On the basis of the data obtained, a procedure was suggested for their separation. I. K. Shvetsov (SSSR) reported his investigations on the separation of transplutonic elements with organophosphorus compounds.

Reports on Preparative Chemistry were devoted to the production and study of the structure of the actinide metals: actinium, protoactinium, americium, curium, californium; obtaining and determining the parameters of the crystal lattice of the monochalcogenides and monopnictides (P, N, As, Sb, Bi) of the actinide elements. In discussing the crystalline structure of metallic americium and curium (V. Muller et al., Federal German Republic), the authors arrived at the conclusion that in the case of production of these elements by condensation from the gaseous phase, they have a double hexagonal densely packed lattice.

At the meeting of the section on Physical Chemistry, the results were discussed of studies of the specific heat, electrical resistance, vapor pressure and magnetic susceptibility of metallic americium, curium and californium, and the magnetic susceptibility of the pnictides of americium and curium. New experimental data were presented in these papers, which permit judgement on the electron structure of the metals and their compounds.

In a number of reports, the structure of the compounds of the actinide elements was studied, using methods of infra-red spectroscopy and x-ray structure analysis. The most interesting papers were on the oxides of Pa, U, Np, Am, Cm, and Cf (D. Main, R. Turcott, USA), the investigation of the structure of the complex peroxides, carbonates and acetates of penta- and hexavalent neptunium (S. Myuzicas and J. Borns, USA). The conclusions of the authors of the latter paper, on the general nature of the change of the metal–oxygen and metal–ligand bond strength with transition from Np(VI) to Np(V), are in agreement with the conclusions drawn in the paper by D. N. Suglobov.

A small number of reports concerned investigations of the stability of the valence states of the actinide elements in different media. The reports presented by the Soviet scientists V. S. Koltunov, N. B.

Translated from Atomnaya Énergiya, Vol. 40, No. 3, pp. 270-271, March, 1976.

Mikheev and B. F. Myacoedov attracted great interest. Of the other papers, the report by G. Landress et al. (Belgium) on the pair potentials and chemical properties of uranium, neptunium, and plutonium in alloys of the alkali metal chlorides should be mentioned. The pair potentials were determined for Me(VI)/Me(V), Me(V)/Me(IV), Me(IV)/Me(III), and MeIII/Me, which is the basis for the development of electrochemical methods of extraction and separation of the transuranic elements by the use of melts.

The information presented to the section on the Applied Use of the Actinide Elements was concerned mainly with questions of the practical use of ^{252}Cf neutron sources in industry, medicine, and scientific research. D. Carracer (USA) showed that the principal user of the sources is the atomic industry. In other reports, procedures are described for the preparation of californium sources, the essential equipment, and installations. In April 1976, symposia are to be held in Paris and Brussels especially on the use of ^{252}Cf.

Problems of the Synthesis of the Transactinide Elements were discussed at two meetings. Two papers on this theme were presented by the Soviet Union: "The Experimental Verification of New Methods of Synthesis of the Transuranic Elements" (G. N. Flerov) and the "Results and Prospects of Searches for Superheavy Elements in Nature" (G. M. Ter-Akop'yan). In addition, I. Zvara reported on chemical experiments with elements with Z equal to 102-105, carried out in Dubna. These papers were received with great interest and generated a lively discussion.

Scientists of Berkeley and Livermore reported on the synthesis of an isotope of element-106 with a mass number 263. The authors described in detail the procedures for purifying a ^{249}Cf target from lead, and the irradiation conditions in a beam of heavy ions at Berkeley. The principal results concerning the properties of the isotope $^{263}106$ confirm the data from experiments carried out in the Joint Institute of Nuclear Research (JINR), in which element 106 was discovered.

A group of scientists from Los Alamos and Livermore reported on the synthesis of the heaviest isotope of fermium with mass number 259. Synthesis of the isotope was effected in a beam of tritons, using a target of ^{257}Fm.

Three papers, presented by groups from the Max Planck Institute, Heidelberg, the Technical University of Darmstadt, and the University of Mainz, were devoted to an account of methods for the separation of the actinide elements and elements with Z = 103 by a beam of heavy ions in the UNILAK accelerator in Darmstadt.

In almost all the reports, papers of Soviet scientists on the study of the properties and synthesis of new elements were cited.

A useful exchange of information occurred at the symposium on the urgent problems of the chemistry of the transuranic elements, which will permit the route for further development of investigations in this direction to be planned.

IAEA SYMPOSIUM ON THE NATURAL NUCLEAR REACTOR AT OKLO

V. A. Pchelkin

In the middle of 1972 a unique natural phenomenon – a natural nuclear reactor, which operated about two billion years ago – was observed at the Oklo uranium deposit in Gabon. This was the subject of an international symposium organized by the IAEA, together with the French CEA and the government of the Fabonese Republic, which was held in Libreville, the capital of Gabon, in the summer of 1975. More than 70 specialists (physicists, chemists, geologists, geochemists, etc.) from 17 countries took part in the symposium. The delegations from France, Gabon, the USA, the FRG, and England had the most representatives. Thirty nine talks were included in the program of the symposium, including a talk by A. K. Kruglov, V. A. Pchelkin, M. F. Sviderskii, Yu. M. Dymkov, N. G. Moshchanskaya, and O. K. Chernetsov entitled "Preliminary studies of samples of uranium ore from the Oklo (Gabon) natural atomic reactor." The talks were divided thematically into three groups (earth science, isotopic geochemistry, and reactor physics).

The first group of talks dealt with the place of the Franceville Basin in the geology of Africa, the peculiarities of the Oklo deposit as a whole and in the parts which make up the nuclear reaction zone, mineralogical, chemical, and petrographic studies of the ore-bearing minerals and the surrounding rock, the nature of the organic matter associated with the uranium ores of the Franceville Basin, and a number of other geochemical problems. A large part of the talks dealt with problems of isotopic geochemistry and related problems: geochronology, the duration and date of the nuclear reaction, the geochemical evolution of a natural nuclear reactor, the fission product yield and their isotopic composition, estimates with the aid of isotopic geochemistry of the number and frequency of Oklo-type phenomena in nature, and so on. Special attention was given to the accuracy and sensitivity of isotopic analyses of uranium as well as of a number of fission products, and to the apparatus used in these analyses. In this regard, we should note the talks on the results of high quality systematic analyses of the isotopic composition of uranium and the rare earth elements (Ce, Nd, Sm, Eu, Gd) contained in the Oklo ores, and also on high resolution spectrometry before and after activation of ore samples. It should be emphasized that the very discovery of the remarkable Oklo phenomenon is due to the fact that workers at the French CEA observed uranium containing 0.7171% ^{235}U instead of the accepted 0.7202 ± 0.0006% during isotopic analysis (precision mass-spectrometry).

The problem of the physics of these reactors was presented in full in the talks by the leader of the "Franceville" project, R. Naudet and his co-workers (Department of Reactor Physics and Applied Mathematics at the Center for Nuclear Studies at Saclay). In the talks data were given on studies of the neutron balance, on the neutron flux distribution in the Oklo natural nuclear reactor as determined with the aid of isotopic analysis of rare earth elements, on neutron analysis of the distribution of reaction rates, on a model for the behavior of uranium and fission products in the natural nuclear reactor, and, in addition, the problems generated by the mechanisms controlling the reactions were stated.

Among the remaining questions (the accumulation of uranium, means of propagation of the reaction, etc.) discussed in the final session were the prospects for studying the Oklo phenomenon within a scheme for international cooperation.

The participants in the symposium visited the mining pit with the natural reactor at Oklo, the concentrating (gravitation) plant, a hydrometallurgical factory whose final product is a chemical concentrate containing 55% uranium as U_3O_8, and an analytical laboratory (Munana region). It should be noted that

Translated from Atomnaya Énergiya, Vol. 40, No. 3, pp. 271-272, March, 1976.

at the factory, the production is monitored not only for the overall content of uranium but is also analyzed isotopically for its ^{235}U content by means of an "Oklometer" (using the 186-keV γ-line). The deviation of these results from mass spectrometry does not exceed $\pm 1.5\%$.

The discovery of a natural nuclear reactor in Gabon has led to widespread research on this remarkable phenomenon. Scientists from many countries are involved in active searches for traces of such reactors in other parts of the world. Undoubtedly, the problem of isotopic anomalies in natural uranium is not only of scientific importance, but has significant practical information.

The material from the symposium will be published by the IAEA.

CONFERENCE OF THE INTERNATIONAL COMMITTEE ON NUCLEAR DATA

G. B. Yan'kov

The regular and 8th meeting of the International Committee on Nuclear Data (ICND) took place on October 6-10, 1975 in Vienna. Traditional problems were considered serially at the meeting: the annual reports of countries concerning experimental investigations and work on the assessment of nuclear data, information on new facilities, reports of the permanent subcommittees of the ICND, the work of centers concerned with neutronic and nonneutronic data, the world register of enquiries (WRENDA), the issue of the SINDA compilation, aid to developing countries in the organization of research on nuclear data, the results of past conferences and proposals for the future, and also reports of the nuclear data sections of the IAEA.

The principal attention in experimental investigations continues to be paid to measurements of the constants in regions of the greatest discrepancies (or absence) of data for isotopes which determine the operation of fission reactors, reference standard cross sections and parameters for the quantities used in the designing of models of thermonuclear reactors. The evaluated nuclear data are widely used everywhere not only by customers as the primary data for calculations of different systems, but also by researchers for revealing regions of discrepancy in the data when planning experiments. The accuracy asked for in the values of the principal cross sections is now mostly supported by the accuracy required in determining the principal reactor parameters and their sensitivity to a change of the quantities being measured. The experimental basis, in particular, of the neutron source continues to be improved: new 160-MeV linear electron accelerators are being constructed at Harwell (Great Britain), the source parameters are being improved on the basis of the Los Alamos meson factory (USA), and the first neutron work has been carried out on the "Fakel" linear electron accelerator in The I. V. Kurchatov Institute of Atomic Energy (Soviet Union).

In reactor technology, the importance of interreactor measurements – reactor dosimetry – has increased. The nuclear data sections of the IAEA have prepared and issued (in the form of a report) the second part of a review, which contains the transverse cross sections of reactions used in reactor dosimetry.

A new and extremely vast region has been incorporated this year into the sphere of activity of the ICND – atomic and molecular data (A + M data) – used in plasma research and in thermonuclear technology. This concerns the requirements in data for such sections of research as, e.g., the characteristics proper of a plasma its diagnostics, interaction of the plasma with the metal walls, injection of particles into the plasma, laser and electronic methods of generating a fusion reaction. The nuclear data sections of the IAEA prepared a review of the requirements in A + M data and conducted a small international conference of consultants for discussing these requirements and also the possible forms of international cooperation. These forms, obviously, will be similar to the forms of collaboration in neutronic and nonneutronic data. In 1976 the IAEA is proposing to hold a conference of specialists in A + M data and to discuss more specifically plans for future cooperation.

The ICND has changed its methods of operation somewhat. This concerns, in the first place, its "technical" subcommittees, i.e., the subcommittee on reference standard quantities and the subcommittee on discrepancies and estimates [At. Énerg., 38, No. 3, 190 (1975)]. Beside the ICND there exists a regional committee on nuclear data, the NEANDC, whose members are certain west European countries, the USA, and Japan. In order to reduce duplication of activity of the technical subcommittees, the activities

Translated from Atomnaya Énergiya, Vol. 40, No. 3, pp. 272-273, March, 1976.

of both committees will be coordinated. An example is the suggested method of operation of the committee on reference standard quantities. Each reference quantity within the constitution of each committee for several years has been fixed for the individual scientific or laboratory (correspondent) which, before a meeting of its committee, prepares a report on the status of the data on the stated quantity. For example, for the Soviet Union values have been fixed for the fission cross section of ^{235}U and the spectral energy of the neutrons from the spontaneous fission of ^{252}Cf. After the meeting of the ICND, a report with recommendations will be made to the appropriate correspondent within the constitution of NEANDC (e.g., for the fission cross section of ^{235}U in Great Britain), which supplements the report with new data and presents it at the meeting of its committee; the report with the recommendations is then returned to the correspondent within the constitution of the ICND, etc. Meetings of the committees are staggered in dates, and therefore the reports will be updated continuously on the basis of more recent data and thus with less expenditure of effort. A somewhat different spacing of the meetings also was discussed. Thus, in 1971 and 1975, the All-Union Conferences on Neutron Physics in Kiev and the National Conferences on Nuclear Data in the USA were held in the same half-year. A 3-yr cycle of conferences was proposed at the meeting: e.g., in the Soviet Union in 1977, in Western Europe in 1978 and in the USA in 1979, and then repeated. As a result of this, there will be no need to organize a large and very expensive conference of the IAEA, similar to the conference which took place in 1970 in Helsinki.

It was accepted also that the period between meetings of the ICND should be increased: to sesquiannually. The next conference is to be held in May 1977 in Vienna.

ALL-UNION CONFERENCE ON THE APPLICATION OF CHARGED-PARTICLE ACCELERATORS IN THE NATIONAL ECONOMY

O. A. Gusev

The 2nd All-Union Conference on the Application of Charged-Particle Accelerators in the National Economy was held on October 1-3, 1975 in Leningrad. Specialists from 53 organizations and companies of the Soviet Union participated in the conference, representing the Academy of Sciences of the Soviet Union, the State Committee for Nuclear Energy Research, the chemical, petrochemical, electronic, textile, radio and electrotechnical, timber and tree cultivation, power engineering industries, the Ministries of Public Health and Higher Education. Specialists from Poland, the German Democratic Republic, Czechoslovakia, and Hungary also participated. More than 80 papers were heard on the problems of the development, construction and operation of different types of accelerators, and also their application in radiation chemistry, for industrial defectoscopy and activation analysis, for the sterilization of manufactured goods, the prevention of contamination of the environment, and radiation therapy. More than 100 accelerators of different types are operating at present in branch institutes, in plants and factories and in medical establishments. The economic effect from their utilization amounts to tens of millions of rubles per year. The use of accelerators in the national economy allows a number of technological processes, which are new in principle, to be carried out, manual labor to be eliminated, and the productivity of work and the production quality to be increased.

In the reports devoted to the development and construction of charged-particle accelerators for radiation processes, the advantages of facilities with high-powered accelerators are shown clearly. These accelerators permit the unit cost of installed power of the radiation facilities to be reduced and permit conversion to the industrial utilization of radiation processes with a high energy capacity. For this, during recent years in the Scientific-Research Institute of Power Engineering and Physics of the Atom (NIIÉFA) and the Institute of Nuclear Physics, Siberian Division of the Academy of Sciences of the SSSR, new types of high-voltage electron accelerators have been developed, with a power of 20-25 kW ("Avrora," ÉLB). The accelerators have passed the trials successfully and have been recommended for series production. The development of high-voltage accelerators with an average power of 50 kW or more has started. At the same time, the startup of certain obsolete types of accelerators (KGÉ-500 and KGÉ-2.5) which have unsatisfactory technical-economic indexes, and also accelerators of the ÉLT type which have shown insufficient reliability, has been suspended.

The present-day level of Soviet electron accelerators, designed for radiation facilities, will permit the successful solution of problems of the industrial introduction of a wide circle of radiation processes, including such high-efficiency processes as the output of manufactured articles of radiation cross-linked polyethylene, hardening of colored varnished coatings, the production of perspexes, the manufacture of tissues with special properties, synthesis of a number of polymers, etc.

A considerable part of the reports was devoted to problems of the development of accelerators for industrial defectoscopy. Experience in the use of these accelerators in a number of heavy engineering works (linear, at the Izhorsk plant in Leningrad, betatrons in Barnoul, etc.) has shown clearly their advantages in comparison with the previously used γ-radiation isotope sources. The linear accelerators presently operating in the NIIÉFA enable the quality of steel manufactured articles with a wall thickness of up to 650 mm to be monitored (LUÉ-15-1500D, with a radiation intensity of 15,000 R/min·m). High-powered betatrons are being developed for similar purposes, e.g., the BS-3-25 with an energy of 25 MeV

Translated from Atomnaya Énergiya, Vol. 40, No. 3, pp. 273-274, March, 1976.

and with a maximum radiation intensity of 1400 R/min·m. For the transillumination of steel, with a thickness of up to 100-150 mm, there are the promising small-sized betatron MIB-6-200 (5 R/min·m) and also a defectoscope based on the RTD resonance transformer (50-100 R/min·m). Because of need for ensuring the quality control of steel units with a thickness of up to 900 mm, the use of which is likely in the future for the rapidly developing nuclear power generation, not only a further increase of the radiation intensity produced from the accelerator is very urgent, but also the methods of recording the defects must be improved. An increase of the intensity of the radiation sources and a reduction of the exposure time associated with this (which in a number of cases becomes significantly less than the time of the preparatory operations), raises sharply the question of automation of commercial defectoscopy processes, in particular the construction of industrial robots for the installation and replacement of film.

One of the first directions in which the accelerator found practical application was in beam therapy. For the specialists working in this field, great interest was aroused by the discussions on the positive operating experience with accelerators of the LUÉ-25 type in the Scientific-Research Institute of Oncology and Medical Radiology, Belorussian SSR and the Scientific-Research Institute of Oncology (Leningrad). In addition to the operating characteristics of the accelerator, the results are given of their clinical use. New developments in accelerators for beam therapy were considered in a number of reports. The discussion on the LUÉ-15M accelerator, developed in the NIIÉFA with programmed control, should be mentioned, also the characteristics of the therapeutic microtron and the research capabilities of the use in beam therapy of the small-scale betatron developed in the Institute of Nuclear Physics, Tomsk Polytechnical Institute. Reports were received with interest concerning the work carried out on the synchrotron of the B. P. Konstantinov Institute of Nuclear Physics, Leningrad, by the use of a proton beam with an energy of 1 GeV for medical–biological purposes.

A considerable part of the discussions was devoted to the equipment layout of laboratories and the participants of neutron activation analysis at industrial establishments, and also analysis with the use of photonuclear reactions. As a neutron source, it is proposed to use the NG-150M neutron generator, produced by NIIÉFA, in the majority of laboratories.

The expansion of the scales of introduction of accelerator techniques into the national economy makes the problems of monitoring the parameters of charged particle streams and of technological dosimetry very urgent. Discussion showed that at the present time, a number of devices are being developed which will allow continuous monitoring of the beam current and particle energy at the accelerator outlet. In view of this, the development and introduction of a unified procedure for measuring absorbed radiation doses in commercial radiation facilities is very important.

In its resolution, the conference recommended that work be continued on the improvement of the accelerators currently in production, and also new types of high-powered accelerators for newly developed radiation processes with a high energy capacity, compact accelerators for medical work and defectoscopy, small-sized accelerators for mobile activation analysis laboratories, and proton accelerators for medical purposes. At the same time, further development is recommended of the scientific principles of radiation techniques and improvement of the methods for calculating and designing radiation facilities. It was agreed that it would be advantageous to hold an All-Union Conference on the Use of Accelerators in the National Economy in 1979, with participants from affiliated institutes and industrial establishments.

2nd INTERNATIONAL SYMPOSIUM ON PLASMA CHEMISTRY

Yu. N. Tumanov

The symposium was held in Rome on September 18-23, 1975. One hundred thirteen delegates from 16 countries took part and about 70 papers were discussed. (Five people from the Soviet Union took part and delivered ten papers.) The symposium was organized by the International Union of Pure and Applied Chemistry (IUPAC). All the talks were grouped according to their subject.

Elementary Reactions in Low Temperature Plasmas. The topics discussed included the following: studies of the mechanisms of different chemical reactions in thermodynamically nonequilibrium plasmas; data on electron–atom, electron–molecule, atom–molecule, ion–molecule, etc. interaction cross sections; and, data on the interpretation of parameter measurement results in chemically reacting plasmas. Models of atomic–molecular reactions for Maxwellian velocity distributions and for different deviations from same were studied in a number of concrete cases. The perturbing effect of a laser on the mechanism of these elementary reactions was considered.

Considerable attention was devoted to the kinetics of chemical reactions under the action of electron impact, to the relaxation kinetics of excited atoms and molecules, to the interaction of atoms and radicals in complex mixtures, and to the kinetics of ion-neutral particle interactions. The plasma characteristics and chemical reactions of electronegative gases were studied in detail.

A large group of talks dealt with chemoionization reactions which take place during the strongly exothermic interaction of molecular beams of metal and metalloid atoms with oxidants (oxygen, nitrogen oxides, halogens, hydroxyl group). In this interaction ions are formed with ionization taking place, as a rule, in three ways: electronic transitions (ionization of the atom), reactive ionization (formation of the monoxide ion), and associative ionization (formation of a polyoxide ion).

Chemoionization of uranium in a uranium–oxygen system has been examined in much detail, in particular the dependence of the chemoionization cross section in the above-mentioned processes on the relative energy of atoms and molecules in the beams. Chemoionization of uranium when an atomic beam interacts with oxygen and nitrous oxide in a mirror machine has been investigated. In addition, studies have been made of chemoionization of atoms from the II, III, IV, V, and VI groups of the periodic system (Al, B, Ba C, Ca, Ce, Fe, Hf, Zu, Si, Mg, Nb, Mo, Se, Si, Th, etc.) with not only atomic and molecular oxygen as an oxidant, but also with halides and the hydroxyl group. A preliminary classification of the elements was made according to their behavior in chemoionization reactions and the possibility was discussed of using these reactions for separation of elements and of isotopes of elements, particularly of uranium isotopes. A number of talks dealt with the role of chemoionization reactions in the mechanism for combustion of hydrocarbon fuels as well as with the reactions of ionic clusters in the upper layers of the atmosphere.

Diagnostics of Chemically Reacting Plasmas. The development of a new diagnostic technique for studying the products of chemical reactions in an electric discharge plasma (M. Kaufman, USA) was discussed. Because of the difficulty of using mass spectrometry to observe the neutral intermediate chemical reaction products (excited atoms and molecules, free radicals, etc.), a so-called neutral mass spectrometer has been developed which is a synthesis of the techniques of mass spectrometry and molecular beams.

Considerable attention was devoted to chromatographic analysis (to increase the accuracy of the analysis a gas sample is compressed) and to the so-called actinometric technique for measuring the intensity of a discharge (electron density and energy), which is related to the rate of chemical reactions. The

Translated from Atomnaya Énergiya, Vol. 40, No. 3, pp. 274-275, March, 1976.

remaining talks were on specific results from the use of probe diagnostics, mass spectrometry, optical spectroscopy, contact methods, and modern computers in studies of the mechanism of chemical transformations in plasmas.

Use of Plasma Turbulence to Produce Chemical Reactions. This group of talks was presented by scientists from the USSR (V. A. Legasov and A. A. Ivanov). The problems of nonequilibrium plasma chemistry were considered, as well as the possibility of using powerful electron beams to produce stationary plasma discharges. Studies on the separation of particles of differing molecular weights in a plasma centrifuge as a means of separating the products of plasma chemical reactions were discussed. A plasma centrifuge may be successfully used where the possibility of thermally freezing out the fast reaction products is exhausted. The use of the magnetoacoustic resonance to heat plasma electrons, synthesizing reactions in gaseous discharges, reactions stimulated by a relativistic electron beam, and so on, were considered in a number of talks. Chemical and phase transitions in a uranium–fluorine plasma were discussed (Yu. N. Tumanov).

Plasma Technology. The most interesting talk was given by Academician N. N. Rykalin (USSR). The processes of melting and spheroidizing of metals, synthesizing reactions, and the development of various plasma sources were discussed. Other papers reported on the development of three phase plasma sources, the use of gaseous cooling to increase the efficiency of plasma sources (plasmatrons), the transport properties of flows of plasma thermal conductors, and the use of current carrying thermal conductors for nitride synthesis.

Chemical Reactions in Plasmas. A very promising area for applications of low pressure nonisothermal plasmas is transport reactions (S. Veprek, Switzerland). Three types of chemical reactions have been studied: "chemical" vaporization and condensation of solid substances when they interact with a low pressure chemically active plasma; surface modifications due to heterophase interactions of a plasma with metals; and, heterophase atomic recombination reactions. The role of the thermodynamic and kinetic effects of the chemical interactions in a nonisothermal plasma was considered. Transport reactions in a plasma are a powerful means of obtaining pure materials (for example, for microelectronics and nuclear technology). Part of the talks was devoted to directed polymerization and decarbonylization reactions in a low pressure plasma. Significant attention was paid to the synthesis of carbide and nitride materials by means of plasma heating.

Some Problems in the Development of Plasma Chemistry. The organizational activities of the subcommittee on plasma chemistry of the IUPAC and measures to improve the interaction of industry with the universities in France were discussed.

Based on the talks considered at the symposium, we may draw the following conclusions:

1. Despite the energy crisis which has affected most industrially developed countries, there is great interest in the use of low temperature plasmas in chemistry, chemical technology, and metallurgy. Compared with the first symposium on plasma chemistry (Kiel, W. Germany, 1973) there was an increase in the number of research topics, and the ways to develop the scientific bases of plasma chemistry were noted. This is apparently due to the need to simplify and unify the mechanism for transfer of the energy of an electric current in a reactor, to reduce the energy expended in chemical metallurgical processes, and to intensity the latter and increase the level at which they are controlled.

2. In addition to electric arc and RF plasma sources, electron beam plasma sources are beginning to be used. Plasma centrifuges are beginning to be used beside the traditional methods for separating the products of plasma chemical reactions by thermal freezing.

3. Interest has increased in chemical reactions in nonequilibrium plasmas. Somehow or other, in most talks the properties or applications of low pressure plasmas were discussed. The topic of discussion was the production of pure materials for atomic power and semiconductor technology, for synthesis of products which are unstable under ordinary conditions, for producing polymer films and coatings, and for surface modification.

4. A very interesting method of obtaining a plasma and applying it in chemistry is by means of chemoionization reactions which take place during the strong exothermic interaction of elements in molecular beams. The methods for producing chemoionization reactions may be utilized for separating chemical elements and, possibly, isotopes of elements.

5. There was interest in ionic and ion–molecular reactions in the upper layers of the atmosphere. These studies have great practical interest. It is possible, e.g., to recall the reactions of various materials released to the atmosphere by industrial establishments, and aircraft and rocket engines, with ozone, a band of which occurs at an altitude of about 30 km.

The next symposium on plasma chemistry will take place in Limoges, France in 1977.

3rd INTERNATIONAL CONFERENCE ON THE MEASUREMENT OF LOW LEVELS OF RADIOACTIVITY AND THEIR APPLICATION

A. K. Lavrukhina

The conference took place in October 1975 in Czechoslovakia. It was organized by the Komenskii University (Bratislava) and the Institute for Research, Production and Application of Radioisotopes (Prague). About 150 specialists from 21 countries participated in the conference, approximately 100 papers were read, of which 65 were presented by scientists of the socialist countries. A wide circle of scientific-technical problems were covered on the construction of the most complex radiometric instruments for the measurement of low levels of radioactivity. The solution of many large-scale fundamental problems of solar physics, oceanology, archeology, physics of the terrestrial atmosphere, the origin and time variations of cosmic rays, the origin and evolution of the surface of planets, satellites and the small bodies of the solar system, the search for superheavy elements and also many applied problems of geochronology, hydrogeology, meterorology, glaciology and the radiation charge of the environment, which are impossible without a detailed study of the radioactivity of natural objects of terrestrial and cosmic origin. In connection with this, great attention is being paid in many countries to the construction of specialized low-background radiometric laboratories.

Over the last decade, great successes have been achieved in the field of precision studies of low levels of radioactivity. This was assisted, first of all, by the construction of underground laboratories in the Soviet Union (Institute of Nuclear Research, Academy of Sciences of the USSR and the Joint Institute of Nuclear Research), Japan (Institute of Nuclear Research, Tokyo University), Switzerland (Institute of Physics, Bern), Federal German Republic (Physicotechnical Society, Braunschweig), in Bulgaria (Institute of Nuclear Research and Nuclear Energy, Sofia). These laboratories have a low background of cosmic radiation, for example: the muon flux in the neutrino laboratory of the Institute of Nuclear Research, AN SSSR, located at a depth of 600 m water equivalent, amounts to a total of only 1 muon/day $\cdot$ cm^{-2}. In order to screen the detectors from the radioactive background of the rocks, in this laboratory ultrabasic rock dunite and specially produced concrete with a low radioactivity are used. Great attention is being paid to the choice of pure metals for the passive screening. However, the maximum reduction for the detectors should be achieved by replacing the plastic scintillators with NaI crystals in the "active" screening. Thus, S. Tanaka et al. (Institute of Nuclear Studies, Tokyo University), for a needle-shaped, end-window, gas-flow, copper counter (volume $\sim$0.15 cm^3, window area $\sim$0.75 cm^2) placed in a well in a NaI crystal and connected in anticoincidence with the main counter, obtained an extremely low background of 0.0092 $\pm$ 0.0005 dpm with an efficiency of 43 $\pm$ 3% (for a ^{137}Cs source). The sensitivity of this counter was $5 \cdot 10^{-15}$ Ci.

Great attention was paid to the consideration of the structural features of gas-flow counters for measuring the β activity of solid samples, and also new designs of multiwire counters for measuring the radioactivity of gases (^{14}C, ^{3}H, ^{37}Ar, ^{39}Ar, and ^{82}Kr). The report of I. R. Barabanov et al. (Institute of Nuclear Research, Akad. Nauk SSSR) was devoted to the search for new methods of purifying structural materials from impurities of the natural radioactive elements.

Until recently, one of the main disadvantages of low β-activity measurements was the absence of methods for the simultaneous determination of the intensity of the energy of β particles. Now, the situation has changed significantly: several versions of these methods have been proposed. One of these was discussed in the report by V. A. Alekseev et al. (GEOKhI, Akad. Nauk SSSR).

Translated from Atomnaya Énergiya, Vol. 40, No. 3, pp. 275-276, March, 1976.

A large part of the reports was devoted to the use of liquid scintillators; particular attention was paid to the optimization of the counting cycle. On the basis of the known properties of scintillators and the theory of interaction of radiations with a substance, the response functions were investigated theoretically and experimentally for various types of liquid scintillators (N. Prokhazka, Research Institute of Veterinary Medicine, Brno).

The sensitivity of measurements of low radioactivity levels can be increased not only by reducing the background and its stability, but also by increasing the specific activity of the samples being investigated by isotopic exchange. The data presented at the conference by the scientists of different countries show that this method is the most efficient for measurements of low concentrations of tritium in sea water and radiocarbon in organic objects with a long lifetime (up to 75,000 yr).

The most important and promising trend of work in the field of low activity measurements is the application of γ spectrometry and $\gamma-\gamma$, $\beta-\gamma$, and $\beta-\gamma-\gamma$ coincidences. They open up wide possibilities for studying the radioactivity of samples without their destruction. This permits a unique substance (meteorites, tektites, cosmic dust, and lunar rocks) to be preserved, and laborious chemical processing operations to be avoided, which frequently lead to useless losses and errors. The development of work in this sphere is proceeding in two directions.

1. New radiotechnical schemes for $\gamma-\gamma$, $\beta-\gamma$, and $\beta-\gamma-\gamma$ coincidences are being improved and produced (GEOKhI Akad. Nauk SSSR, Moscow; Komenskii University, Bratislava; Institute of Nuclear Research, Akhmesabad, India; Central Institute of Nuclear studies, Rossendorf, German Democratic Republic). The greatest sensitivity in determining ^{22}Na and ^{26}Al has been obtained in a $\beta-\gamma-\gamma$ coincidence cycle on an instrument consisting of two NaI (Tl) crystals, 150 $\times$ 100 mm, β counters and a plastic scintillation anticoincidence counter (Komenskii University). The background of the instrument in the energy counting regions of ^{22}Na and ^{22}Al is equal to 0.75 pulses/d and the sensitivity is $\sim 5 \cdot 10^{-15}$ Ci.

2. In many countries, γ spectrometers with Ge(Li) semiconductor detectors have been produced, which are being used successfully for determining the contents of radioactive products from nuclear explosions, in atmospheric dust and fallout, cosmogenic isotopes in lunar and meteoritic material, and also for the activation determination of ultrasmall amounts of elements in pure substances and natural objects. The greatest sensitivity ($5 \cdot 10^{-15}$ Ci) is achieved on the γ spectrometer of the Institute of Organic Chemistry and Biochemistry in Prague, where unique measurements have been made of the content of ^{22}Na, ^{26}Al, K, Th, and U in samples of lunar soil with a weight of 247 mg, obtained by the Luna-20 automatic station.

One of the interesting aspects of the application of methods for measuring low levels of radioactivity is the possibility of interpreting cosmic phenomena (cyclic and flare activity of the sun, variations of the earth's magnetic field, the time and space variations of cosmic radiation of solar and galactic origin, volcanic activity of the earth and other planets) in both the present time and in the past. Reports were devoted to these problems by scientists of the Soviet Union, Czechoslovakia, Japan, and Federal German Republic (G. E. Kocharov, V. A. Dergachev, A. K. Lavrukhina, P. Povinets, C. Tanaka, et al.). In some papers, questions were touched upon connected with estimating the age of soil, archeological samples, water, ice, volcanic ash, and also with searching for superheavy elements in meteorites and terrestrial samples.

The proceedings of the conference will be issued in 1976.

ALL-UNION SEMINAR ON THE RADIATION STABILITY OF ORGANIC MATERIALS

Yu. Ya. Shavarin

The All-Union Seminar on the Radiation Stability of Organic Materials took place in Obninsk from October 6-9, 1975. About 150 people participated in the work of the seminar. Sixty-five reports were presented from various organizations using organic materials under conditions of the interaction of different types of radiation. Problems were considered concerning changes of the electrophysical, physico-mechanical, structural, and other properties of organic materials both during and after irradiation, and also problems in studying the damage mechanisms of organic materials used in the construction of nuclear reactors, electron accelerators, and other facilities. Problems were discussed concerning increasing the radiation stability of these materials.

A meeting of specialists in the radiation stability of organic materials is proposed for November 1976.

Translated from Atomnaya Énergiya, Vol. 40, No. 3, p. 277, March, 1976.

A FACILITY FOR PRODUCING A BEAM OF ELECTRONS WITH ENERGIES OF UP TO 250 KeV AND WITH A POWER OF UP TO 1000 kW

M. M. Brovin, A. A. Bushuev,
V. A. Gapanov, A. I. Grishchenko,
S. S. Zhukovskii, V. E. Nekhaev,
V. S. Nikolaev, V. V. Ryazanov,
R. A. Salimov, E. P. Semenov,
and A. F. Serov

A facility has been started up in the Institute of Nuclear Physics, Siberian Division of the Academy of Sciences of the USSR, in which an electron beam is produced with energies of up to 250 keV and with a power of up to 1000 kW. The one-shot duration of operation of the facility is limited by the thermal cycle and amounts to a time of order of a few tens of seconds. By the introduction of forced cooling, the facility can be used for the production of an electron beam in a continuous cycle.

In beam power, the facility significantly exceeds direct-action accelerators of similar energy, the useful power of which does not exceed hundreds of kW. The facility can be used for investigating various energy-capacious radiation processes; in the continuous cycle, it may find application in industrial scale processes.

The facility consists of an accelerator tube, located in a powerful longitudinal magnetic field, and a high-voltage rectifier, made in the form of individual units and connected by high-voltage cable. A 12-phase system of rectification is used in the rectifier. The energy pulsations of the beam, as a result of this, amount to ±5%. The rectifier is fed from an ac three-phase supply at a potential of 6.3-10 keV. The rectifier is mounted in a tank with diameter of 2 m and height of 3.3 m. The equipment of the accelerator tube unit, without the beam catcher, is arranged in a volume of 2.5 × 2.5 × 3 m. The parameters of the electron beam obtained are limiting for this facility. The beam energy attained at present is limited by the magnitude of the breakdown voltage of the accelerator tube. It has been suggested that, by reducing the level of electromagnetic radiation and secondary particles in the region of the accelerator tube, it should be possible to produce an electron beam with even higher energy and power parameters. The high-voltage rectifier used in the facility has been tested in operation on active load to a magnitude of the output voltage of up to 400 kV and a power of up to 4,000 kW. Shielding of the rectifier elements from objectionable surges, which can originate as a result of breakdowns in the accelerator tube, is ensured by a high-voltage screened choke-coil installed at the rectifier output.

Translated from Atomnaya Énergiya, Vol. 40, No. 3, p. 277, March, 1976.

BIBLIOGRAPHY

A. I. Moskvin

COORDINATION CHEMISTRY OF THE ACTINIDES*

Reviewed by A. M. Rozen

The available information on the coordination compounds of the actinides is disjointed, although the flow of experimental data is very large. Therefore, the publication of A. I. Moskvin's monograph is expedient and timely.

In the book being reviewed, extensive data on the complex-formation of all the actinide groups are systematized and classified. In the first two chapters, the characteristics are introduced of the complex compounds of the actinides with inorganic and organic ligands (composition, most important physicochemical properties). The principal statements are discussed concerning the types of complex compounds, the state of the actinide ions in solutions and their hydrolytic behavior; the mechanism of hydrolysis and polymerization of the actinide ions is discussed in accordance with modern views concerning mono- and polynuclear hydrocomplexes forming genetic series. Great attention is paid to a description of synthetic chemistry and the equilibrium of complex-formation, taking account of reaction mechanisms and with the inclusion of structural, spectroscopic, and thermodynamic data. Complex-formation is considered of heptavalent neptunium and plutonium. Numerous data on the composition and stability constants of the actinide compounds formed in solutions are tabulated; a critical estimate of the constants is given and the effect of different factors on the stability of the compounds is explained. Section 2.4 is interesting, which is devoted to the laws of chemism of actinide extraction processes and the effect of different factors on the extraction capacity of extractants. By an example of compounds of the actinides with phospho- and arseno-organic reagents, the large role is stressed of the induction effect of group-substituents (e.g., by an atom of phosphorus or arsenic).

Section 2.7 is devoted to the composite complex compounds of the actinides, where the most important results are summarized, obtained in the work of numerous researchers. It is shown, that in order to carry out the synthesis of composite compounds, the theory of oriented synthesis is very fruitful, which is based on the rule of mutual substitution of ligands, determined by I. I. Chernyaev and further developed by R. N. Shchelokov. Certain laws also are discussed, determining the solubility of the compounds, and the correlation of the solubilities produced with the properties of the components forming them.

The third chapter, devoted to the laws of complex-formation of the actinides in aqueous solutions, is based to a considerable degree on original research of the author.

The correlations are discussed which relate the stability constants of the coordination compounds with the properties of the metals forming their ions and of the ligands (charge, radius, structure, electronegativity, atomic number, stereochemistry, and basicity of the donor atoms). The greatest attention is paid to the stereochemistry of the actinide ions, the effect of substitution and dentoticity of the ligands, and also cycloformation to the magnitude of the stability constants of the compounds. An explanation is given for the diversity and complexity of composition of the actinide compounds, especially of the first half of the actinide series, starting from the ideas concerning the formation of donor–acceptor coordination bonds. It is shown that their coordination capabilities, the types of chemical bonds formed by them and the stability of the compounds, are found in a definite interrelationship with the electron structure of the actinides. Some prospective developments of the coordination chemistry of the actinides are formulated briefly.

* Atomizdat, Moscow (1975).

Translated from Atomnaya Énergiya, Vol. 40, No. 3, p. 278, March, 1976.

There are certain inadequacies in the book: the practical application of the complex compounds for distinguishing and separating the actinides is not considered, and the location of the actinide group in the periodic system is not discussed on the basis of modern achievements in the coordination chemistry of the elements. These problems merit individual consideration. Unfortunately, many sections of the book are discussed with too much sketchiness, in an extremely condensed form.

On the whole, the book is quite a complete review of the existing data on the chemistry of the coordination compounds of the actinides. The large bibliographical information (907 references) makes it possible to use the book as a reference book. It will be useful for a wide circle of scientific workers and engineer–industrialists (radiochemists, geochemists, biophysicists, biochemists, oceanologists, etc.). occupied with the chemistry and technology of nuclear fuel. A repeat issue of the book is desirable, with the appropriate additions and revisions.

V. M. Gorbachev, Yu. S. Zamyatnin, and A. A. Lbov

THE PRINCIPAL CHARACTERISTICS OF ISOTOPES OF THE HEAVY ELEMENTS*

Reviewed by N. A. Vlasov

The book being reviewed is a very useful handbook on the properties of the isotopes of the heavy elements. Their list starts with ^{212}Th and concludes with element ^{262}105, which has still not been named, and includes all the isotopes of the intermediate elements known up to 1974. The largest section of the handbook contains data on the physical characteristics of the isotopes: masses, decays (period, energy) and the radiation characteristics. Besides the detailed tables, nuclear level schemes are assembled from all the data (energy, moment and parity, de-excitation scheme with an indication of the relative transition intensities), obtained as a result of a great number of original nuclear-spectrometric investigations. All the tables are accompanied by references to the papers in which these or other figures have been determined.

In addition to the nuclear-spectrometric tables, the handbook contains tables with the characteristics of the elements and their compounds. For example, the principal minerals, crystalline structures of the most important compounds, etc. are enumerated. The last section is devoted to methods of producing the isotopes of the heavy elements. Data are assembled in it, obtained in experiments on nuclear reactors, on charged particle accelerators and in nuclear explosions.

The handbook is extremely useful for physicists, chemists, engineers, biologists, medical, and other specialists using preparations and samples of heavy elements. It rids one of tedious searching for the requisite data in the multiplicity of journals, as it contains almost all the data obtained by science and used in the development of the various laboratory and technical equipments. The diversity of properties of the isotopes of the heavy elements stimulates the growth of a number of regions for their application. A knowledge of the numerous characteristics of the isotopes will assist in accelerating their utilization in the future in applications already being encountered and even as yet unknown.

Table 1.2, containing data on the minerals of uranium, may cause some perplexity. The principal regions of dispersal, stated in the table, are incomplete without any explanations. There is only a reference to the papers from which the table is quoted.

The arrangement of the material on the whole is logical, but for the sake of economy of space, its convenience of use is impaired. From the long title of the book, the words "Principal Characteristics" can be totally excluded. The cover of the book, gaudily inscribed, does not beautify the book, but on the contrary it gives it a frivolous aspect.

Replenishment and updating of the data undoubtedly will soon require the handbook to be reprinted. This reprint is welcomed in advance and every success is wished to the authors in renewing and updating this handbook.

* Atomizdat, Moscow (1975).

Translated from Atomnaya Énergiya, Vol. 40, No. 3, pp. 278-279, March, 1976.

A. P. Zimon

DECONTAMINATION*

Reviewed by O. M. Zaraev

During the last 30 years, a great number of publications have appeared in the Soviet and foreign literature devoted to the results of theoretical and experimental investigations of the various aspects of the decontamination of surfaces contaminated with radionuclides.

The monograph being reviewed is the first large-scale generalization of universal experience in solving important and urgent problems for the removal of radioactive contamination.

In the first chapter, the author attempts to analyze the still inadequately studied physicochemical processes of contamination of surfaces and their decontamination. It proposes to classify these processes into three groups: adhesion, surface, and depth. Adhesion contamination is equivalent to nonfixed contamination, and surface (as a result of adsorption, ion exchange, chemosorption) and depth (in consequence of diffusion, formation of an oxide film, corrosion) contamination corresponds to weakly fixed and firmly fixed contaminations. This classification and the generalized physicochemical representations based on it are, in our opinion, those sufficient solutions which permit the required theoretical basis to be set up for the treatment of decontamination processes.

In the second chapter, modern methods of decontaminating processes and the basic mechanisms of contamination of surfaces with radionuclides are discussed, and the problem of reproducing the parameters which characterize surface contamination is dealt with.

In chapters three to five, the author considers in detail the problems currently attracting the greatest attention of specialists and which are still inadequately dealt with in the literature – the decontamination of surfaces as a result of their adhesion contamination with radioactive particles, and surface and depth contamination with radionuclides. An important part of this material are the results of his own investigations. The author analyzes the processes affecting decontamination, for which he investigates several quantitative models, gives alternatives for describing phenomena, the physical mechanisms of which is still not interpreted, and gives much consideration to the generalization of the results of the experimental investigations.

The sixth and seventh chapters reveal the special features of decontamination of varnished-color, lining and polymer materials, and also leather coats and protective clothes. These data carry the mark of the author's personal opinions, in view of which some problems are incompletely represented.

An analysis of the urgent problems of decontamination of plant, buildings, localities, and also foodstuffs is given in the concisely written eighth chapter. Certain problems recounted are of a discussion nature and could become the theme of a separate book.

In the last, the tenth chapter, interesting problems are discussed concerning the intensification of decontamination processes by means of ultrasonic and electric fields.

In the monograph being reviewed, the author gives an account of the various problems of decontamination from unique positions. The monograph has a number of inadequacies, associated to a considerable degree with its multiaspect nature. The principal ones are the nonuniformity of the discussion of the various chapters, mathematical formalism which is not always justified in the statements of individual sections

* Atomizdat, Moscow (1975).

Translated from Atomnaya Énergiya, Vol. 40, No. 3, pp. 279-280, March, 1976.

(especially the third chapter), and a certain sketchiness in the description of technical and medical-biological applications.

The book reviewed encompasses a very wide circle of problems and contains much useful data on the methods and scientific basis of decontamination, and valuable practical recommendations. It is of great interest for scientific workers, engineering-technical workers, and also university lecturers, graduate students and students specializing in this field.

breaking the language barrier

WITH COVER-TO-COVER ENGLISH TRANSLATIONS OF SOVIET JOURNALS

The Soviet Journal of Bioorganic Chemistry

Bioorganicheskaya Khimiya

Editor: **Yu. A. Ovchinnikov**
Academy of Sciences of the USSR, Moscow

Devoted to all aspects of this rapidly-developing science, this important new journal includes articles on the isolation and purification of naturally-occurring, biologically-active compounds; the establishment of their structure; the mechanisms of bioorganic reactions; methods of synthesis and biosynthesis; and the determination of the relation between structure and biological function.

Volume 1, 1975 (12 issues) $225.00

The Soviet Journal of Coordination Chemistry

Koordinatsionnaya Khimiya

Editor: **Yu. A. Ovchinnikov**
Academy of Sciences of the USSR, Moscow

The synthesis, structure and properties of new coordination compounds; reactions involving intraspheral substitution and transformation of ligands, homogeneous catalysis; complexes with polyfunctional and macromolecular ligands; complexing in solutions; and the kinetics and mechanisms of reactions involving the participation of coordination compounds are among the topics this monthly examines.

Volume 1, 1975 (12 issues) $235.00

The Soviet Journal of Glass Physics and Chemistry

Fizika i Khimiya Stekla

Editor: **M. M. Shul'ts**
Academy of Sciences of the USSR, Leningrad

This new bimonthly publication presents in-depth articles on the most important trends in glass technology. Both theoretical and applied research are reported.

Volume 1, 1975 (6 issues) $95.00

Soviet Microelectronics

Mikroélektronika

Editor: **A. V. Rzhanov**
Academy of Sciences of the USSR, Moscow

Offering invaluable reports on the latest advances in fundamental problems of microelectronics, this new bimonthly covers • theory and design of integrated circuits • new production and testing methods for microelectronic devices • new terminology • new principles of component and functional integration.

Volume 4, 1975 (6 issues) $135.00

Lithuanian Mathematical Journal

Lietuvos Matematikos Rinkinys

Editor: **P. Katilyus**

A publication of the Academy of Sciences of the Lithuanian SSR, the Mathematical Society of the Lithuanian SSR, and the higher educational institutions of the Lithuanian SSR.

In joining the ranks of other outstanding mathematical journals translated by Plenum, *Lithuanian Mathematical Transactions* brings important original papers and notes in all branches of pure and applied mathematics. Topics covered in recent issues include complex variables, probability theory, functional analysis, geometry and topology, and computer mathematics and programming. Translation began with the 1973 issues.

Volume 16, 1976 (4 issues) $150.00

Programming and Computer Software

Programmirovanie

Editor: **N. P. Buslenko**
Academy of Sciences of the USSR, Moscow

This important new bimonthly is a forum for original research in computer programming theory, programming methods, and computer software and systems programming.

Volume 1, 1975 (6 issues) $95.00

send for your free examination copies!

PLENUM PUBLISHING CORPORATION, 227 West 17th Street, New York, N.Y. 10011

Prices slightly higher outside the US. Prices subject to change without notice.